

**EMISSION CONTROL SYSTEM FOR AN X-RAY TUBE**

**JAISINGH RAJWADE**

**Bachelor of Engineering (B.E.) - Industrial Electronics  
University Of Pune, India  
November 1997**

**A Thesis submitted in partial fulfillment  
Of the requirements for the degree of**

**MASTER OF SCIENCE OF ELECTRICAL ENGINEERING  
(M.S.E.E.)  
CLEVELAND STATE UNIVERSITY**

**August 2001.**

## ACKNOWLEDGMENTS

First and foremost, I would like to thank my employers-the management and engineering staff at Marconi Medical Systems, Inc for their support of this thesis work at their facility in Cleveland, Ohio.

Among the above I would specifically like to thank Mr. Alan Cunningham, Electronics Section manager in CT engineering for his constant support in facilitating my research, my thesis technical advisors at Marconi Medical Systems -Ted Resnick and Lester Miller without whose guidance this project would not have been possible, and my other engineering colleagues Ron St. Julian, Gary Angeline, Bart Ziganti, Don Hescht, Greg Loya, Randy Luhta and Mark Herold for providing me with all the help that I required during my thesis work.

I would also like to thank my mentor and thesis advisor at CSU, Dr Dan Simon for his tireless effort and guidance in enabling me to complete this work. Of the community at Cleveland State University I wish to thank Dr E. Villaseca, Adrienne Fox, Allen Morinec, Richard McGuire, Nayeem Sayeed and the rest of the electrical engineering department for their support during my years at Fenn College of Engineering.

Lastly, I would like to thank my family and friends for their encouragement and support during my college days, with a special thanks to my childhood buddy and roommate Anant Gairola, who constantly played the role of my conscience and pushed me into doing my work. Without their love and support, my goals could never have been achieved.

## **EMISSION CONTROL SYSTEM FOR AN X-RAY TUBE**

**JAISINGH RAJWADE**

### **ABSTRACT**

A new control method is needed for cyclic power applications as applied to an X-Ray tube in high power CT scanners in order to minimize the radiation exposure to the patient. The emission control system of an X-Ray tube is highly nonlinear and is typically linearized about an operating point for constant power applications. There exists a need to vary the power over a large range and it is necessary for the linearization of the control loop to be dynamic and have the set point characteristics change via a look up table type of approach. The control loop is implemented using a combination of fuzzy logic and conventional control methods. I have developed a model of the control loop in Simulink to prove out the concept.

This thesis develops a Simulink model of an existing CT scanner control system, and then augments the control system with fuzzy logic to improve the dynamic response of the CT scanner. The development of the Simulink model allows control algorithms to be evaluated before hardware implementation, and the incorporation of fuzzy logic reduces the error in the CT scanner tube current from 9 % to 0.75 %. The system model, design and results are discussed.

## TABLE OF CONTENTS

Chapter 1: INTRODUCTION .....	8
<b>1.1 COMPUTED TOMOGRAPHY</b> .....	8
1.1.1 CT SCANNER .....	8
1.1.2 Dose Modulation .....	11
<b>1.2 LITERATURE REVIEW</b> .....	12
<b>1.3 THESIS CONTRIBUTION</b> .....	16
Chapter 2: SYSTEM MODELING AND SIMULATION .....	18
<b>2.1 X-RAY CONTROL SYSTEM</b> .....	19
<b>2.2 EXPLANATION OF BLOCKS IN MODEL</b> .....	22
2.2.1 Simulink Model 1 .....	22
2.2.2 X Ray Tube Sub-Block .....	29
2.2.3 Simulink Model 2 .....	33
<b>2.3 HISTORICAL PERSPECTIVE</b> .....	34
<b>2.4 SIMULATION RESULTS</b> .....	35
2.4.1 Static mA .....	35
2.4.2 Output of the system .....	36
2.4.3 Percentage Error between reference and actual output of system .....	37
2.4.4 Dynamic mA .....	38
2.4.5 Output of the Dynamic system .....	39
2.4.6 Percentage Error between reference and actual output of the system .....	40
<b>2.5 SYSTEM VERIFICATION</b> .....	41
Chapter 3: CONTROLLER DESIGN AND SIMULATION .....	44
<b>3.1 DESIGN OBJECTIVE</b> .....	44
<b>3.2 A BRIEF LOOK AT FUZZY LOGIC</b> .....	44
3.2.1 Fuzzy Set Theory .....	45
<b>3.3 A CLOSER LOOK AT THE X-RAY CONTROL LOOP</b> .....	45
<b>3.4 FORMATION AND OPTIMIZATION OF MEMBERSHIP FUNCTIONS</b> ..	46
3.4.1 Selection of Inputs and Outputs of the controller .....	46
3.4.2 Selection of values for Inputs .....	49
3.4.3 Membership Functions of “Error” Input .....	51
3.4.4 Membership functions of “DeltaError” Input .....	55
3.4.5 Selection of values for Outputs .....	56
3.4.6 Membership IF-THEN rules .....	59
<b>3.5 SIMULATION OF MODEL</b> .....	64
<b>3.6 DISCUSSION OF SIMULATION RESULTS</b> .....	68
3.6.1 Input to the Fuzzy Logic Controller (FLC) .....	68
3.6.2 mA reference .....	69
3.6.3 Output of the System .....	70
3.6.4 Output of the Fuzzy Controller .....	71
3.6.5 Input to summing block 2 .....	72
3.6.6 Percentage Error between reference and actual output of the system .....	73
3.6.7 Fuzzy Enhanced Model simulation for non Varying Reference .....	74

Chapter 4: SIMULATIONS WITH IMPROVEMENTS TO MODEL AND CHANGES IN PARAMETERS.....	75
<b>4.1 MODIFICATIONS IN MEMBERSHIP FUNCTIONS</b> .....	75
4.1.1 Membership functions of “Error” input.....	76
4.1.2 Membership functions of “DeltaError” input .....	77
4.1.3 Membership functions of “ErrorOut” Output .....	78
<b>4.2 SIMULATION RESULTS</b> .....	79
4.2.1 Percentage Error between reference signal and actual output of system .....	80
<b>4.3 FREQUENCY LIMITATIONS</b> .....	81
4.3.1 Frequency of reference signal .....	81
4.3.2 Simulation at 24 radians /second tube current reference (4 Hertz).....	82
4.3.3 Simulation at 48 radians/second (8 Hertz) tube current reference .....	84
4.3.4 System Output at 48 radians/ second.....	86
4.3.5 Simulation at 6 radians/second (1 Hertz) tube current reference .....	87
<b>4.4 ROBUSTNESS OF THE CONTROLLER TO NOISE CONDITIONS AND ANOMALIES</b> .....	88
4.4.1 Impulse of 600mA.....	90
4.4.2 Impulse of 2000mA (2 Amps) .....	92
4.4.3 Impulse of 4000mA (4 Amps) .....	94
4.4.4 Impulse of 4000mA (4 Amps) on original model.....	95
Chapter 5: CONCLUSION AND FUTURE DEVELOPMENTS.....	96
APPENDIX .....	98
REFERENCES .....	109

## TABLE OF FIGURES

Figure 1. CT Block Diagram .....	9
Figure 2. Anatomy of an X-Ray Tube .....	10
Figure 3. X-Ray Control System .....	19
Figure 4. Model of Existing X-Ray Control System. ....	21
Figure 5. Filament Preheats.....	23
Figure 6. X-Ray Tube Block .....	29
Figure 7. X-Ray Tube Emission Characteristics .....	30
Figure 8. Tube System Model with varying current reference.....	32
Figure 9. Tube Current Reference .....	35
Figure 10. Actual Current of System .....	36
Figure 11. Percentage Error of Static Reference System.....	37
Figure 12. Reference Tube current for dynamic system.....	38
Figure 13. Actual Tube Current of Dynamic System .....	39
Figure 14. Error of System using Dynamic Reference .....	40
Figure 15. Table Showing Comparison of Real System and Simulink Model .....	42
Figure 16. Error of Actual System for static current reference. ....	43
Figure 17. Structure of Fuzzy Controller .....	47
Figure 18. Measurement Setup on Model. ....	48
Figure 19. Error Signal with Dynamic Reference .....	49
Figure 20. Membership Functions of “Error” Input .....	51
Figure 21. “Negative Large” Membership Function Range .....	52
Figure 22. Rate of Change of Error Signal.....	53
Figure 23. “DeltaError” Input.....	54
Figure 24. “Negative Small” Membership Function of “DeltaError” Input .....	55
Figure 25. “ErrorOut” Output of Fuzzy Controller .....	57
Figure 26. “Positive Small” Membership Function of “ErrorOut” Output.....	58
Figure 27. Membership Rules “1 Through 13” .....	60
Figure 28. Membership Rules “13 Through 25” .....	62
Figure 29. Tube Model with Fuzzy Controller.....	63
Figure 30. Surface View of Fuzzy Controller .....	64
Figure 31. Rule viewer during simulation.....	65
Figure 32. Another Rule Viewer Output.....	66
Figure 33. Rule Viewer Output showing multiple rule triggering .....	67
Figure 34. Input Signal to the Fuzzy Logic Controller During Simulation .....	68
Figure 35. Tube Current Reference .....	69
Figure 36. Actual Tube Current of Fuzzy Enhanced Model.....	70
Figure 37. Output of Fuzzy Controller During Simulation.....	71
Figure 38. Correction Signal .....	72
Figure 39. Error of Fuzzy Enhanced System. ....	73
Figure 40. System error for static tube reference. ....	74
Figure 41. Gaussian Membership Functions of “Error” Input. ....	76
Figure 42. Membership Functions of “DeltaError” Input.....	77
Figure 43. Membership Functions of “ErrorOut” Output.....	78

Figure 44. Ruleviewer for simulation with gaussian Membership functions .....	79
Figure 45. Surface view of Fuzzy Controller using Gaussian Membership Functions ....	80
Figure 46. Error of System using Gaussian Membership Functions .....	81
Figure 47. Error at 4 Hertz. ....	82
Figure 48. Original Model Error at 4 Hertz. ....	83
Figure 49. Error at 8 Hertz Reference.....	84
Figure 50. Original Model Error at 8 Hertz .....	85
Figure 51. System Output at 8 Hertz Reference Signal .....	86
Figure 52. Error at 1 Hertz. ....	87
Figure 53. Original System Error at 1 Hertz. ....	88
Figure 54. Setup for noise handling.....	89
Figure 55. Error signal to the controller.....	90
Figure 56. Error of system with 600mA impulse noise .....	91
Figure 57. Error signal to the controller.....	92
Figure 58. Error of system with 2 Amps of impulse noise .....	93
Figure 59. Error of system with 4 Amps of impulse noise. ....	94
Figure 60. Error of original system with 4 Amps of impulse noise. ....	95

## **Chapter 1: INTRODUCTION**

### **1.1 COMPUTED TOMOGRAPHY**

Computed Tomography is a major branch of diagnostic radiology. The term 'Tomography' is derived from the Greek tomos, (ref 14) meaning section. A conventional tomogram is an image of a section of the patient. CT uses a procedure called image reconstruction from projections to produce sharp, clear images of cross-sectional anatomy.

The formation of CT images by a CT scanner involves a three-step process

#### **1. Data Acquisition.**

This refers to the collection of X-Ray transmission measurements from the patient. Once X-Rays have passed through the patient, they fall onto special detectors that measure transmission/attenuation values. Enough transmission measurements (data) must be recorded to meet the requirements of the reconstruction process. The signals from the detectors are then converted into data that the computer can use to process the image.

#### **2. Image reconstruction.**

Once the detectors have collected enough transmission measurements, they are sent to the computer for processing. The computer uses special mathematical techniques to reconstruct the CT image in a finite number of steps called reconstruction algorithms.

#### **3. Image display, manipulation, storage and recording.**

Once the computer has performed the image reconstruction process, the reconstructed image can be displayed and recorded for subsequent viewing

#### **1.1.1 CT SCANNER**

A traditional CT Scanner (*Figure 1*) is primarily made up of an X-Ray tube and its supporting hardware and detectors. When X-Rays pass through the patient, they are

attenuated and subsequently measured by detectors. The X-Ray tube and detectors are hidden inside the gantry (which is the entire frame structure of the CT Scanner- consists of a stationary part fixed to the ground (termed “stator”) and a rotating part (termed “rotor”)) of the scanner. The X-Ray tube is mounted on the rotor, which rotates around the patient during scanning (sometimes stationary scans are also done). The detectors convert the X-Ray photons into electrical signals (analog), which in turn are converted to digital data to input to the computer. The computer then performs image reconstruction on the acquired data.

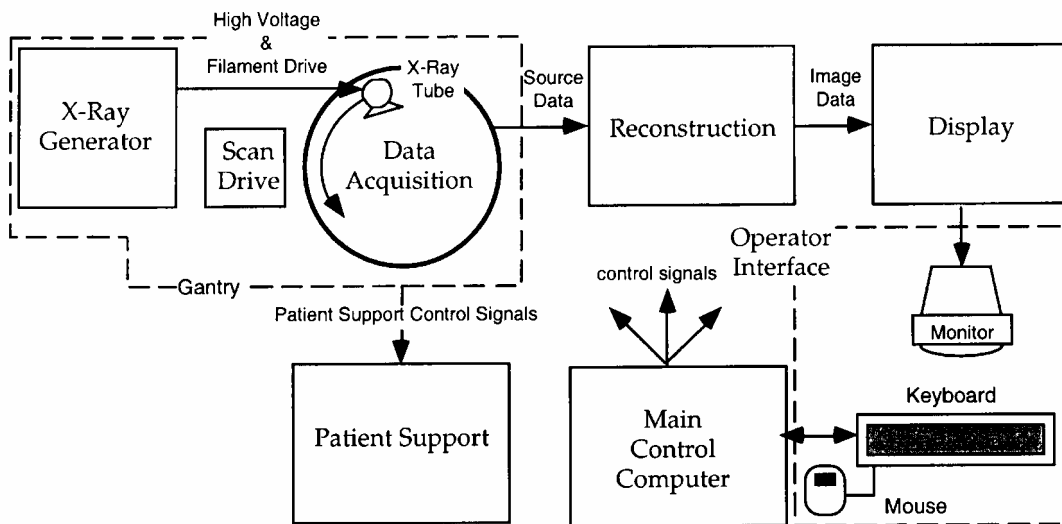


**Figure 1. CT Block Diagram**

The most important unit of a CT scanner is the X-Ray tube, which is the source of X-Rays. A typical X-Ray tube is shown in figure 2.

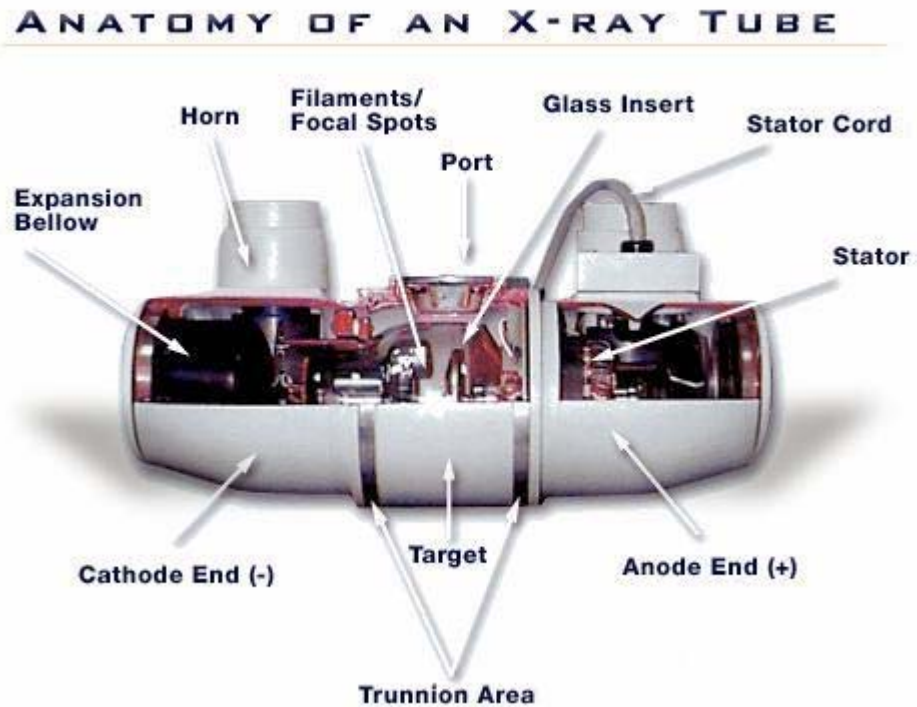


**Figure 2. Anatomy of an X-Ray Tube**

An X-Ray tube consists of a filament cathode and a target anode. A High Voltage (HV) potential of the order of 150 KV is applied across the tube to accelerate electrons emitted by the filament. These electrons hit the target with high impact, which causes the emission of energy in the form of X-Rays. The electron beam energy in these tubes is basically controlled by the potential difference across the tube.

In order to obtain better control over the width of the electron beam, two plates are placed along the cathode assembly of the tube to which a potential is applied. These plates are called Grids. By applying varying negative potentials to the grid the shape of the electron beam can be altered. The potential applied creates an electric field, which has an inward pressing or squeezing effect on the electron beam. By controlling the electron beam in

this way it is possible to control the intensity, focusing area or density of X-Rays generated by the tube.

Alternately, in some scanners, there are 2 different filaments (small and large), which perform the same function of achieving differences in the shape and size of the electron beam.

### **1.1.2 Dose Modulation**

So far in Computed Tomography, the patient has been radiated with a constant amount of radiation during a scanning cycle. Patient dose values in CT are relatively high when compared to standard radiological exams. Because of their increasingly frequent use, CT examinations contribute a substantial portion to the total radiation exposure to the patient [ref 13]. Dose reduction has always been a major concern for medical and health physicists. Several investigators have suggested reducing patient dose by simply lowering tube current. This approach increases image noise, which often deteriorates low contrast detectability.

A more sophisticated method adapts the tube current to X-Ray attenuation as it changes with projection angle. The basic idea is to lower tube current only for projections associated with low attenuation.

The tube current is controlled by the current in the filament, which determines the heat produced in the filament, which in turn determines emission (number) of electrons in the tube. The actual tube current includes those electrons that are emitted from the cathode/filament and pass into the anode/target. A few of the emitted electrons do not reach the anode and do not constitute tube current.

In order to achieve dose modulation, the control system modulates the filament current in accordance with the required tube current. It must be noted that the relation between tube current and filament current is highly nonlinear. Thus the Simulink model used in this

thesis makes use of a look up table with actual values of filament current required to achieve particular tube currents. It should be noted that the real system also uses this look up table (in control software) approach to minimize starting error. This shall be discussed in detail when the model is presented.

## **1.2 LITERATURE REVIEW**

Fuzzy logic, invented by Professor Lotfi Zadeh of UC-Berkeley in the mid-1960s, provides a representation scheme and a calculus for dealing with vague or uncertain concepts [ref 16]. It provides for the facile manipulation of such terms as "large," "warm," and "fast," which can simultaneously be seen to belong partially to two or more different, contradictory sets of values. Zadeh originally devised the technique as a means for solving problems in the soft sciences, particularly those that involved interactions between humans, and/or between humans and machines. Within the United States, with some exceptions, the technique had remained mainly of basic research interest for a long time until the 90's.

The situation in Japan was quite different. Professor Toshiro Terano of Hosei University, inspired by Zadeh's work, introduced the idea to the Japanese research community in about 1972. Perhaps because of a Japanese cultural view of the vagueness of human nature (all concepts belonging partially to contradictory sets), there was almost immediate enthusiasm for the idea. This led to active research and a host of commercial applications, almost entirely in the area of physical systems control. The currently fielded applications range from large-scale electro-mechanical processes, like subway systems and elevators, to mass-market consumer applications like camcorder focus or smooth operation of automobile cruise controls. It is interesting to note that the actual applications of fuzzy logic are far afield from Zadeh's original notion of help for the soft sciences. It is estimated that there are well over 200 (as of May 1993, ref 16) fuzzy control systems in fully fielded use, and there are more than 2,000 engineers in the Japanese Fuzzy Control Society. Over the years, especially in the 90's, fuzzy logic has found immense applications in a large spectrum of fields. Since this thesis deals with an

application in a medical field, let us look at abstracts of some medical applications of Fuzzy Logic.

For example, Ref 1 is a survey dealing with the use of fuzzy logic to replicate the human minds capability to use approximate data to extract meaningful information from massive data, and produce crisp solutions. In practice, a precise model may not exist for biological systems or it may be too difficult to model. In these cases fuzzy logic is considered as an appropriate tool for modeling and control, since our knowledge and experience are directly contained and presented in control strategies without explicit mathematical models. This paper (ref 1) surveys the utilization of fuzzy logic in medical sciences, with an analysis of its possible future penetration.

Ref 2 is a discussion on the use of fuzzy logic to extract a blood vessel in a CT image. This paper proposes a method for segmenting the cerebrovascular region from the Computed Tomography angiography (CTA) images. The proposed method first derives a rough image by combining a raw image and the difference image. The difference image is obtained by applying a Laplacian filter. For the rough image, the venae and arteries are segmented by fuzzy inference. The experimental result shows that this method can extract the blood vessels in CTA images with high accuracy.

Ref 3 presents a novel approach for fully automated boundary extraction and rectification of bony tissue from planar CT data. The approach extracts and rectifies the feature boundary in a hierarchical fashion. It consists of a fuzzy multilevel threshold operation, followed by a small void cleanup procedure. Then a binary morphological boundary detector is applied to extract the boundary. Two innovative anatomical knowledge based algorithms are used to remove the undesired structures and refine the erroneous boundary. Results of applying the approach on lumbar CT images are presented, with a discussion of the potential for clinical application of the approach.

Ref 4 is similar to ref 2 since it presents another image segmentation application of fuzzy logic, this time to an MR (magnetic resonance) image. In this paper, an automated

segmentation and lesion detection algorithm are proposed for axial MR brain images. The proposed segmentation algorithm consists of two steps in order to reduce computation time for classifying tissues. In the first step, the cerebrum region is extracted by using thresholding, morphological operation, and labeling algorithm. In the second step, white matter, gray matter, and cerebrospinal fluid in the cerebrum are detected using fuzzy C-means (FCM) algorithm.

Ref 5 proposes a fuzzy expert system scheme for 3D CT foot image segmentation. The method aims at segmenting a fractured foot bone into ossa (bone) and fractions, as a framework for developing a computer-aided orthopedic surgery system. It employs fuzzy knowledge representation to express the surgeons' knowledge: this includes knowledge of the distance (to extract the fractions) and knowledge of the intensity distribution (to decompose ossa on facies articularis). Their knowledge, which is evaluated in the segmentation procedure, is totally compiled. Qualitative evaluation by a medical doctor shows that this method can correctly segment their ossa and fractions.

Ref 6 describes useful fuzzy logic techniques for medical image segmentation. Specific methods reviewed include fuzzy information granulation, fuzzy inference and fuzzy cluster identification. Fuzzy information granulation is introduced as a powerful scheme to find the thresholds to obtain the whole brain region in MR data. A fuzzy inference technique succeeds in segmenting the brain region into the left cerebral hemisphere, right cerebral hemisphere, cerebellum and brain stem. The fuzzy inference aided segmentation procedure is also useful for human foot CT images as reviewed earlier in ref 5.

Ref 7 presents an automated, knowledge-based method for segmenting chest Computed Tomography (CT) datasets. Knowledge is represented at a high level using an explicit anatomical model. The model is stored in a frame-based semantic network and anatomical variability is incorporated using fuzzy sets. An inference engine uses fuzzy logic to match image to model objects based on the feature constraints. Strict separation of model and image domains allows for systematic extension of the knowledge base. In

preliminary experiments, the method has been applied to a small number of thoracic CT datasets.

In Ref 8 the authors offer an alternative to the manual editing that is commonly used to remove clutter due to artifacts in MR and CT images. The method utilizes recently developed fuzzy connected object delineation algorithms to extract the vessels of interest. Since the resulting definition is nonbinary, it can be displayed via MIP or more sophisticated volume rendering.

In Ref 9, a rule-based approach to the labeling of computed Tomography (CT) head images containing intracerebral brain hemorrhage (ICH) is presented. Fully automated segmentation of CT images is achieved by the method composed of two components: an unsupervised fuzzy clustering and a rule-based labeling. The unsupervised fuzzy clustering algorithm outlines the regions in the input CT head image. Region features and region-neighborhood relations are used to create the knowledge base for the rule-based system. The method has been applied to a number of real CT head images and has shown satisfactory results.

In Ref 10, a neuro-fuzzy approach to computerized Tomography (CT) for the reconstruction of smooth distribution of some material parameters is proposed. The performance of the method is tested using computer generated data and experimental data collected by seismic probing. The tomographic images of time-of-flight information agreed with previously available borehole logs information.

In Ref 11, the authors present their endeavors to segment some cross-sections of the human brain obtained from the two modalities-X-Ray Computed Tomography (CT) and magnetic resonance imaging (MRI), using the fuzzy C-means technique developed by Bezdek. The two advantages of the technique are that it is unsupervised and is robust to missing and noisy data. Attempts at integrating the images from these two modalities are also mentioned.

Ref 12 describes a knowledge-based image interpretation system for the segmentation and labeling of a series of 2-D brain X-Ray CT-scans, parallel to the orbito-meatal plane. The system combines the image primitive information produced by different low-level vision techniques in order to improve the reliability of the segmentation and the image interpretation. The linguistic variables, introduced to describe the prepositional features of the brain model, are defined by fuzzy membership functions. Procedural knowledge has been integrated into different knowledge sources. Experimental results illustrate the reliability and robustness of the system against small variations in slice orientation and interpatient variability in the images.

### **1.3 THESIS CONTRIBUTION**

As we have seen from the above literature reviews, there have been extensive applications of fuzzy logic in the medical field. The majority of these applications have been in handling and manipulation of image data, with very few applications being implemented in the electronics of the medical systems. The purpose of this thesis work has been to apply the principles of fuzzy logic control to enhance the emission control system of an X ray tube for applications in a CT scanner. I use a fuzzy logic controller to implement dose modulation (variable tube current) in a Simulink model of an X Ray tube system. The existing system, whose modeling in Simulink comprised a major portion of the thesis work, shows relatively less accuracy than that with the enhanced fuzzy control model. This improvement in accuracy is beneficial and advantageous in numerous ways:

- 1) There is better control of radiation dose to the patient, thus reducing risks of radiation related ailments like cancer.
- 2) Longer life of the X-Ray Tube, since higher current in the X-Ray Tube affects the life of the filament, thus resulting in cost savings.
- 3) Better quality of images obtained from the CT Scans, as dose modulation optimizes the quantity of radiation required for different views of the body.

The results of the simulation will be discussed.

Chapter 2 presents the development of a Simulink model of the X-Ray system as it exists in the CT system now. The purpose of each block is described in detail and the simulation results are shown to prove the closeness of the model to the real system. I have also shown the same model with a variation of tube reference to emphasize the loss of accuracy in dynamic conditions.

Chapter 3 explains my design of the controller to improve system performance. There is a discussion of the selection of membership functions for the fuzzy logic controller and simulation of the enhanced model. The simulation of the model with the fuzzy controller block is also presented and its results are shown.

Chapter 4 introduces modifications to the fuzzy design and also shows simulations with variation of parameters. It compares the simulation results of the old and the new design. The system is then subjected to noise impulses of high magnitude to simulate real life noise conditions. It is found to be extremely robust to this noise.

Chapter 5 will convey the achievements of the research and design covered here and will talk about further applications and enhancements of this thesis work.

## **Chapter 2: SYSTEM MODELING AND SIMULATION**

A new control method is needed for varying power applications as applied to an X-Ray tube in CT scanners. The emission control system of an X-Ray tube is highly nonlinear and is typically linearized about an operating point for constant power applications. There exists a need to vary the power over a large range and it is necessary for the control loop to be dynamic. The control loop will be implemented using a combination of fuzzy logic and conventional control methods. I have developed a model of the existent control loop, which was originally designed for only static power applications, and have augmented the loop with a fuzzy logic controller to enhance performance for dynamic conditions. The original model will be explained in this chapter and the new designs will be covered in subsequent chapters.

The first step in designing a controller is to mathematically model the system characteristics of the plant that is to be controlled. The mathematical model of the plant contains all of the plant characteristics with the most important being the overall input – output relationship of the system. Plant modeling is necessary for an effective and robust controller to be designed. A model of a plant allows the designer to test and tune different control schemes in computer simulation without putting the actual plant at risk because of errors in controller design.

## 2.1 X-RAY CONTROL SYSTEM

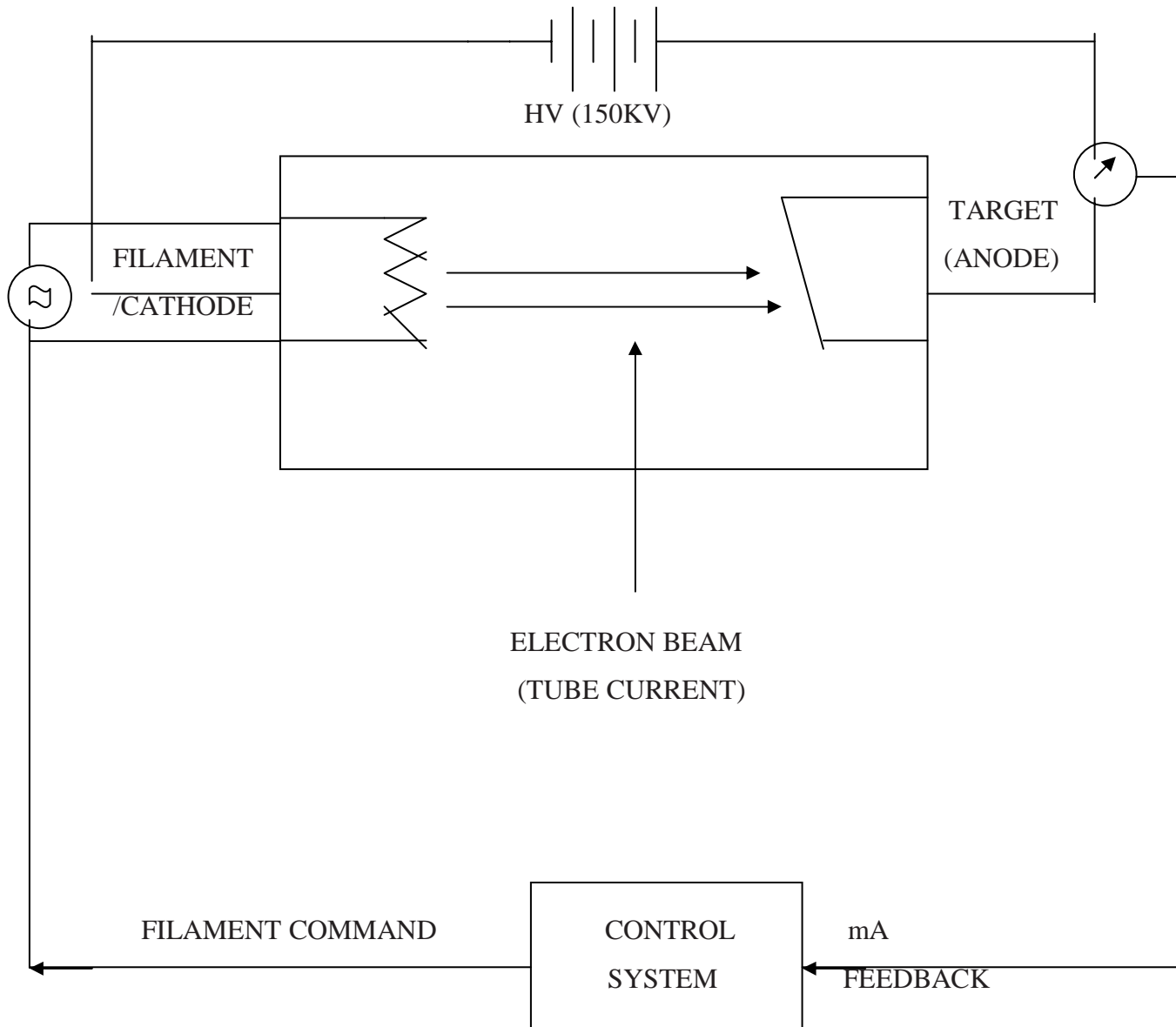
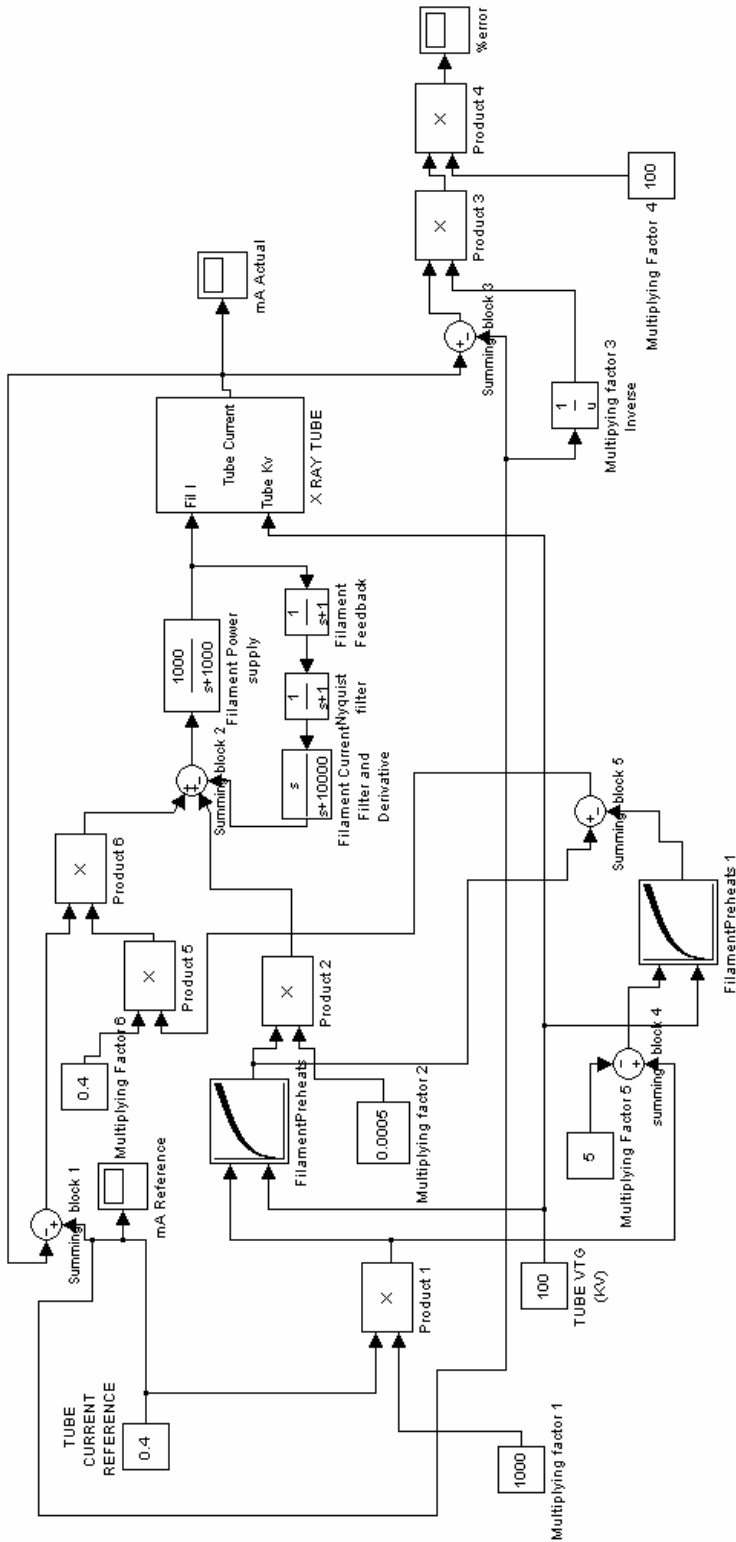


**Figure 3. X-Ray Control System**

The X-Ray system of a CT scanner is shown in *Figure 3*. It shows an X-Ray tube consisting of a cathode, which is the filament and an anode, which serves as the target for the electron beam. An HV potential of the order of 150 KV is applied across the tube to

accelerate electrons emitted by the filament. These electrons hit the target with high impact, which results in generation of X-Rays. The tube current is defined as the electron flow between the anode and the cathode. The tube current therefore depends on the electron emission from the filament, which in turn is dependent on the level of heating of the filament. The current flowing through the filament decides its degree of heat. Thus, controlling the current flowing through the filament can control the tube current. The filament current – tube current relationship, being decided by thermal characteristics, is nonlinear and is also dependent on the potential applied across the tube. This relationship can be seen in the tube emission characteristics graph shown in *figure 7*.

The entire control loop of the X-Ray system is therefore centered on controlling the filament current. The system feeds back the measured tube current, which is used by the controller to determine the required value of filament current. Depicted in the Simulink model is the control system for an X-Ray tube (ref 19), as it exists on Marconi Medical Systems PQ Series of CT Scanners (PQ 2000, PQ 5000, PQ 6000).



Simulink Model of X-Ray Control System (static mA)

Figure 4.

Figure 4. Model of Existing X-Ray Control System.

## **2.2 EXPLANATION OF BLOCKS IN MODEL**

### **2.2.1 Simulink Model 1**

The block of the model (*Figure 4*) depicts the logic of the real system. In the Q series of scanners, this system is implemented in a control box called the XSC + (X-Ray System Control). The heart of this controller is the Motorola 68332 MicroController, where the entire control loop is implemented in code. The filter functions of the systems are implemented in a Digital Signal Processor, the Analog Devices DSP 2105. The Anti Aliasing filters are implemented in hardware. The Tube and Filament current feedback information is received from vendor hardware (High Voltage Generators). Also the filament power supply is provided in the generator

#### **Tube Current Reference**

The desired value of tube current is set in this block. It is a constant value block, so the reference has to be changed manually by the user. In the real system as well, either the user sets the tube reference directly or the imaging selections made result in automatic selection of current reference through parameter selections of software.

#### **Multiplying factor 1 and Product 1**

These blocks convert the tube current reference, which is set by the user in Amps, into milliamps by multiplying by 1000. Even though our final output of interest is in standard units of Amps, some blocks require unit conversions for their internal use. For example, we are doing this particular conversion into milliamps because the next block, which is a look-up table, has data in these units.

In the real system, this is done in micro controller software.

#### **Filament Preheats**

This a look up table which selects default filament current values corresponding to the Tube current reference and Tube voltage reference selections. As the name suggests, this table provides filament current values to heat/preheat the filament to a temperature as

close to the required heat value as possible. The purpose of this table is to provide the filament power supply with the closest starting value of filament current to that that will be required to produce the selected outputs. This helps to minimize the change in filament current when the feedback control loop closes once the system is activated. It also causes the control loop to stabilize faster since the error signal produced in the loop is low from the start. A large value of filament current is detrimental to the life of the filament due to over heating, therefore making it important that the transient response of the filament is well controlled.

This method of applying a default preheat is used in real systems where the filament preheats are set by software according to the parameter selections made by the user. Preheat tables similar to the one used in the model are used, depending on the characteristics of the tube and generators.

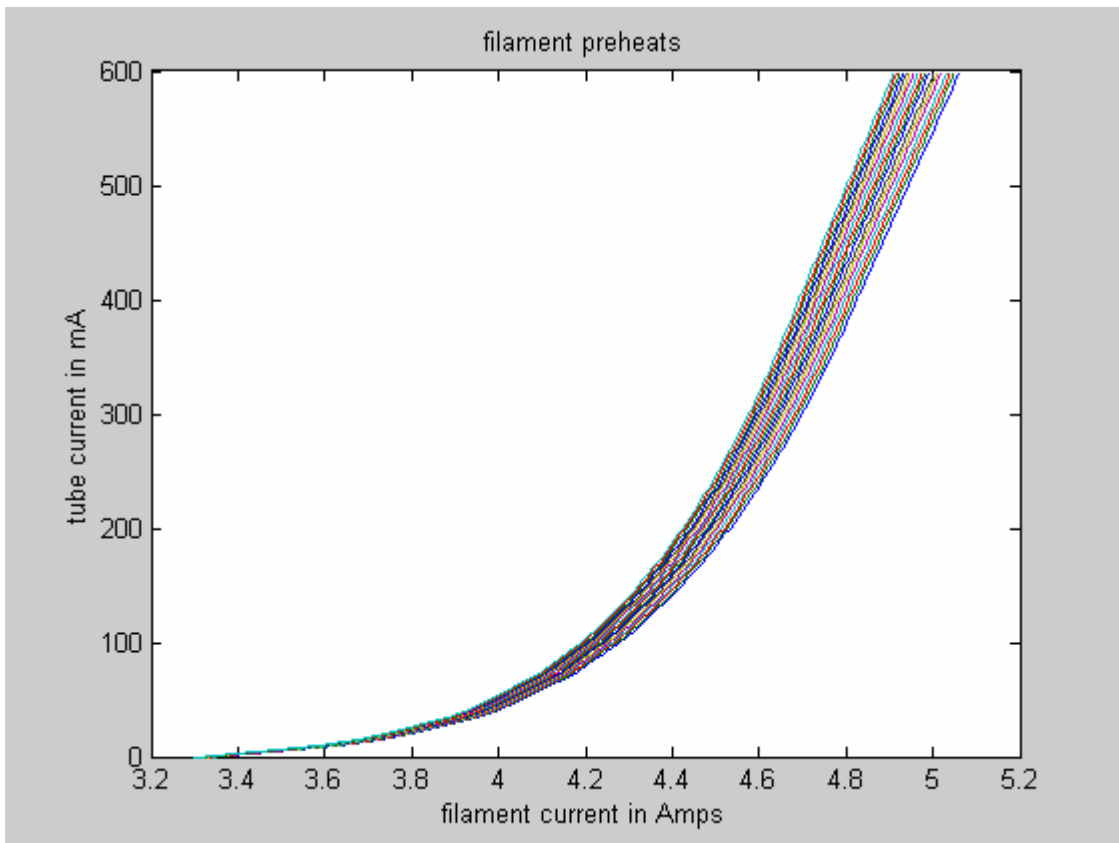


**Figure 5. Filament Preheats**

A plot of the look-up table in *figure 5* shows the preheat values for various values of KV and Tube Current selections (Characteristics are shown for KV Values ranging from 80KV to 165 KV in steps of 5 KV, which explains the band like appearance in the plot). In the plot, we can also see that the filament current does not go to zero even for a zero value of tube current. This is because a standby current of approximately 2 Amps is maintained in the filament when the system is powered 'On' even when X-Rays are not being made. This is also done to prevent sudden inrush of current into the filament, which could affect its life.

NOTE: The immense importance given to the life of a filament should be noted because the filament is the heart of the X-Ray tube. Any damage inflicted to the filament, causes irreparable damage to the functioning of the tube and therefore the production of X-Rays. So one can say that the life of the X-Ray tube is defined by the life of its filament.

### **Multiplying factor 2 and Product 2**

This is another conversion of units scheme. The output values of the preheat table are in (filament ma)\*2 since the preheat DAC has 0.5 ma steps. Therefore to convert to Amps we have to divide by 2000 or multiply by 1/2000 (0.0005).

In the real system, this is done in micro controller software.

### **Summing Block 1**

This block generates the error signal of the system. The actual mA (tube current) is subtracted from the desired value (tube reference) and serves as a control signal to the system.

In the real system, this is done in micro controller software.

### **Gain Calculation**

This involves a function (in the real system is implemented in software) which, using the set points of KV and tube current reference calculates and returns a value of gain which, when implemented in the feedback, maintains a loop gain of 400. This value of 400 was

empirically found (by the designers of the feedback loop in 1988, ref 19) to be the most effective loop gain to maintain the stability of the system.

The formula for calculation of the gain 'K' is as follows

$$K = \text{DESIRED GAIN} / (\text{Tube Gain} * \text{Controller Static Gain} * \text{Generator Gain})$$

Where:

Tube Gain = DELTA tube current / DELTA FILAMENT (This is essentially the only calculation in the gain equation. It represents the slope of the graph of the tube characteristics (filament preheats) at different set points. The other elements in the equation are all constant values determined by system requirements and feedback circuit electronics)

$$\text{DELTA FILAMENT} = \text{FIL2} - \text{FIL1}$$

This is the difference in the preheat values of filament current for a change in tube current of 5 mA.

$$\text{Controller static Gain} = 10$$

$$\text{Generator Gain} = 20$$

$$\text{DELTA tube current} = 5 \text{ mA}$$

$$\text{DESIRED GAIN} = 400$$

Substituting the above constants in the equation for "K"

$$K = 400 / (\text{Tube Gain} * 10 * 20)$$

$$= 400 / (\text{Tube Gain} * 200)$$

$$= 2 / \text{Tube Gain}$$

$$= 2 / (\text{DELTA TUBE CURRENT} / \text{DELTA FILAMENT})$$

$$= 2 / (5 / \text{DELTA FILAMENT})$$

=0.4 \* DELTA FILAMENT

This final equation is the one implemented in the Simulink block. The delta filament is simply the difference in filament current for a corresponding change of 5 mA in tube current.

This calculation is implemented using the following blocks:

#### **Multiplying Factor 5 and Summing block 4**

These are used to subtract 5 mA from the reference value. So this provides the value of the lower filament current on the slope of the mA –Filament current graph.

#### **Filament Preheats 1**

This is the same filament preheat table as that used earlier. The only difference here being the different selection made using a lower value of tube current reference. So the selection inputs to the look-up table are:

Tube reference (in mA) – 5 mA

Tube Voltage (KV reference) – same as the one selected earlier.

#### **Summing block 5**

The DELTA FILAMENT value is calculated here i.e. the difference in filament current corresponding to a 5 mA change in tube current (in the block it is the difference between the outputs of the filament preheats and filament preheats 2 blocks).

#### **Multiplying Factor 6 and Product 5**

These represent the final calculation of the gain equation (i.e. 0.4 \* DELTA FILAMENT)

#### **Product 6**

The error signal is multiplied by the calculated gain of the system here (i.e. the gain is applied at this block to the loop)

## **Summing block 2**

The error signal (with gain) and filament preheat value are summed here. Depending on whether the error is positive or negative, the filament current value is increased or decreased respectively. The third signal entering this block is the derivative of the filament current control signal going to the X Ray tube block. This signal is being subtracted at this point to ensure that the change in filament current does not occur at a very rapid rate. So if the derivative is high or low (filament current changing rapidly or slowly), the loop maintains the change to a slow rate.

## **Filament Power Supply**

In the X Ray system, the loop feeds the control signal to the filament power supply, which is the driving unit of the filament. This power supply uses the control signal to generate the filament current desired. Its transfer function was observed to be similar to a filter as shown in the block, with a bandwidth of about 1 kHz and a gain approximately equal to 1.

In the real system, this is done in generator hardware.

## **Filament feedback**

This block accounts for the time constant of the feedback circuit.

## **Nyquist filter**

There is a filter to reduce aliasing of ripple and noise frequencies in the feedback signal, to ensure faithful representation of the feedback signal.

In the real system, this is done in DSP software.

## **Filament Current Filter and Derivative**

This is represented by a transfer function instead of a derivative block because a pure derivative block cannot be realized in real life. This is because as frequency increases to a very high value, the system will cease to respond (its gain will become zero). Therefore, I have used a transfer function as shown in the block to provide a derivative of the signal.

In the real system, this is done in DSP software.

Thus the control signal in the form of the filament current and the user selected tube voltage (KV) enter the X Ray Tube Sub-Block, which produces the tube current values corresponding to the 2 selection signals.

### **Summing Block 3**

This is an extra block for calculating the error of the system to view simulation results. The difference of the actual output of the tube and the desired output (reference tube current) is calculated at this block. Please note that the output of this block is the same as the output of summing block 1. It is repeated here just to perform some additional calculations to find the error of the system as a percentage of the reference. In the real system, this is done in controller software.

### **Multiplying factor 3 and Product 3**

Taking the error of the system and dividing by the desired output (multiplying by its inverse) gives the error as a fraction of the reference. The output of the Product 3 block is therefore

$$= \frac{\text{Desired output} - \text{Actual output}}{\text{Desired output}}$$

### **Multiplying factor 4 and Product 4**

These are used to convert the above error figure to a percentage value.

### **mA Reference, mA Actual and % error**

These are 3 scope blocks of Simulink, which allow us to view the model simulation in real time.

## 2.2.2 X Ray Tube Sub-Block

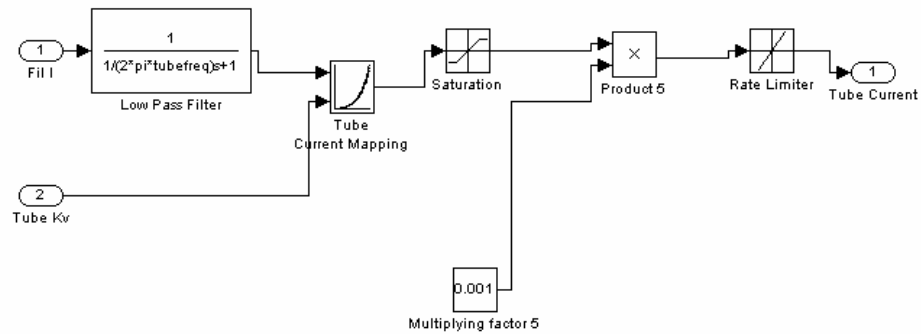


**Figure 6. X-Ray Tube Block**

### Low Pass Filter

Since when the filament current is changed by a certain amount, an equivalent change in its thermal emission has a certain time delay, I have added a low pass filter with a cutoff frequency of 2 Hz which very closely represents the time constant of the filament.

### Tube Current Mapping

The tube is essentially modeled using a look up table that contains actual measured data values of filament current and tube current. We select the filament current and tube voltage (KV) values and the look up table provides the corresponding tube current values.

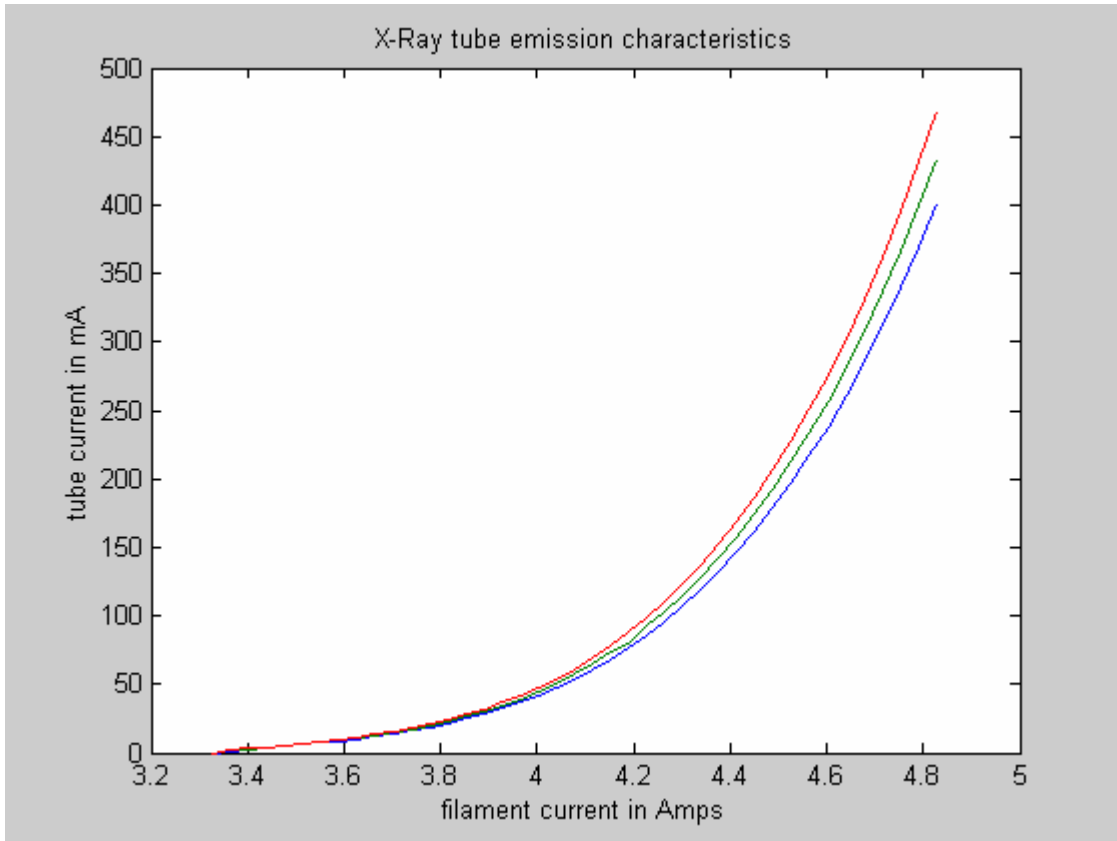


**Figure 7. X-Ray Tube Emission Characteristics**

### **Saturation Block**

Coming out of the look-up table is a saturation limit block. I have set an upper limit of saturation of a constant value of 500 and a lower limit of 0. The value of 500 was chosen because we do not want the tube to run at over 500 mA of current. This is actually a limit imposed by the capabilities of the X –Ray tube and its high voltage power supply (generator). The look up table does not have current values of over this value (500), but the Simulink software interpolates by itself if it receives values that are not defined in the row and column selections and produces outputs corresponding to the characteristics of the table. In the case where the user inputs a reference beyond the capability of the system, the saturation block serves as a safety element to limit this current output. The lower value of 0 is included because the flow of current is in one direction only (no negative current).

In the real system, this is done in micro controller software.

**Multiplying factor 5 and Product 5**

These are used to simply convert the output of the look-up table, which is in milliamps, into the standard unit being used for the reference, which is in Amps.

**Rate Limiter**

Here I have set the rising slew rate limit to 3.5 and the falling slew rate limit to – 4.5. This is a rate limiting for change of tube current. This comes into use in the case of varying tube mA reference. It represents maximum rate of change of tube current that is expected within our limits of operation of the tube.



### **2.2.3 Simulink Model 2**

This is the same as the first model, with an added block to vary the tube reference sinusoidally. (*Figure 8*)

Please note that all the blocks related to dynamic tube current (dose variation) do not exist on the real system yet. It is a new requirement, which will be implemented over the next few design modifications.

#### **Dose Variation**

This is a sinusoidal wave block to superimpose a variation on the tube current reference. I have set the amplitude to 0.1 Amps (100 milliamps). This will be the maximum amplitude of variation of the reference in both the positive and negative direction. The block has a programmable frequency of output. In our application we will be varying the frequency to a maximum of 4 Hz. This is the maximum requirement of dose modulation in imaging applications so far.

#### **Summing block 4**

We add the sinusoidal variation to the tube current reference at this block. The output of this block is therefore a sinusoidal output riding on a dc level set in the tube current reference block.

## **2.3 HISTORICAL PERSPECTIVE**

The above Control System for the tube current in an X-Ray Tube first came about with the invention of the concept of the tube current control loop by Ted Resnick (ref 19) in 1978 at Picker International, Cleveland, Ohio. At that time this was implemented fully in hardware in what was internally called the “Big Shot Generator” and used on Picker’s SX 600 and SX 1200 CT Scanners. An application for a patent was made sometime prior to 1980.

This design went through many stages of evolution, with patents being issued in the early '80,s for the hardware version, to a partial implementation of tube heat calculations in a Microprocessor soon afterwards. The next version, which had a patent issued in 1988(ref 19), used an Analog devices DSP chip to implement filter functions, and the control loop was implemented in code in a Motorola 68332 microcontroller. This design was being used till very recently. At present, there is a new development to implement this loop in more modern Microcontrollers like the MPC 555. So from 1978 till 2001 this design went from full implementation in hardware, to partial software implementation using a 68,000 family Microprocessor, to a combination of implementation in a micro controller and DSP, to the latest implementation in high-speed micro controllers and DSP chips.

Even through all these evolutions of this system over the years, the fundamental concept of control has remained the same; only implementation methods have changed. This concept is what has been implemented in the Simulink model in this thesis. It is also possible that the next iteration in this evolution process will implement the fuzzy logic design proposed in this thesis.

## 2.4 SIMULATION RESULTS

### 2.4.1 Static mA

Setting reference to 400mA (0.4A) and running the Simulink model for 3 seconds (*figure 9*). We can see the constant reference over the simulation period.

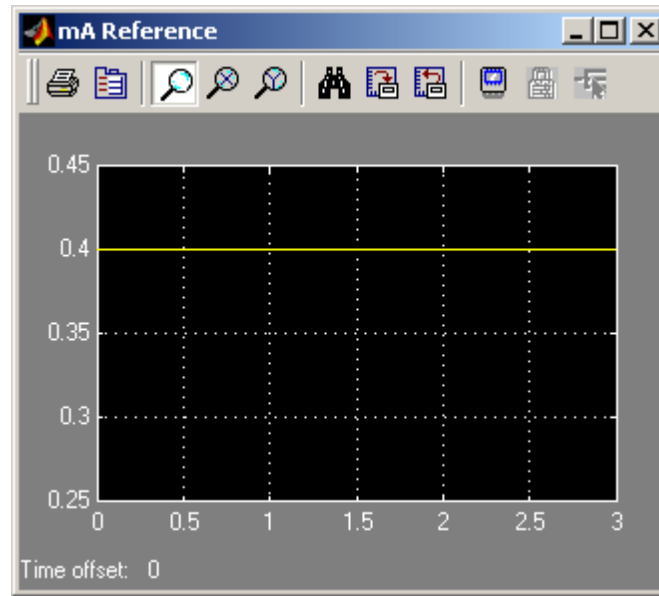


**Figure 9. Tube Current Reference**

Vertical Axis shows current in Amps.  
Horizontal Axis shows time in Seconds.

### 2.4.2 Output of the system

The actual tube current of system when a constant reference of 0.4 A is applied (*Figure 10*)

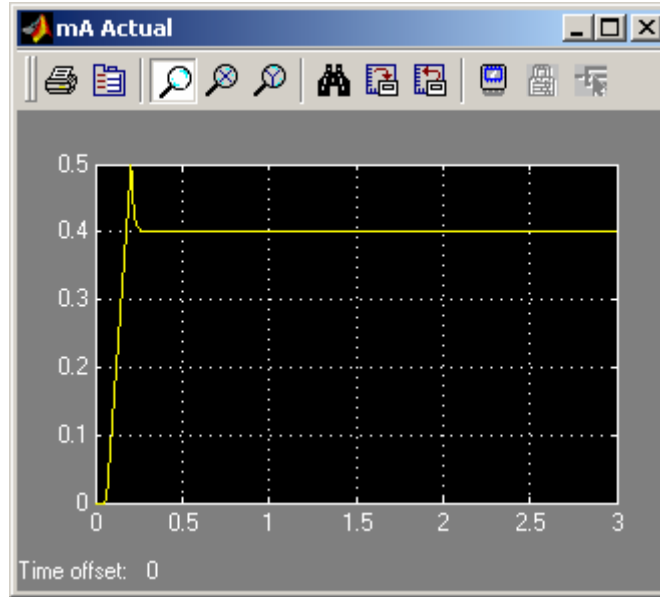


**Figure 10. Actual Current of System**

Vertical Axis shows current in Amps.  
Horizontal Axis shows time in Seconds.

### 2.4.3 Percentage Error between reference and actual output of system

Note how small the value of error is after the system stabilizes (*Figure 11*) In fact the error is almost zero in this case. This shows the faithful tracking of the control system.

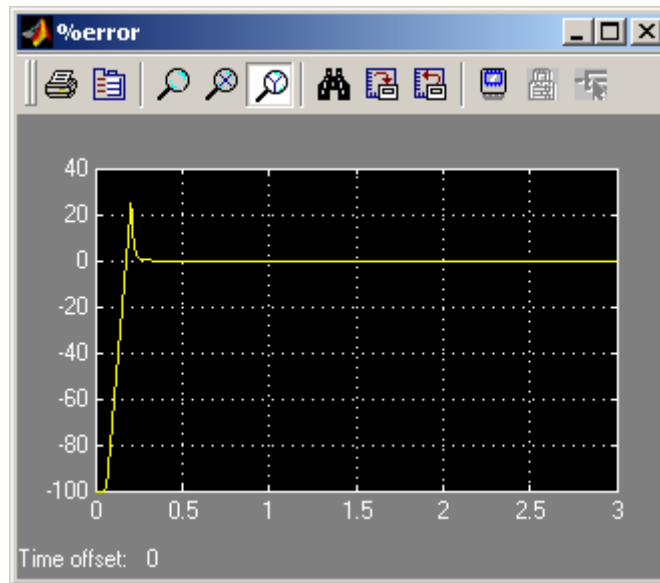


**Figure 11. Percentage Error of Static Reference System**

Vertical Axis shows Percentage error.  
Horizontal Axis shows time in Seconds.

#### 2.4.4 Dynamic mA

Setting reference to 400 mA and adding a sine wave with amplitude of 100 mA (0.1 A). So the reference is being varied by 100mA about the 400mA DC value. The graph in *Figure 12* shows the total reference varying between 0.3 Amps and 0.5 Amps.

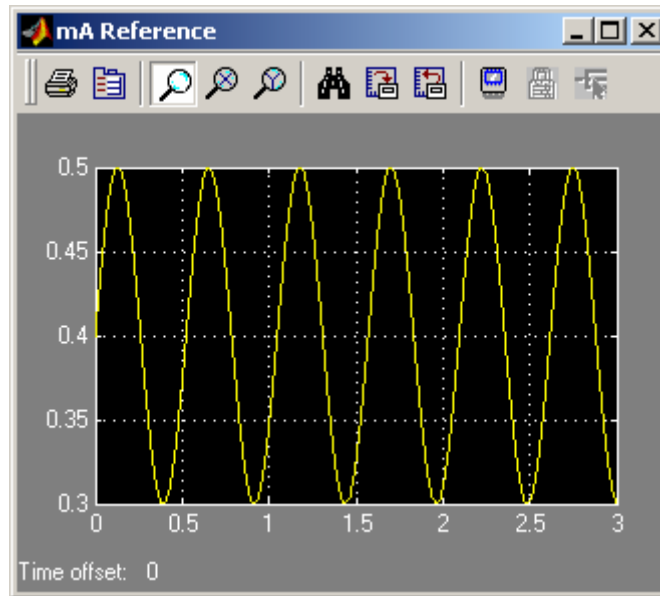


**Figure 12. Reference Tube current for dynamic system**

Vertical Axis shows current in Amps.  
Horizontal Axis shows time in Seconds.

## 2.4.5 Output of the Dynamic system

The actual current of the tube when a sinusoidal reference is applied (*Figure 13.*)

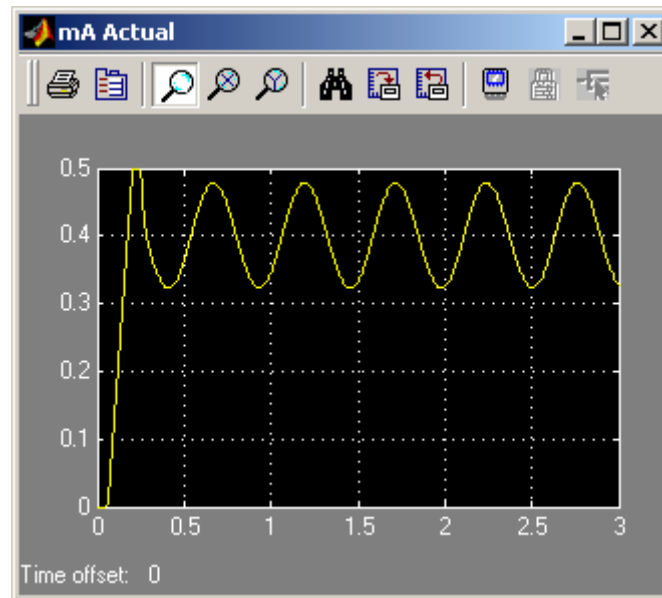


**Figure 13. Actual Tube Current of Dynamic System**

Vertical Axis shows current in Amps.  
Horizontal Axis shows time in Seconds.

## 2.4.6 Percentage Error between reference and actual output of the system

Note the magnitude of error in this case (*Figure 14.*) It varies between approximately 6 % on the negative end and almost 9% on the positive end. This is a high error value as compared to the static system, which had an error closer to zero. This is because the control system for the X-Ray tube had been designed only for static systems. It will need to be modified and enhanced for dynamic performance.

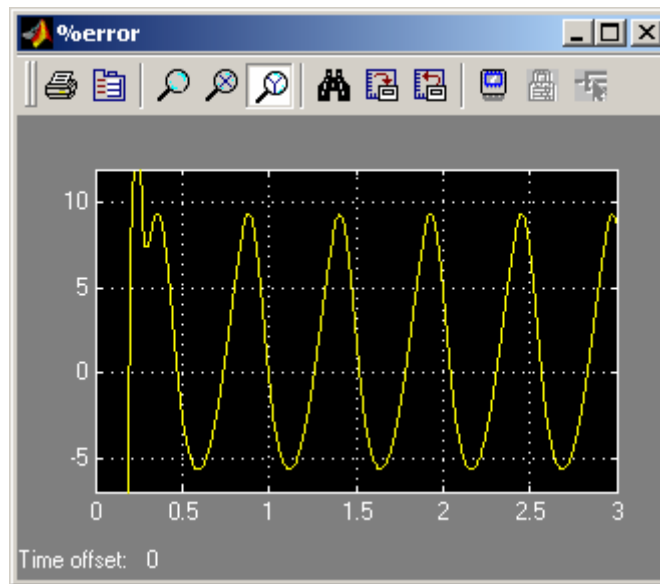


**Figure 14. Error of System using Dynamic Reference**

Vertical Axis shows Percentage error.  
Horizontal Axis shows time in Seconds.

The subsequent chapter deals with a modification/enhancement in the control system to improve performance for dynamic mA. This is because an error of this magnitude will not serve the purpose of dose modulation, which is to optimize the level of radiation according to imaging requirements. It will result in image artifacts. Therefore, there is a need to minimize this error for the dynamic situation.

## 2.5 SYSTEM VERIFICATION

The model using non-varying reference for tube current was compared with results obtained from a real X-Ray system. The results of the simulation and measured outputs were as shown in *figure 15*. It verifies that the Simulink model is a very close representation of the actual system.

FIXED Current(mA) Reference

Ref (mA)	Measured Voltage (1V/80mA)	measured anode ma (mA)	measured Anode ma (amps)	model anode ma (amps)	model anode ma (mA)	error(A) b/w sys and model	error(mA) b/w sys and model	error in amps	%error
<b>80KV</b>									
100	1.23	98.4	0.0984	0.1	100	-0.0016	-1.6	-0.0016	-1.6
150	1.88	150.4	0.1504	0.15	150	0.0004	0.4	0.0004	0.266667
200	2.504	200.32	0.20032	0.2	200	0.00032	0.32	0.00032	0.16
250	3.127	250.16	0.25016	0.25	250	0.00016	0.16	0.00016	0.064
300	3.732	298.56	0.29856	0.3	300	-0.00144	-1.44	-0.00144	-0.48
350	4.355	348.4	0.3484	0.35	350	-0.0016	-1.6	-0.0016	-0.45714
400	4.987	398.96	0.39896	0.4	400	-0.00104	-1.04	-0.00104	-0.26
450	5.621	449.68	0.44968	0.45	450	-0.00032	-0.32	-0.00032	-0.07111
500	6.264	501.12	0.50112	0.5	500	0.00112	1.12	0.00112	0.224
					0		0	0	
<b>100KV</b>									
100	1.229	98.32	0.09832	0.1	100	-0.00168	-1.68	-0.00168	-1.68
150	1.872	149.76	0.14976	0.15	150	-0.00024	-0.24	-0.00024	-0.16
200	2.512	200.96	0.20096	0.2	200	0.00096	0.96	0.00096	0.48
250	3.127	250.16	0.25016	0.25	250	0.00016	0.16	0.00016	0.064
300	3.73	298.4	0.2984	0.3	300	-0.0016	-1.6	-0.0016	-0.53333
350	4.349	347.92	0.34792	0.35	350	-0.00208	-2.08	-0.00208	-0.59429
400	4.984	398.72	0.39872	0.4	400	-0.00128	-1.28	-0.00128	-0.32
450	5.621	449.68	0.44968	0.45	450	-0.00032	-0.32	-0.00032	-0.07111
500	6.264	501.12	0.50112	0.5	500	0.00112	1.12	0.00112	0.224
<b>120KV</b>									
100	1.229	98.32	0.09832	0.1	100	-0.00168	-1.68	-0.00168	-1.68
150	1.867	149.36	0.14936	0.15	150	-0.00064	-0.64	-0.00064	-0.42667
200	2.527	202.16	0.20216	0.2	200	0.00216	2.16	0.00216	1.08
250	3.124	249.92	0.24992	0.25	250	-8E-05	-0.08	-8E-05	-0.032
300	3.729	298.32	0.29832	0.3	300	-0.00168	-1.68	-0.00168	-0.56
350	4.345	347.6	0.3476	0.35	350	-0.0024	-2.4	-0.0024	-0.68571
400	4.997	399.76	0.39976	0.4	400	-0.00024	-0.24	-0.00024	-0.06
450	5.615	449.2	0.4492	0.45	450	-0.0008	-0.8	-0.0008	-0.17778
500	6.255	500.4	0.5004	0.5	500	0.0004	0.4	0.0004	0.08

<b>140KV</b>									
100	1.227	98.16	0.09816	0.1	100	-0.00184	-1.84	-0.00184	-1.84
150	1.864	149.12	0.14912	0.15	150	-0.00088	-0.88	-0.00088	-0.58667
200	2.508	200.64	0.20064	0.2	200	0.00064	0.64	0.00064	0.32
250	3.13	250.4	0.2504	0.25	250	0.0004	0.4	0.0004	0.16
300	3.736	298.88	0.29888	0.3	300	-0.00112	-1.12	-0.00112	-0.37333
350	4.354	348.32	0.34832	0.35	350	-0.00168	-1.68	-0.00168	-0.48
400	4.993	399.44	0.39944	0.4	400	-0.00056	-0.56	-0.00056	-0.14
450	5.62	449.6	0.4496	0.45	450	-0.0004	-0.4	-0.0004	-0.08889
500	6.247	499.76	0.49976	0.5	500	-0.00024	-0.24	-0.00024	-0.048

**Figure 15. Table Showing Comparison of Real System and Simulink Model**

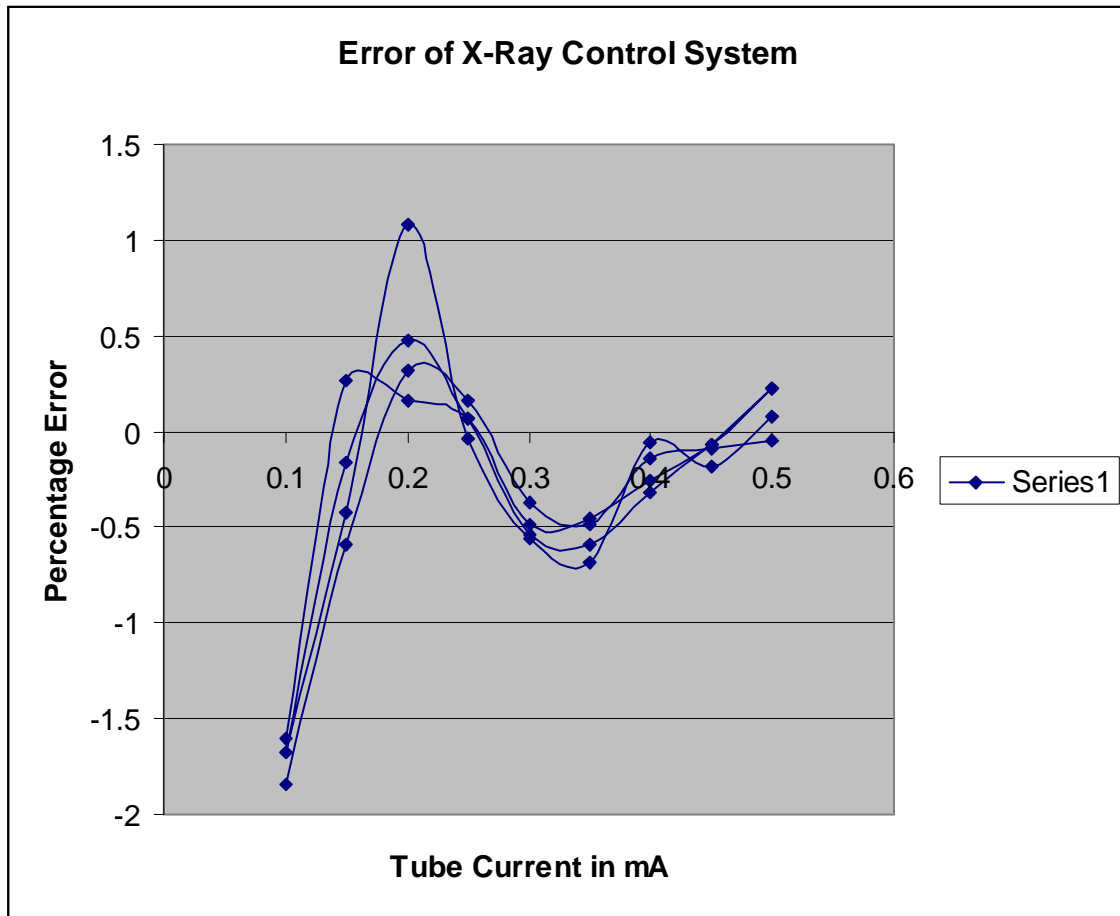


**Figure 16. Error of Actual System for static current reference.**

Figure 16 shows a plot of the error data (figure 15) of the real control system as measured on a PQ 6000 CT Scanner at Marconi Medical Systems. A LeCroy 4 GHz oscilloscope was used to measure filament and tube current feedbacks. As can be seen, the maximum error of the system is in the range of 2%. The error of the Simulink model is of smaller magnitude (closer to zero), but this is a result of inaccuracies resulting from real systems like measurement, noise etc. However, this is good enough verification to prove that our Simulink model closely resembles the real system.

## Chapter 3: CONTROLLER DESIGN AND SIMULATION

### 3.1 DESIGN OBJECTIVE

In the previous chapter, I developed a model of the X-Ray system, as it exists in a Marconi Medical Systems Q Series CT Scanner today. The last portion of the chapter also emphasized the loss of accuracy of desired outputs when the scanner is subjected to varying reference parameters that will be required in future applications of the system. The objective of this thesis work is to present an enhancement to the existing system to adapt it to the additional performance requirements of dose modulation. This chapter will explain in detail the design approach in Fuzzy logic and the implementation of this design.

### 3.2 A BRIEF LOOK AT FUZZY LOGIC

The basic structure of a fuzzy system (Ref 17) consists of three conceptual components: a **rule base**, which contains a selection of fuzzy rules; a **database (or dictionary)**, which defines the membership functions used in the fuzzy rules; and a **reasoning mechanism**, which performs the inference procedure (**fuzzy reasoning**) upon the rules and given facts to derive a reasonable output or conclusion.

**Soft Computing** is an innovative approach to constructing computationally intelligent systems. Complex real world problems require intelligent systems that combine knowledge, techniques, and methodologies from various sources. These intelligent systems are supposed to possess humanlike expertise within a specific domain, adapt themselves and learn to do better in changing environments. In confronting real-world computing problems, it is frequently advantageous to use several computing techniques synergistically rather than exclusively. This leads to the concept of neuro-fuzzy systems, which combine fuzzy logic and neural network techniques. Using the same principle of applying systems synergistically, I have used a fuzzy controller to enhance the

performance of the conventional control system used for the X-Ray tube. The details of the system will be discussed.

### **3.2.1 Fuzzy Set Theory**

The human brain interprets imprecise and incomplete sensory information provided by perceptive organs. Fuzzy set theory provides a systematic calculus to deal with such information linguistically, and it performs numerical computation by using linguistic labels stipulated by membership functions. Moreover, a selection of fuzzy if-then rules forms the key component of a fuzzy inference system (FIS) that can effectively model human expertise in a specific application.

Presented in this chapter is the selection and formation of fuzzy membership functions, fuzzy if-then rules and the implementation of this fuzzy system in the previously presented model of the X-Ray tube.

In Contrast to a classical set, a fuzzy set, as the name implies, is a set without a crisp boundary. That is, the transition from “belong to a set” to “not belong to a set” is gradual, and this smooth transition is characterized by membership functions that give fuzzy sets flexibility in modeling commonly used linguistic expressions, such as “the water is hot/very hot/extremely hot”.

## **3.3 A CLOSER LOOK AT THE X-RAY CONTROL LOOP**

It was evident in the previous chapter that the X-Ray system produced significant error when subjected to a varying tube current reference. From the structure of the model, I found that a good method of reducing the error of the system would be applying additional controls in the control loop where the correction factor was applied to the filament drive (at summing block 2 in *figure 8*).

The error signal being generated at summing block 1 is being multiplied by a fixed gain, and the product is the control signal to the next block to vary the filament current

accordingly. However, since the rate of change of the error signal is high (due to the reference varying rapidly), the system cannot apply a correction fast enough to maintain the output close to the reference.

This observation implies that there could be an enhancement to performance, were the correction signal applied with certain manipulations to the gain error product of the loop. Being the prime factor in the correction of the control signal, it is also the most appropriate modification from a control point of view. This is how I identified a possible application for another controller (fuzzy controller) in the system.

### **3.4 FORMATION AND OPTIMIZATION OF MEMBERSHIP FUNCTIONS**

#### **3.4.1 Selection of Inputs and Outputs of the controller**

For the fuzzy controller, the error signal is the main deciding factor (being a feedback of the real error of the system) for the magnitude of control required to ensure closeness to desired output. Therefore, this is an essential input. However, this signal is already being used in the loop to perform corrections to the control signal. We need a way to improve the control signal or change it at a faster rate to further enhance performance. This is where we see the rate of change of error as a possible signal that could be observed to improve system performance. Therefore I selected these 2 signals as the inputs to the fuzzy controller (*figure 16*). They are named “Error” and “DeltaError”. The controller is of the Mamdani type (which uses if-then rules to calculate the output of the system). The output is simply called “ErrorOut”. This is the control signal to the loop (our manipulated control signal).

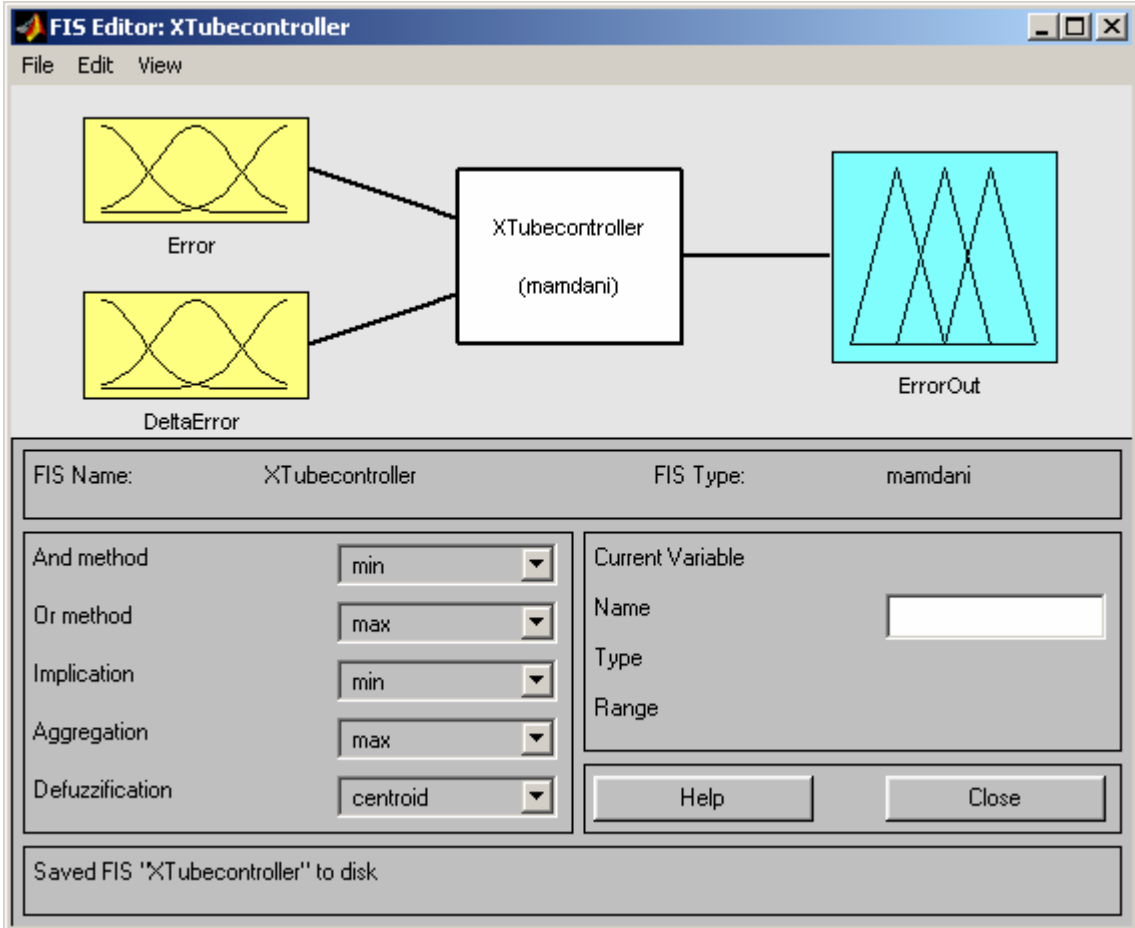
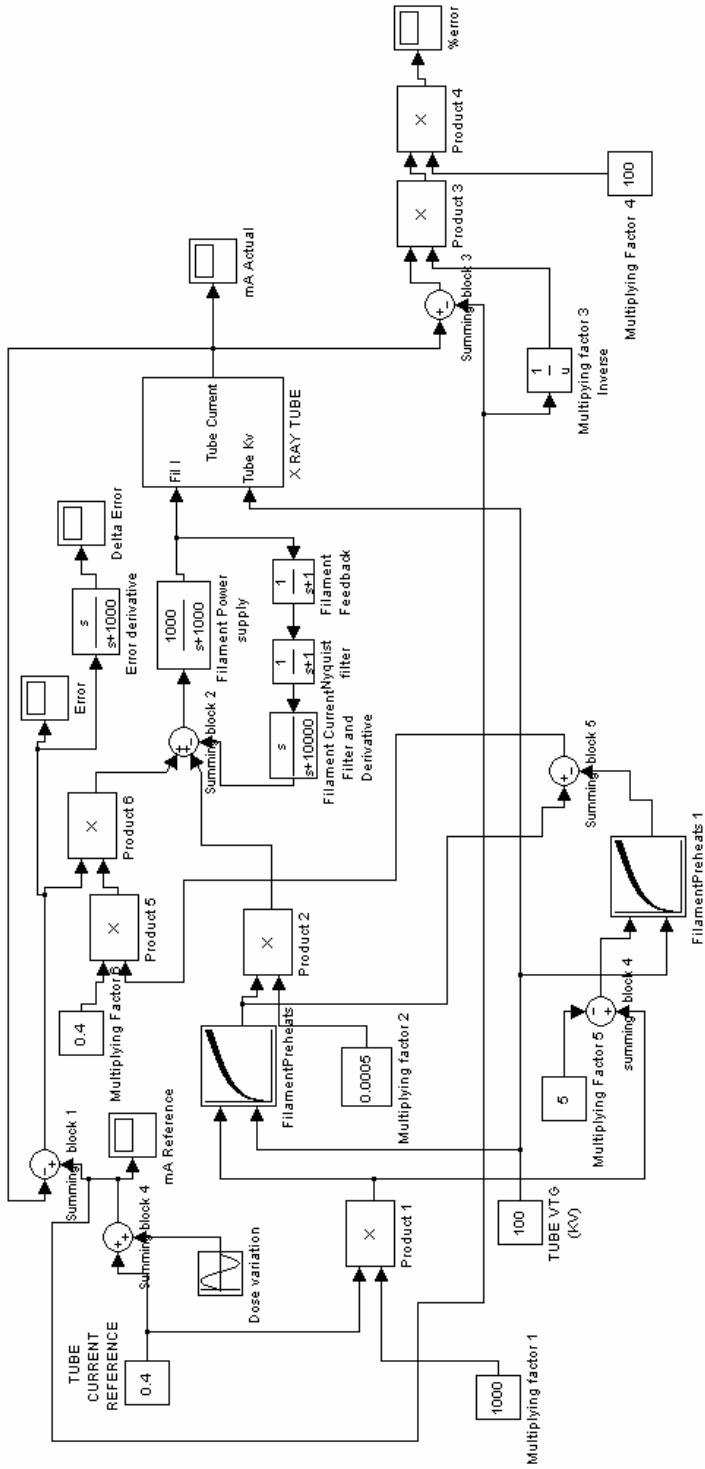


Figure 17. Structure of Fuzzy Controller



Measurement setup on model of X-Ray Tube

Figure 18. Measurement Setup on Model.

### 3.4.2 Selection of values for Inputs

In order to ascertain a starting point for the range of values of the error and change rate of error, I set up scopes in the old model as shown in *figure 18*. The error signal was read as shown in *figure 19*.

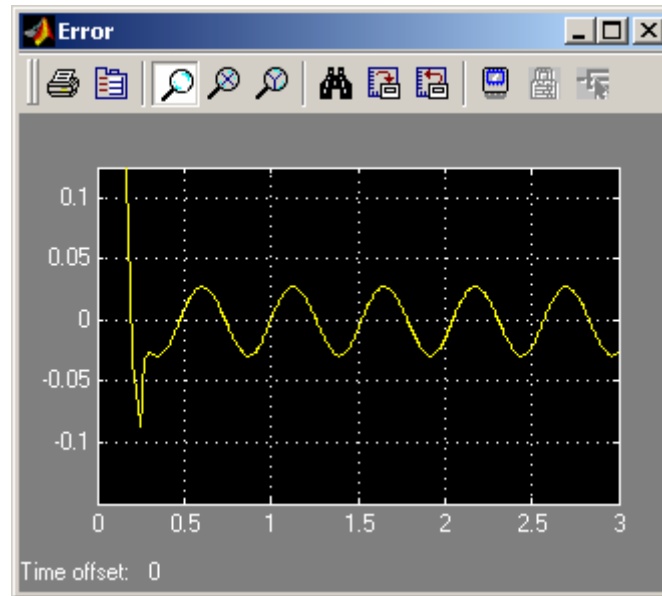


**Figure 19. Error Signal with Dynamic Reference**

Vertical Axis shows error values  
Horizontal Axis shows time in Seconds.

We can see that after the large settling error, the error values range between  $-0.3$  and  $+0.3$ . This was therefore selected as the range of the error input to the fuzzy controller (*figure 20*).

Also, as shown in *figure 20*, I selected 5 trapezoidal membership functions to represent the error range. The reason for this selection was the number of different linguistic ranges that I desired to break the input into. It was a practical and reasonable segmentation of the error values to start with. Fewer membership functions means less control and less

resolution, more membership functions means extra computational effort, so there is a tradeoff between the two.

During the course of the systems design and simulation, I also tried using triangular membership functions and changed the number of functions. The final selection is depicted in *figure 20*.

A Trapezoidal membership function is specified by four parameters {a, b, c, d} as follows:

$$\begin{aligned} \text{Trapezoid}(x; a, b, c, d) = & 0, & x \leq a. \\ & \frac{x - a}{b - a}, & a \leq x \leq b. \\ & \frac{d - x}{d - c}, & c \leq x \leq d. \\ & 0, & d \leq x. \end{aligned}$$

The parameters {a, b, c, d} with (a < b ≤ c < d) determine the x coordinates of the four corners of the underlying trapezoidal membership function.

I have chosen a membership function having four parameters (trapezoidal) because it has a more gradual transition into neighboring sets as compared to triangular functions.

NOTE: The selection of ranges and values in this design involved a long period of trial and error based on reasoning and inferences made after running numerous simulations of the model. The iterations and changes have not been depicted in this written part because they would seem redundant. Hence only the initial and final selected ranges and values will be shown and explained here.

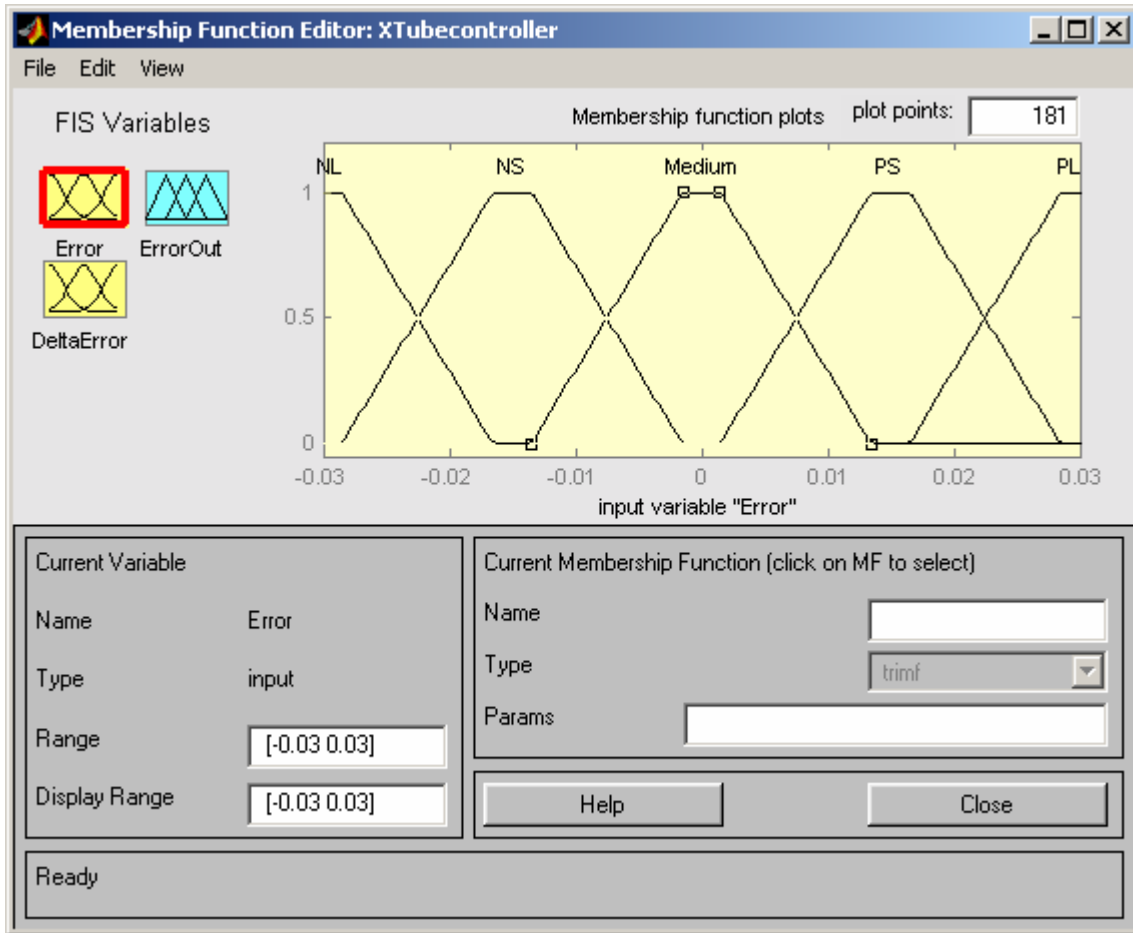


**Figure 20. Membership Functions of “Error” Input**

### 3.4.3 Membership Functions of “Error” Input

Figure 20 also shows the membership functions of the “Error” input signal. These are conventionally named as follows:

#### **Negative Large (NL) (figure 20)**

Ranges from  $-0.01652$  and is an “open left” function i.e. all negative values lower than (more negative-so higher in magnitude) the above value of  $-0.01652$  are considered to be Negative Large.

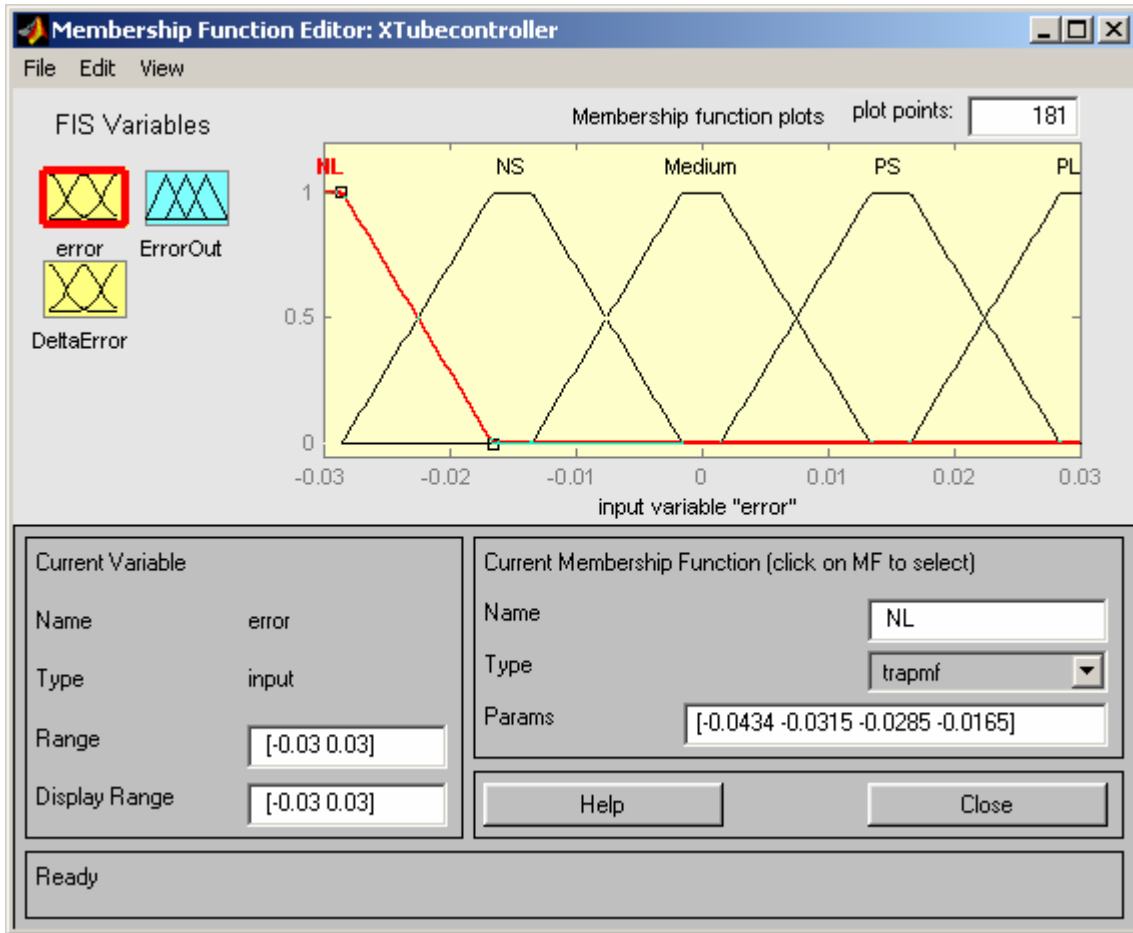


**Figure 21. “Negative Large” Membership Function Range**

**Negative Small (NS)**

Ranges from  $-0.02851$  to  $-0.001501$ .

**Medium**

Ranges from  $-0.01351$  to  $0.01348$ .

**Positive Small (PS)**

Ranges from  $0.001499$  to  $0.02848$ .

**Positive Large (PL)**

Ranges from  $0.01649$  to any positive value larger than that. It is an “open right” function.

**Note:** The overlap of all the membership functions as is evident from the figures means that there are some values that are part of more than one membership function. In the event that an input falls in this overlapping region, the controller triggers multiple rules and the output is derived from this multiple triggering. This will be discussed later in the chapter.

Figure 22 shows the derivative of the error signal as obtained from the Simulink model of figure 18. Here again please note that the transfer function block has been used to provide derivative action (instead of a derivative block) for the same reason as that of the filament current derivative loop (summing block 2 in figure 18). Reiterating the observation, a pure numerical derivative control element is not possible to implement in Matlab due to its frequency response (the fact that as frequency increases to a very high value, the system gain becomes zero). This problem is solved by using a derivative transfer function with a high cutoff frequency, which acts as a conventional derivative at frequencies of our interest.

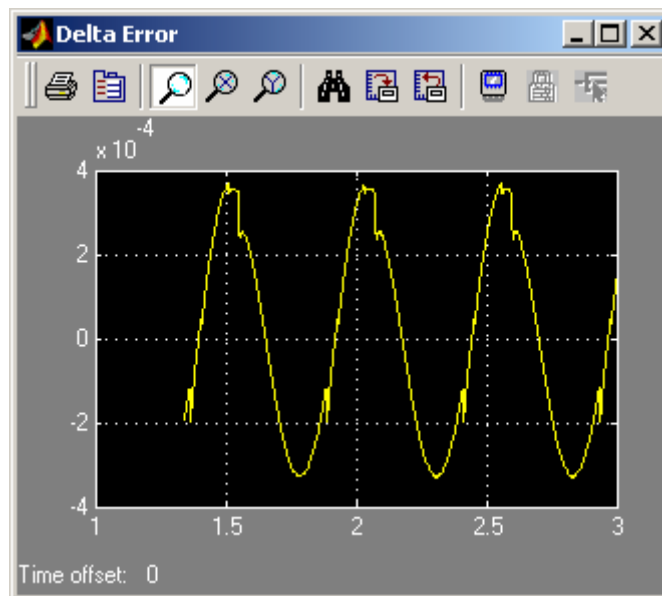


**Figure 22. Rate of Change of Error Signal**  
Vertical Axis shows rate of change of error

Horizontal Axis shows time in Seconds.

As seen in *figure 22*, the derivative of the error signal ranges from a value of 0.0004 to –ve 0.0004. This value was used as the range for DeltaError initially. However, when the simulation was run with the fuzzy block added to the model, I observed the input to the fuzzy block displaying an error rate of one order higher than the selected limit, and the error of the system was even higher than before using the fuzzy block. Therefore, the error rate range had to increase by one order of magnitude. So the final selection for the DeltaError was chosen to be between 0.004 and –0.004 as shown in *figure 23*.

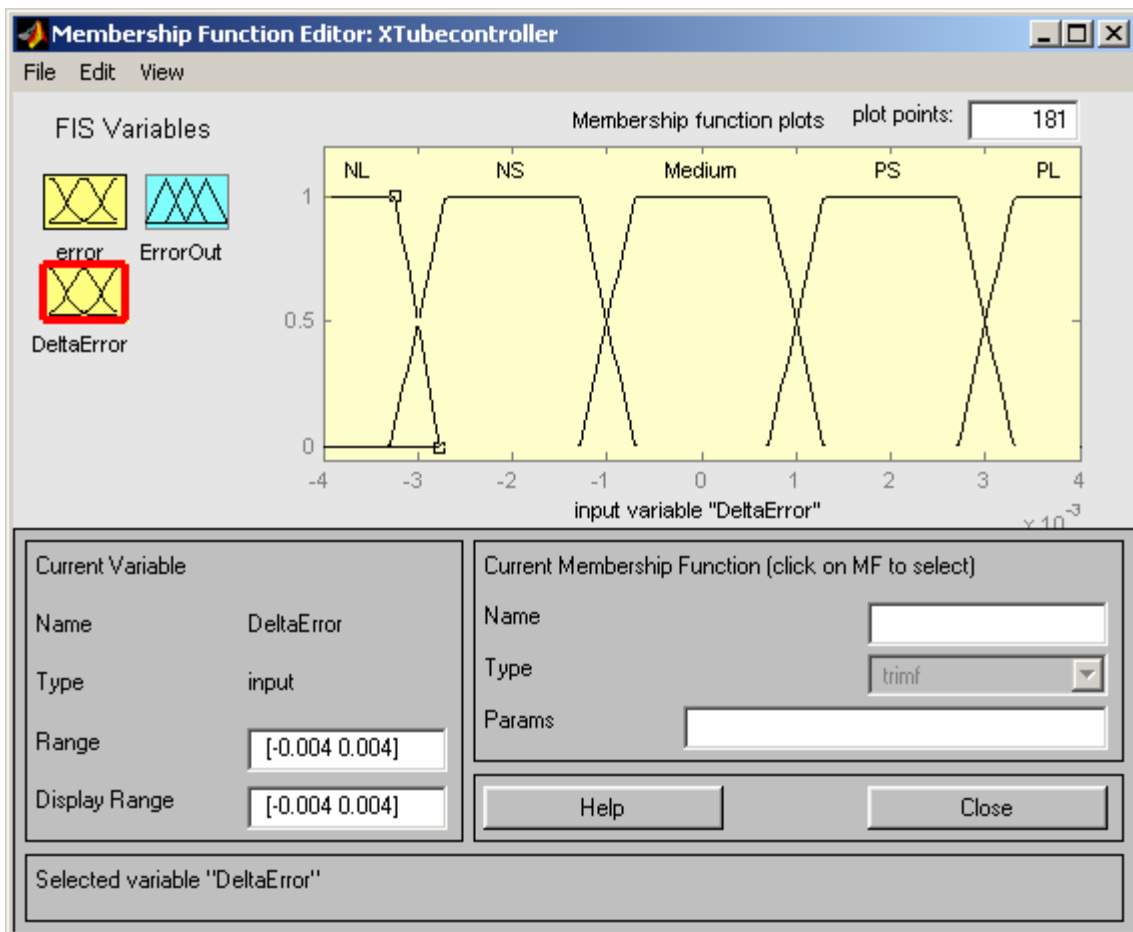


**Figure 23. "DeltaError" Input**

### 3.4.4 Membership functions of “DeltaError” Input

#### Negative Large (NL)

Ranges from  $-0.00276$  and extends to any value larger in magnitude in the negative direction. It is an “open left” function.

#### Negative Small (NS) (figure 24)

Ranges from  $-0.003297$  to  $-0.0007$ .

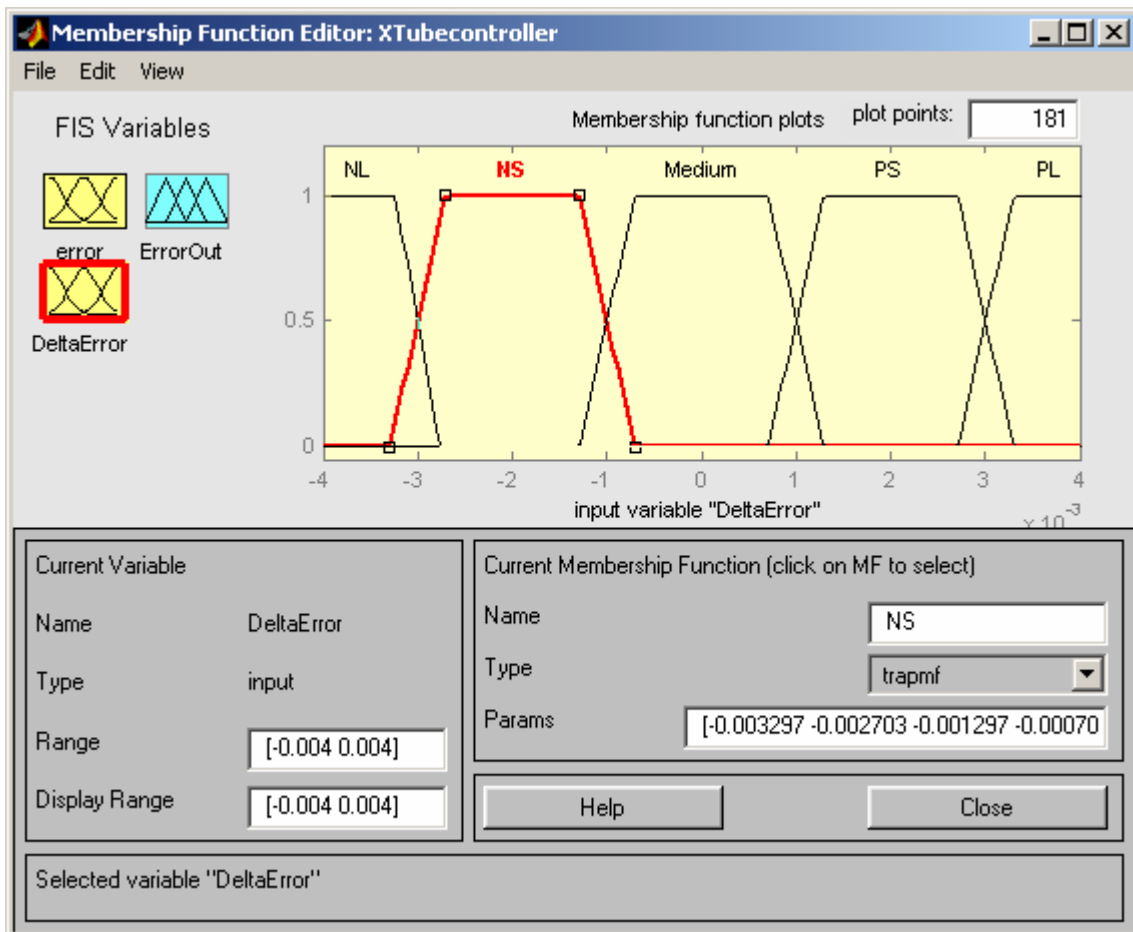


Figure 24. “Negative Small” Membership Function of “DeltaError” Input

**Medium**

Ranges from -0.001297 to 0.0012.

**Positive Small (PS)**

Ranges from 0.0007036 to 0.003298.

**Positive Large (PL)**

Ranges from 0.002706 to any positive value larger than that. It is an “open right” function.

**3.4.5 Selection of values for Outputs**

The range of values for the “ErrorOut” membership function was arrived upon by numerous simulations and deductions based on trial and error. Initially I started with the same range as the error input, with an attempt to optimize the values to get a more accurate control signal, but then found that an increase in magnitude of error signal gave better results. The final range of values I arrived at was between  $-0.8$  and  $0.8$  as shown in *figure 25*.

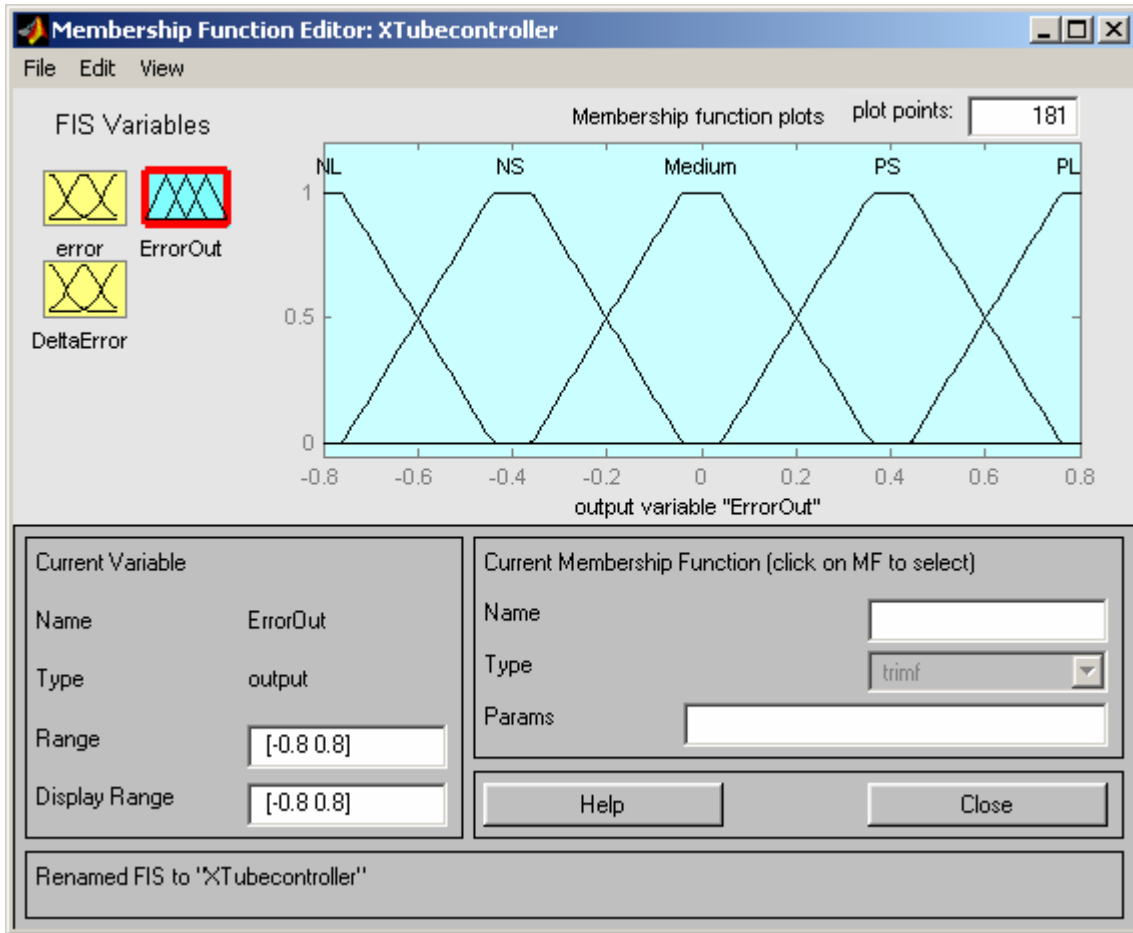


**Figure 25. “ErrorOut” Output of Fuzzy Controller**

### **Negative Large (NL)**

Ranges from  $-0.44$  and extends to any value larger in magnitude in the negative direction. It is an “open left” function.

### **Negative Small (NS)**

Ranges from  $-0.76$  to  $-0.04$ .

### **Medium**

Ranges from  $-0.36$  to  $0.3608$ .

**Positive Small (PS) (figure 26)**

Ranges from 0.04 to 0.7614.

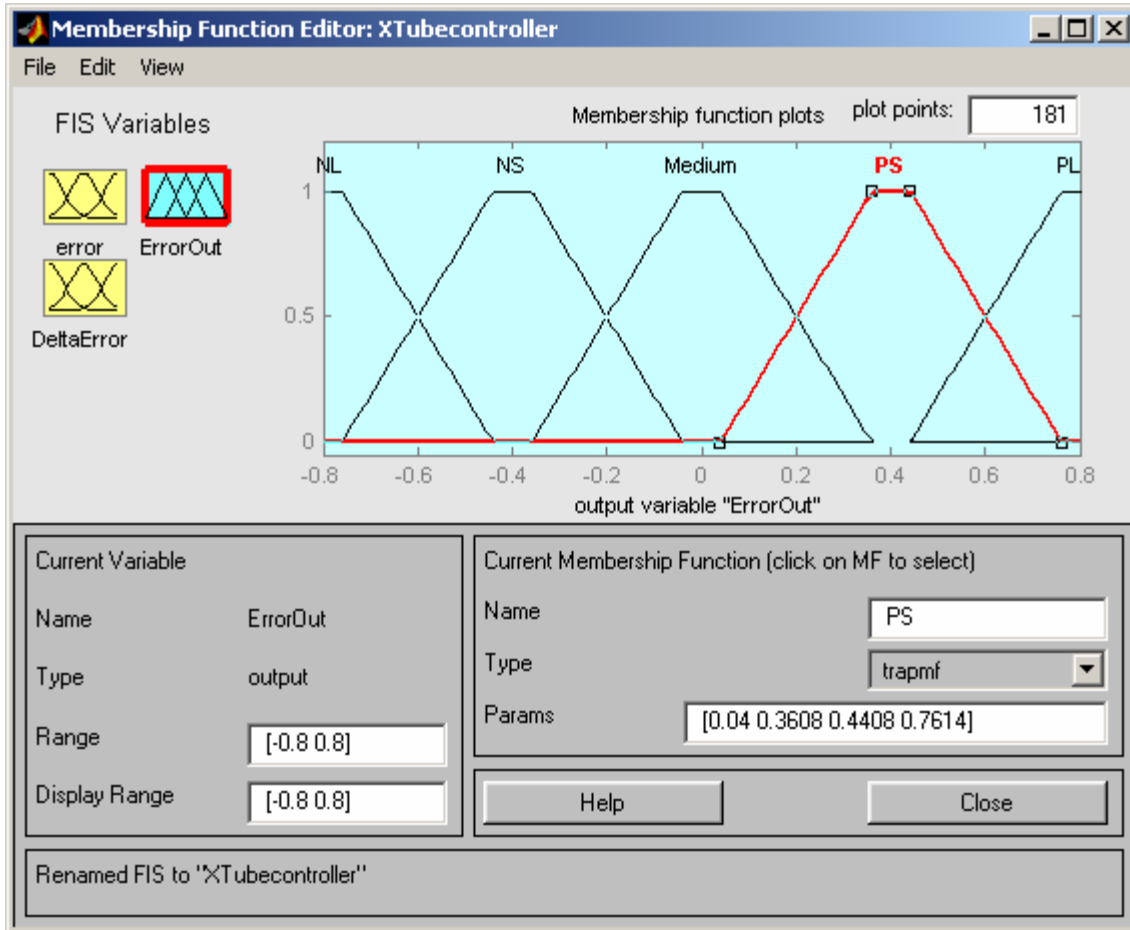


**Figure 26. “Positive Small” Membership Function of “ErrorOut” Output**

**Positive Large (PL)**

Ranges from 0.4408 to any positive value larger than that. It is an “open right” function.

### 3.4.6 Membership IF-THEN rules

A Fuzzy **if-then rule** (also known as a **fuzzy rule**, **fuzzy implication**, or **fuzzy conditional statement**) (ref 17) assumes the form

If x is A then y is B,

Where A and B are linguistic values defined by fuzzy sets on universes of discourse X and Y, respectively. Often “x is A” is called the **antecedent** or **premise**, while “y is B” is called the **consequence** or **conclusion**. In essence, the above expression describes a relation between two variables x and y. This can be extended to multiple antecedents as will be done in the design here, where we will be using two antecedents or inputs.

After numerous simulations and manipulations of inputs and outputs, I arrived at an effective logic for control. The magnitude of the error signal must be augmented in the direction of its trend so as to apply a larger control signal than that which the error block generates. The amount of augmentation is decided by the fuzzy membership rules as shown in *figures 27 and 28*. Please note that there are other ways of arriving at a rule base. There are methods that make use of genetic algorithms to form rule bases, where a function called the fuzzy implication function performs the task of transforming membership grades of the antecedents and conclusions into outputs for the system. The Mamdani Fuzzy model used here makes use of If-Then Rules, while there are others like the Sugeno Fuzzy Model where the conclusion is represented as a function of the antecedents. (ref 17)

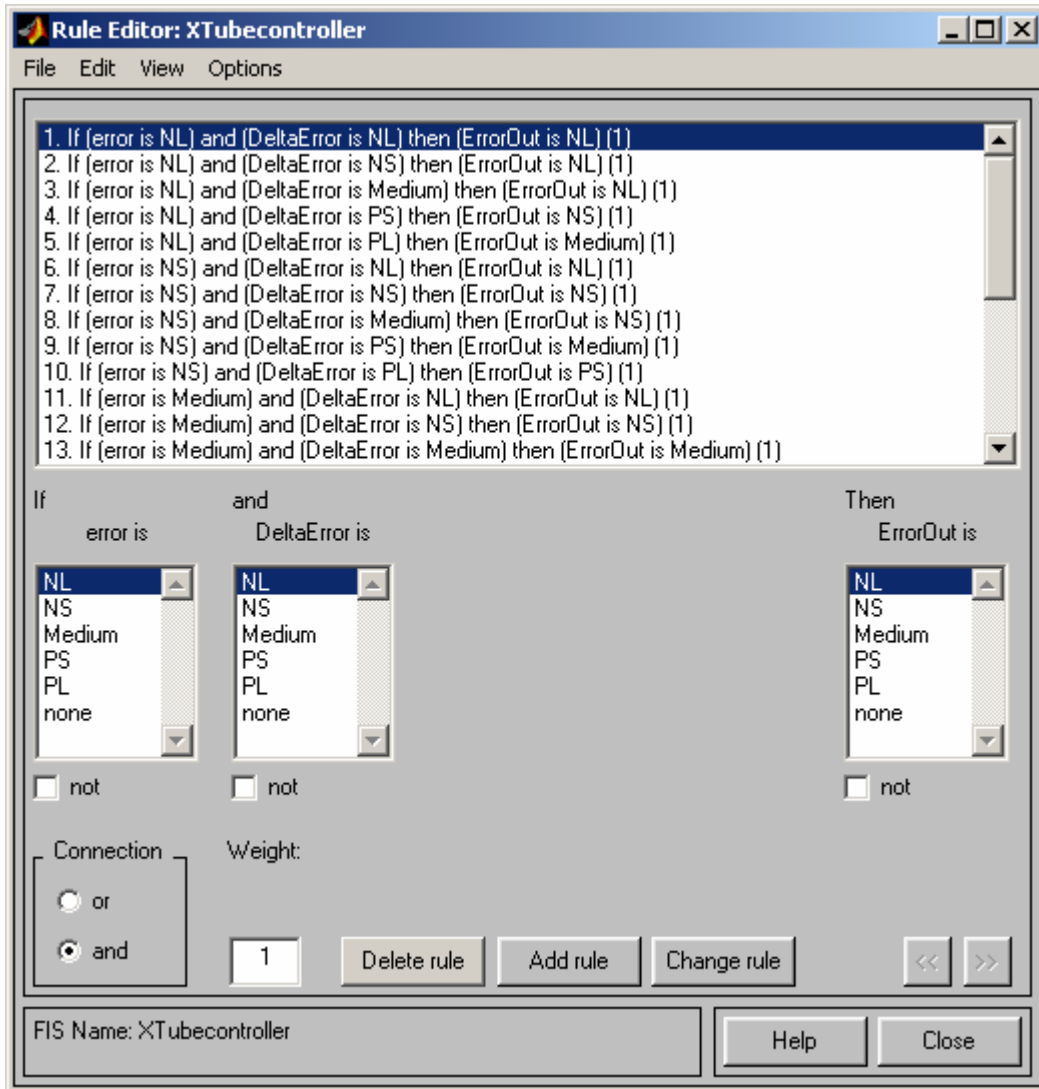


**Figure 27. Membership Rules “1 Through 13”**

Let us look at the first rule from *figure 27* as an example.

If (Error is Negative Large) and (DeltaError is Negative large) then (ErrorOut is Negative Large)

This means that IF the error signal is anywhere from  $-0.0165$  to any negative value of higher magnitude AND the rate of change of error is  $-0.00276$  or of larger negative value THEN the Output of the fuzzy controller will be in the range of  $-0.44$  to any larger

negative value. This means that if the error is a large negative value and it is also increasing in the negative direction (the actual output is larger than the desired reference value and is increasing in that direction), then the controlling action of the system should be to increase the error signal in the negative direction. This will result in feeding a high negative value at summing block 2, which in turn will lower the filament current drive and cause the output to be lowered, thus lowering the error. The effect of getting a higher magnitude of output from this block is to rectify the error at a faster rate than before.

The rest of the 25 rules just deal with every combination of the membership functions of “Error” and “DeltaError” (both have 5 membership functions each, so every possible combination leads to a total number of  $5 \times 5 = 25$  combinations, thus giving rise to 25 rules). Here again it should be noted that due to the overlap of membership functions, the fuzzy controller will trigger more than one rule if the values of the inputs fall in the overlap regions. This is the feature of fuzzy logic which gives adequate representation to linguistic terms like “negative large” etc.

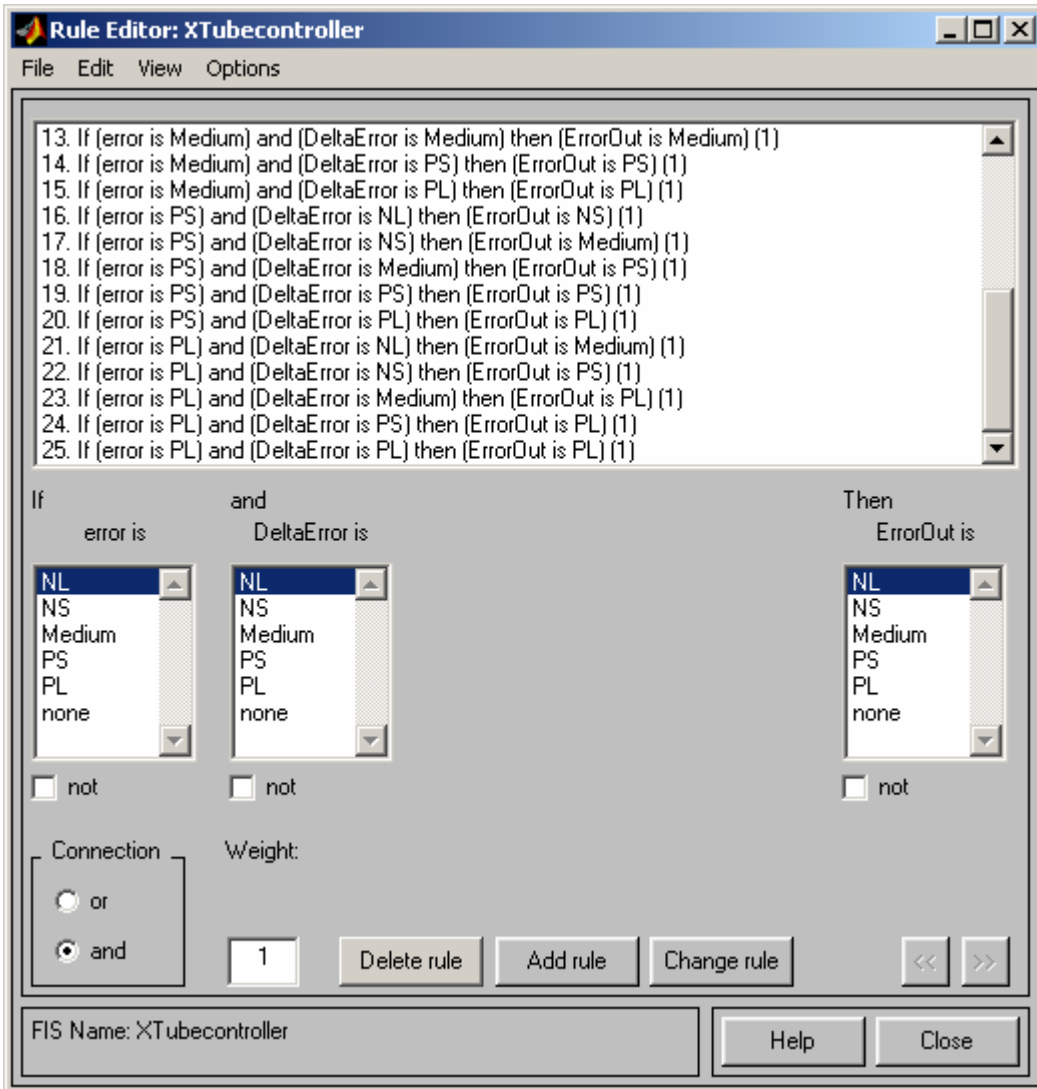
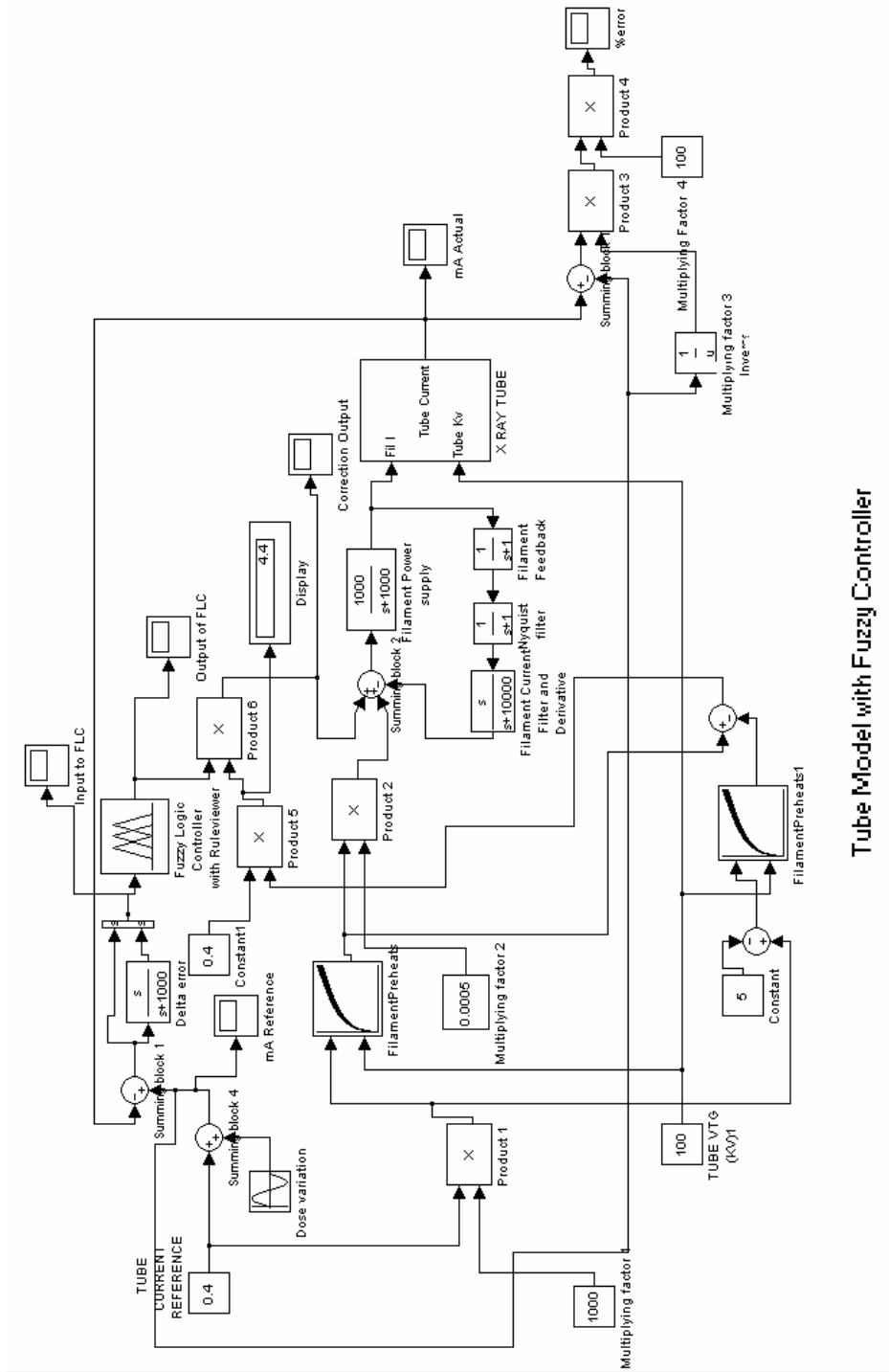


**Figure 28. Membership Rules “13 Through 25”**



Tube Model with Fuzzy Controller

Figure 29. Tube Model with Fuzzy Controller

### 3.5 SIMULATION OF MODEL

Figure 30 shows the surface view of the fuzzy controller. It is a 3 dimensional display of the membership functions with their range of values and the mapping to the output as defined by our membership rules.

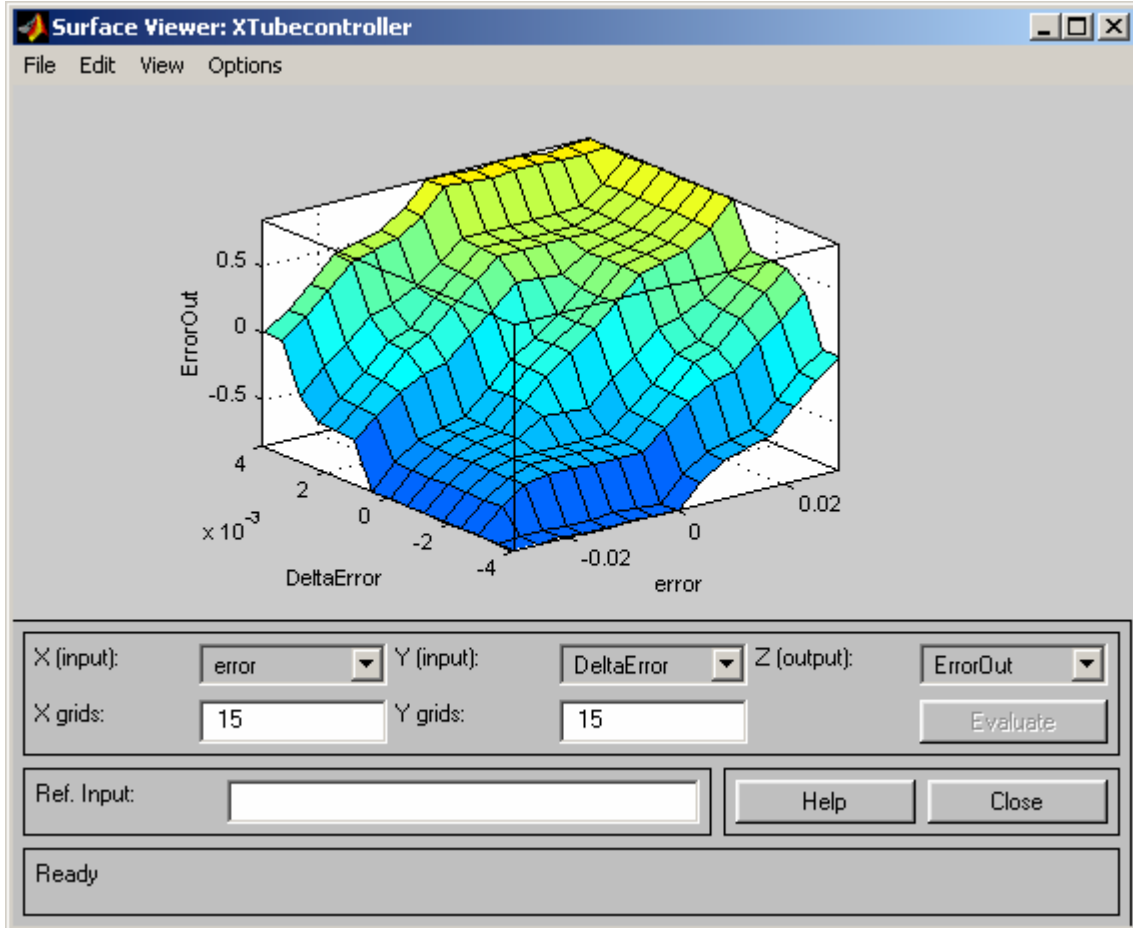


**Figure 30. Surface View of Fuzzy Controller**

The model in figure 29 was run with the following simulation parameters

Simulation time = 3 seconds.

Reference mA = 400mA (0.4 Amps) summed with a sine wave variation of 0.1 Amps.

Sine wave frequency = 12 radians per second (approximately 2 Hertz).

The fuzzy logic controller block has a rule viewer, which displays the values of inputs and the rules being triggered during the course of the simulation. It also shows the rules

corresponding to the input membership functions being triggered and the outputs being generated by the fuzzy controller at each instance.

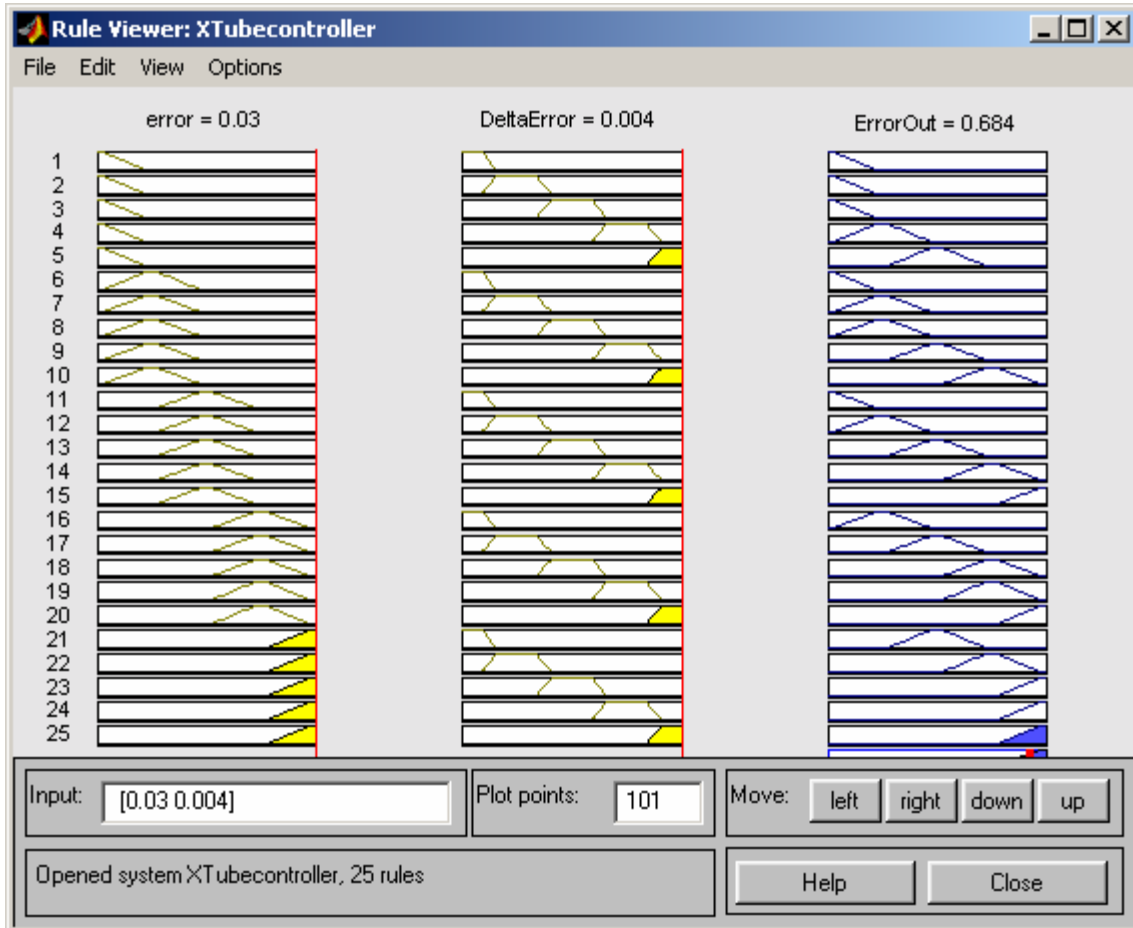


**Figure 31. Rule viewer during simulation**

Figures 31 and 32 are two different instances of fuzzy rule triggering during the simulation of the model.

From figure 31, we can see the rule viewer at the extremes of the ranges of inputs. The error at this point in time is 0.03 and the DeltaError value is 0.004. From the membership functions of these inputs (Figures 21 and 24), we see that they both fall in the Positive Large membership functions of their respective inputs. Thus this would trigger rule number 25 (figure 28) and the output of the controller should be in the Positive Large Membership Function (figure 26) of ErrorOut i.e. be of a value larger than 0.55 The

output as is evident from *Figure 31* is 0.684, which is in the PL membership function. The value is arrived at by the centroid defuzzification method of fuzzy logic theory, which uses certain mathematical algorithms (fuzzy reasoning) to calculate the outputs of the controller. More details of these methods can be found in reference 17.

Now if we look at *figure 32*, we find that the Error input value is  $-0.00177$  and the DeltaError has a value of  $9.81e-006$ . Looking at their Membership functions (*figures 21 and 24*), we see that both these values fall in the “Medium” Membership function of their respective inputs. So this triggers rule number 13 (*figure 27*) and so the output value is  $-0.0121$ , in the “Medium” membership function of the ErrorOut output.

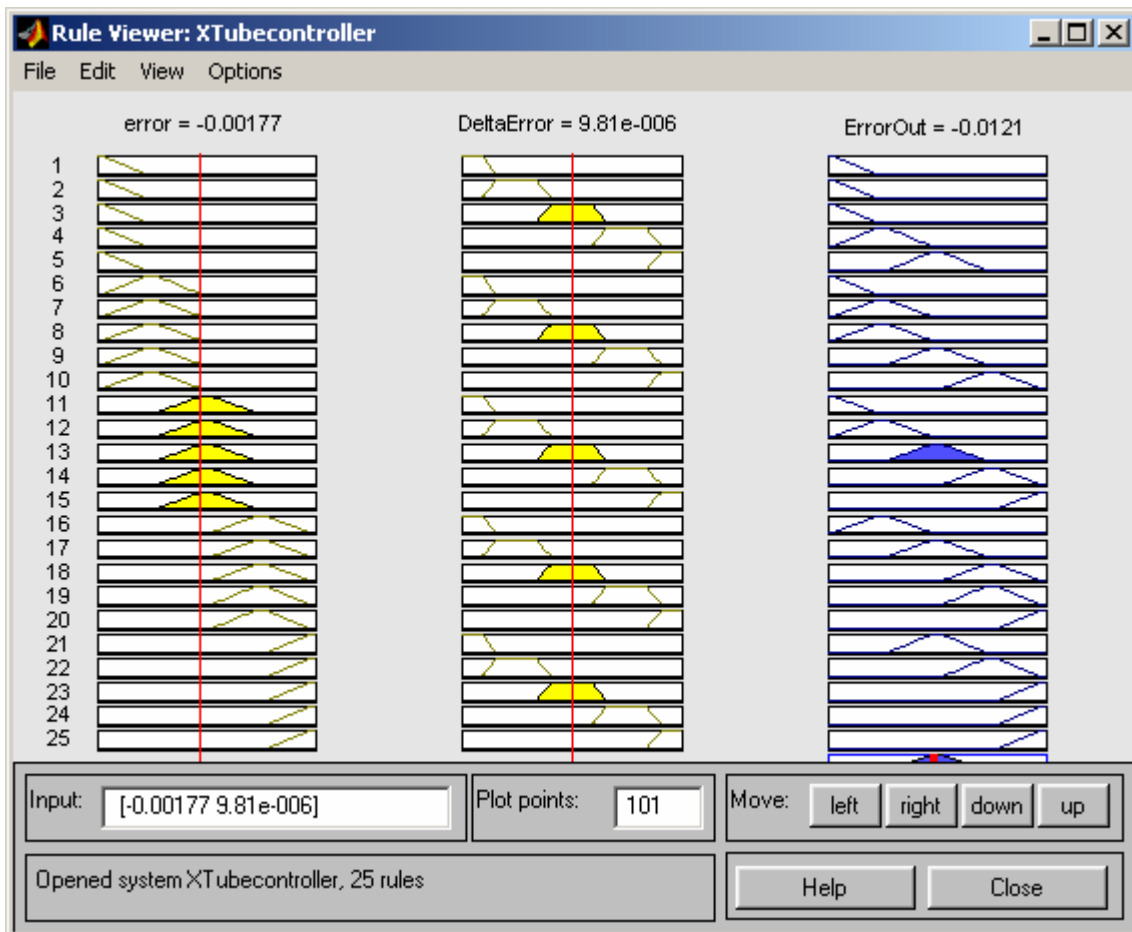


**Figure 32. Another Rule Viewer Output.**

The triggered rule is shown as the full blue trapezoid in the row for the 13<sup>th</sup> rule as can be seen in *figure 32*. The red streak in the blue block at the end of the rule column simply depicts the triggered rule and marks the value chosen by the controller.

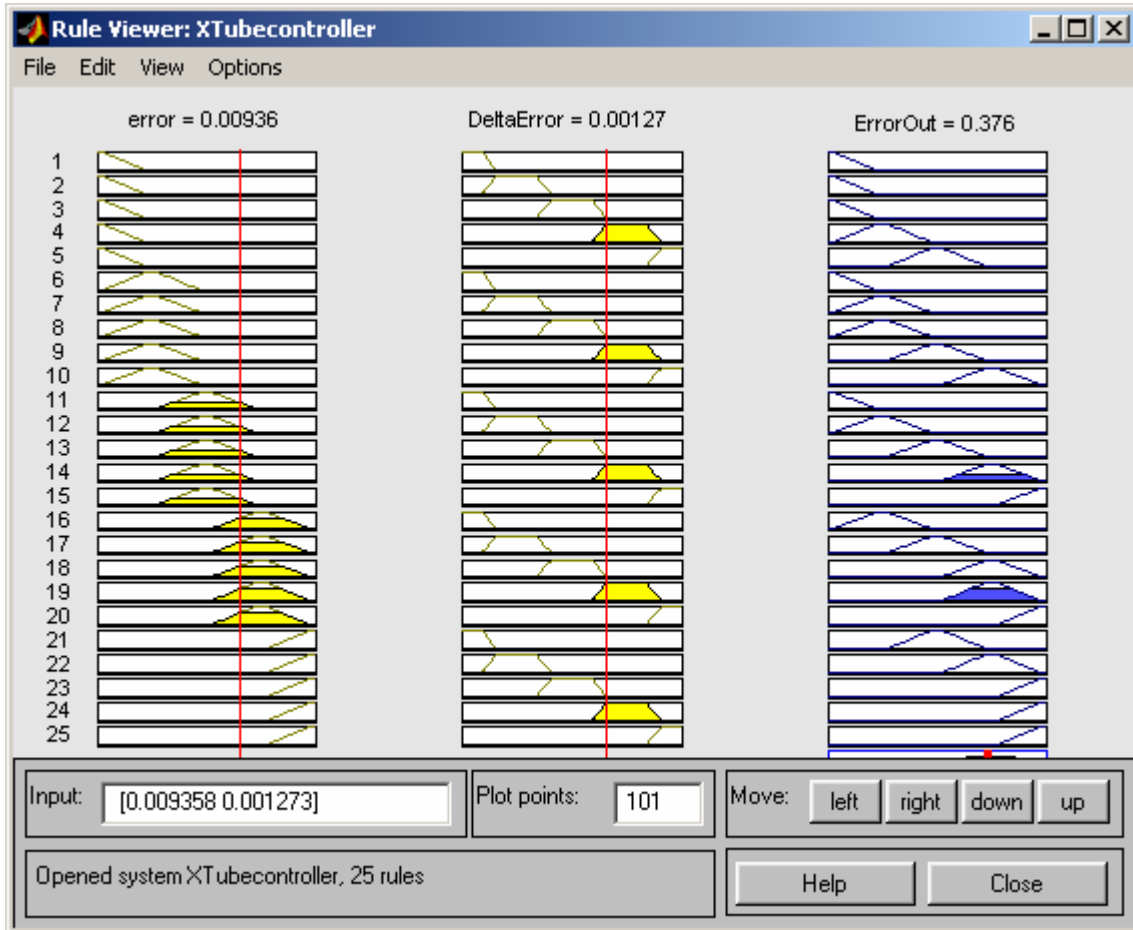


**Figure 33. Rule Viewer Output showing multiple rule triggering**

*Figure 33* is a good example of multiple rules triggering in fuzzy logic. As seen in the figure, the “Error” input is a value of 0.00936 which falls in the “Medium” membership function (*figure 21*) and the “ErrorOut” input is 0.00127 which falls in the “Positive Small” membership function (*figure 24*). This causes rule 14 to trigger (*figure 28*) and the output would be in the Positive Small range of “ErrorOut”. However if we look closely at the “Error” input value of 0.00936, we can see that this value also falls in the “Positive

Small” membership function (*figure 21*). Thus this will also cause rule 19 to trigger. The output of both of these rules happens to be “Positive Small” just by coincidence and the value of 0.376 is output by the controller. The calculation involved in the controller, however, weighs the impact of the membership functions and the rule base to give out the final value.

### 3.6 DISCUSSION OF SIMULATION RESULTS

#### 3.6.1 Input to the Fuzzy Logic Controller (FLC)

Depicted in the scope display in *figure 34* are the two inputs to the fuzzy controller. The “Error” input is displayed in yellow and the “DeltaError” is in pink.

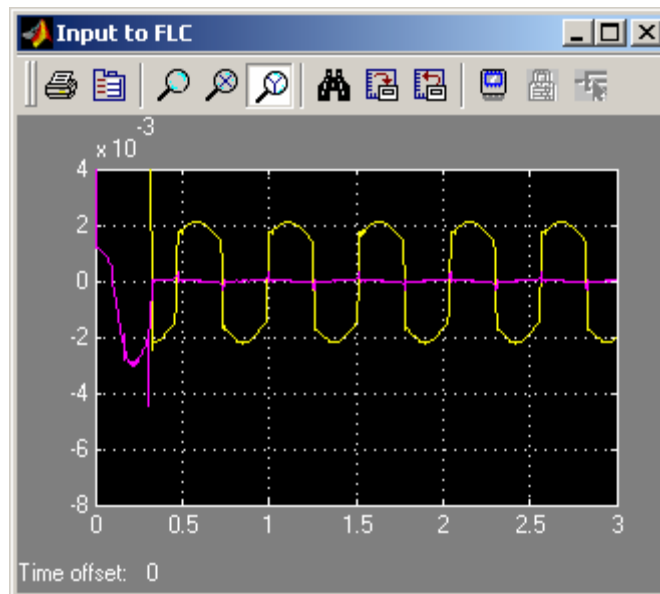


**Figure 34. Input Signal to the Fuzzy Logic Controller During Simulation**

Vertical Axis shows magnitude of inputs.  
Horizontal Axis shows time in Seconds.

### 3.6.2 mA reference

The desired tube current reference to the system, (*figure 35*) in this case with a frequency of 12 radians per second or approximately 2 Hertz.

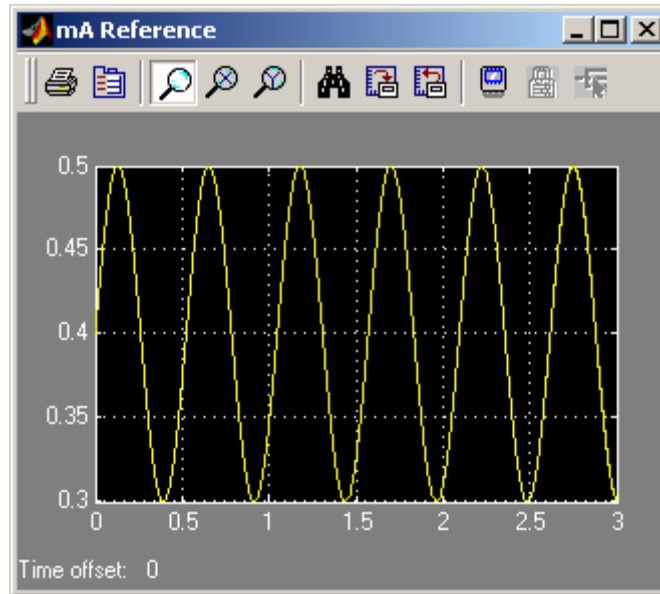


**Figure 35. Tube Current Reference**

Vertical Axis shows current in Amps.  
Horizontal Axis shows time in Seconds.

### 3.6.3 Output of the System

The actual tube current over the simulation period can be seen in *figure 36*.

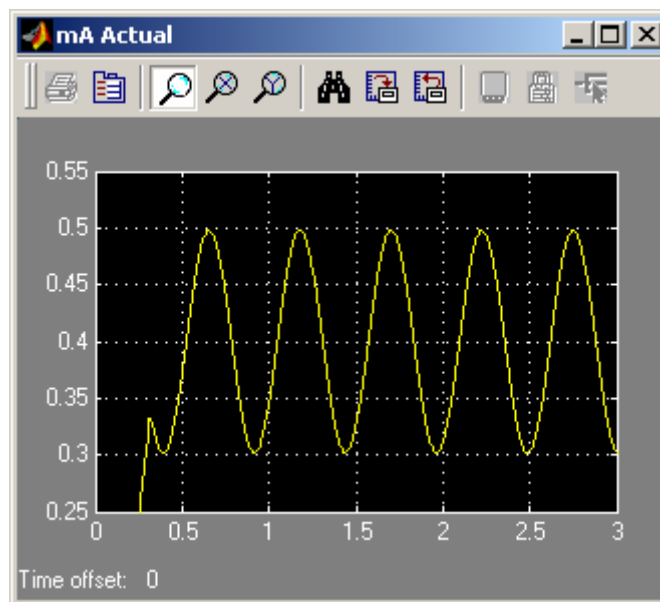


**Figure 36. Actual Tube Current of Fuzzy Enhanced Model**

Vertical Axis shows current in Amps.  
Horizontal Axis shows time in Seconds.

### 3.6.4 Output of the Fuzzy Controller

This is essentially the control signal being generated by the fuzzy controller based on its inputs and rule base. (Figure 37)

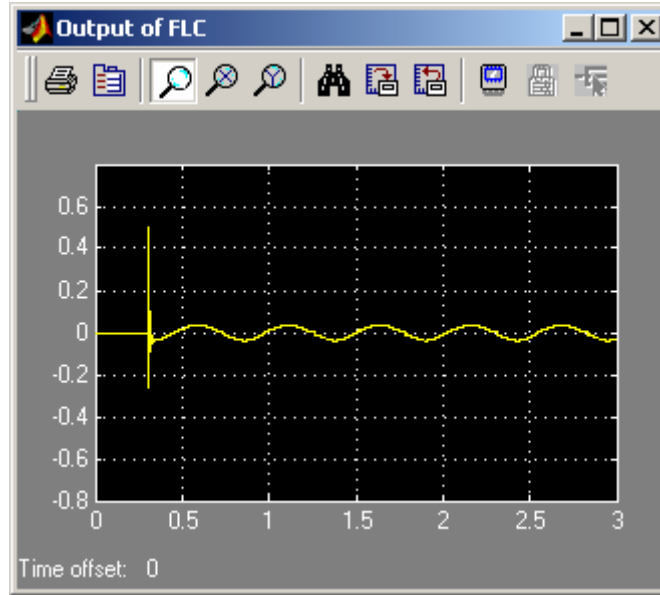


**Figure 37. Output of Fuzzy Controller During Simulation**

Vertical Axis shows magnitude of control signal.  
Horizontal Axis shows time in Seconds.

### 3.6.5 Input to summing block 2

The product of the gain and the output of the fuzzy controller. (*Figure 38*)

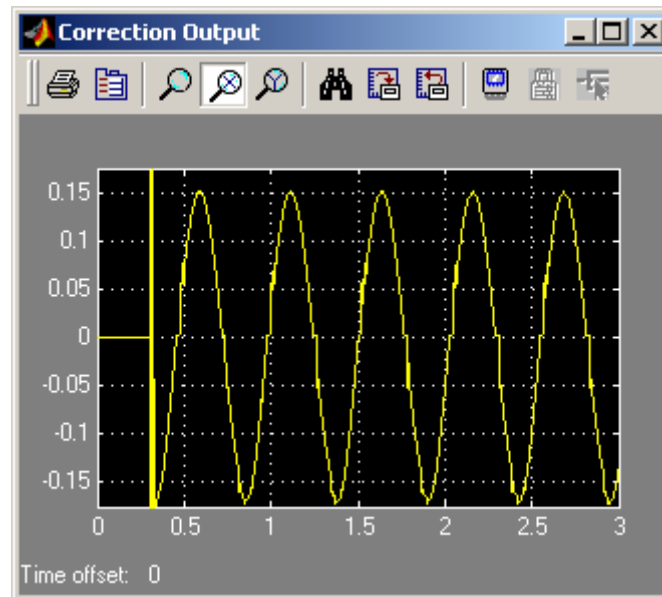


**Figure 38. Correction Signal**

Vertical Axis shows magnitude of signal.  
Horizontal Axis shows time in Seconds.

### 3.6.6 Percentage Error between reference and actual output of the system

This is the basic performance goal of our design. As can be seen from *figure 39*, the error of the system ranges approximately between  $-0.5\%$  and  $0.75\%$ , as compared to  $-6\%$  and  $9\%$  in the original model. We have successfully reduced the error of the system by approximately  $92\%$ . Such is the effectiveness of our fuzzy controller!!!!

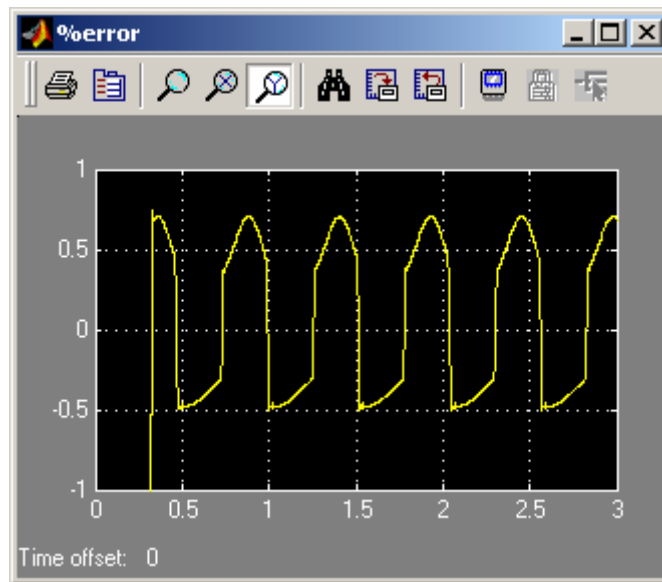


**Figure 39. Error of Fuzzy Enhanced System.**

Vertical Axis shows percentage error.  
Horizontal Axis shows time in Seconds.

As seen in the simulations so far, there is a startup error of relatively large magnitude, which settles to the consistent values in less than 0.4 seconds. This initial error, though undesirable, can be allowed in the system since the imaging data acquisition system can be made to wait (time delayed) for a specified time period before beginning the sampling, thus keeping the scan images free from artifacts that could be caused in this period. Also, the time taken by the error to settle is very small and will have very minimal adverse effect on the system.

### 3.6.7 Fuzzy Enhanced Model simulation for non Varying Reference.

Figure 40 shows the output of the System model using the fuzzy control, when the current reference is constant. So this shows that the Fuzzy model will also function well in a static situation. The fuzzy controller works better when the reference is sinusoid, but this shows that it still works well when the reference is constant also. In fact, we can see that the fuzzy controller even has a lower starting error as compared to the original model.

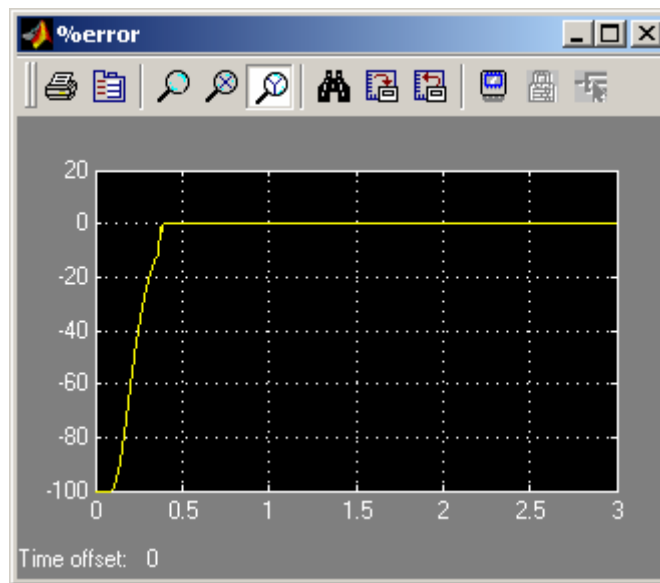


**Figure 40. System error for static tube reference.**

Vertical Axis shows percentage error.  
Horizontal Axis shows time in Seconds.

## **Chapter 4: SIMULATIONS WITH IMPROVEMENTS TO MODEL AND CHANGES IN PARAMETERS**

### **4.1 MODIFICATIONS IN MEMBERSHIP FUNCTIONS**

As we have seen in the previous chapter, the fuzzy controller successfully reduced the percentage error of the system by a significant amount. However, we also see that the shape of the error graph (*figure 39*) is a waveform with sharp edges. Since our reference is a sine wave, we would ideally like an error signal that also follows the same shape since this would indicate some uniformity in the error and be easier for the system to handle. Therefore a smoother error signal would be more desirable than the sharp one that is seen in *figure 39*.

According to the fuzzy set theory as mentioned in chapter 3, a fuzzy set has a boundary, which makes a smooth transition from one set to another. A trapezoidal membership function as used in the fuzzy controller in chapter 5 is one such set. It has gently sloping sides, which combine with its neighboring functions smoothly. Yet using this as a membership function results in slightly sharp error transitions. In order to improve on this performance, I tried using gaussian membership function in the model as shown in *figure 41*.

#### 4.1.1 Membership functions of “Error” input

(Figure 41)

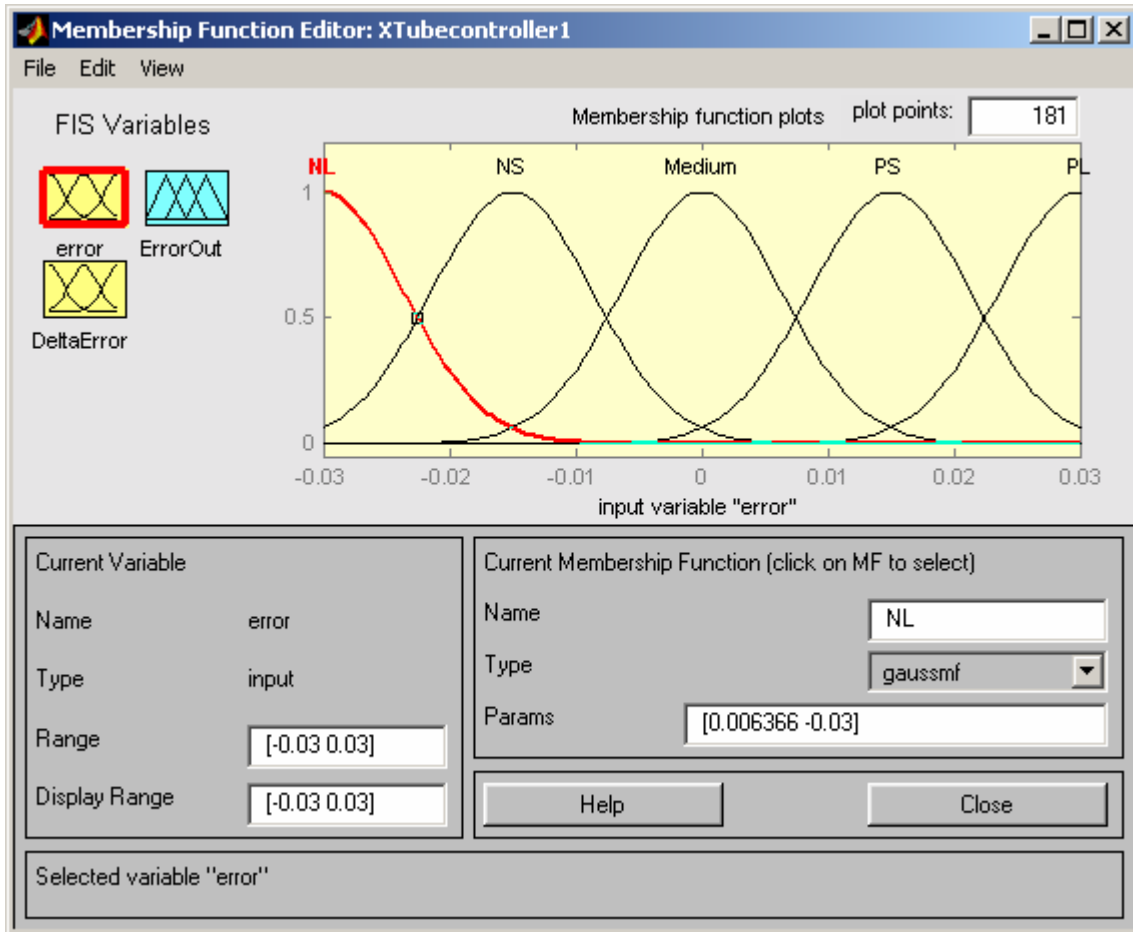


**Figure 41. Gaussian Membership Functions of “Error” Input.**

As can be seen in *figures 41,42 and 43*, I have simply replaced the membership functions of chapter 3 by gaussian membership functions, keeping their ranges of values the same. Gaussian curves are relatively smoother than the trapezoidal shapes, thus indicating that there would be a smoother transition between neighboring membership functions.

#### 4.1.2 Membership functions of “DeltaError” input

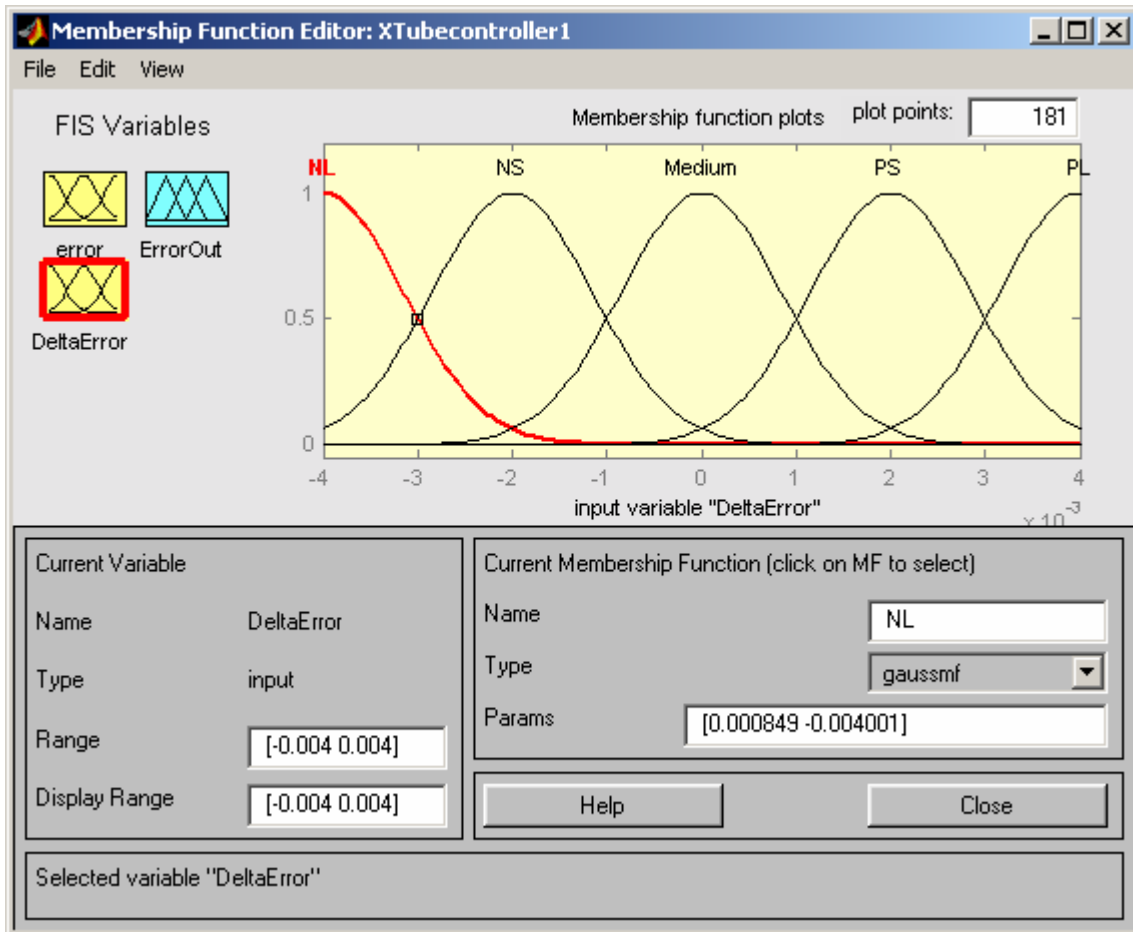


**Figure 42. Membership Functions of “DeltaError” Input**

A Gaussian Membership function is specified by 2 parameters

{ $c$ ,  $\sigma$ } as follows:

$$\text{gaussian}(x; c, \sigma) = \exp\left(-0.5 \frac{(x-c)^2}{\sigma}\right)$$

where ‘ $c$ ’ represents the membership functions center and ‘ $\sigma$ ’ determines its width.

### 4.1.3 Membership functions of “ErrorOut” Output

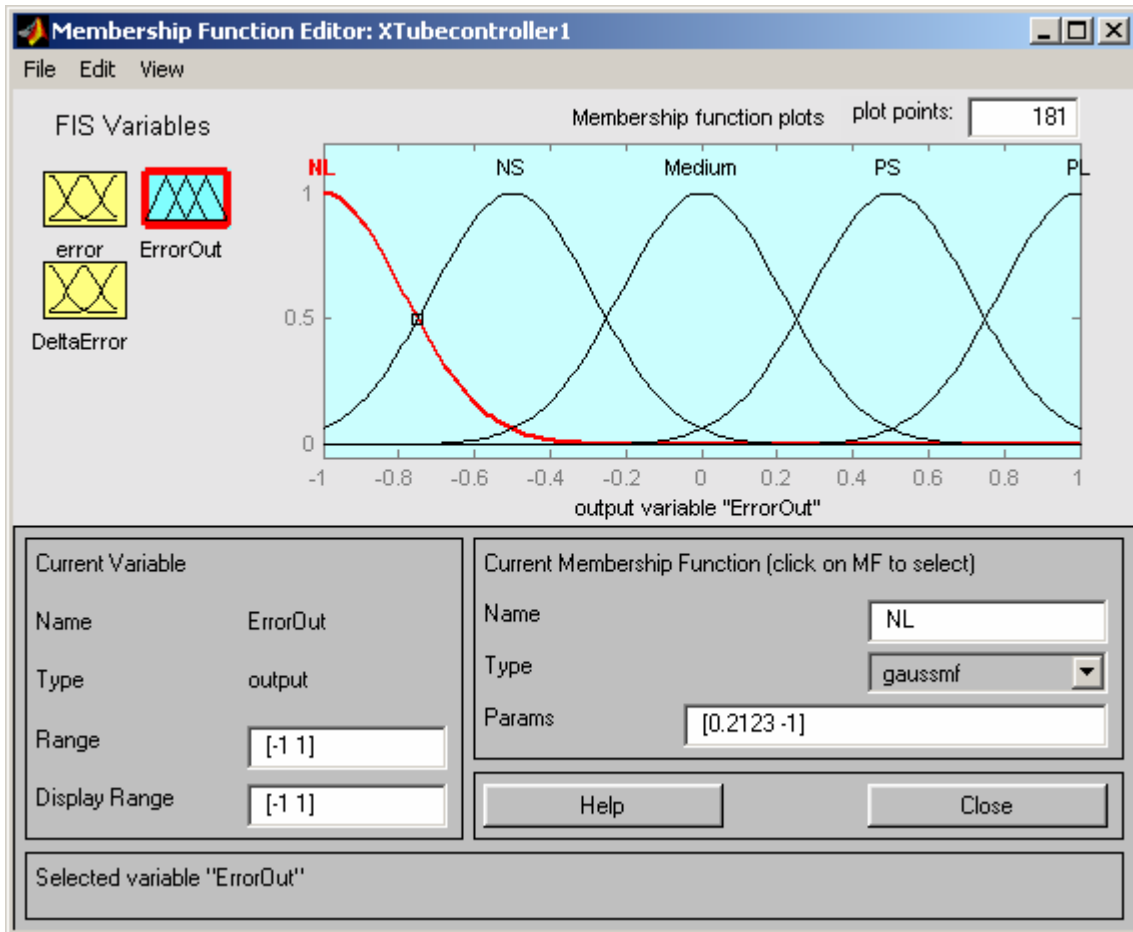


**Figure 43. Membership Functions of “ErrorOut” Output**

The Simulink model was run using the above gaussian membership functions and the same parameters (references) as before. The results of the model are shown.

## 4.2 SIMULATION RESULTS

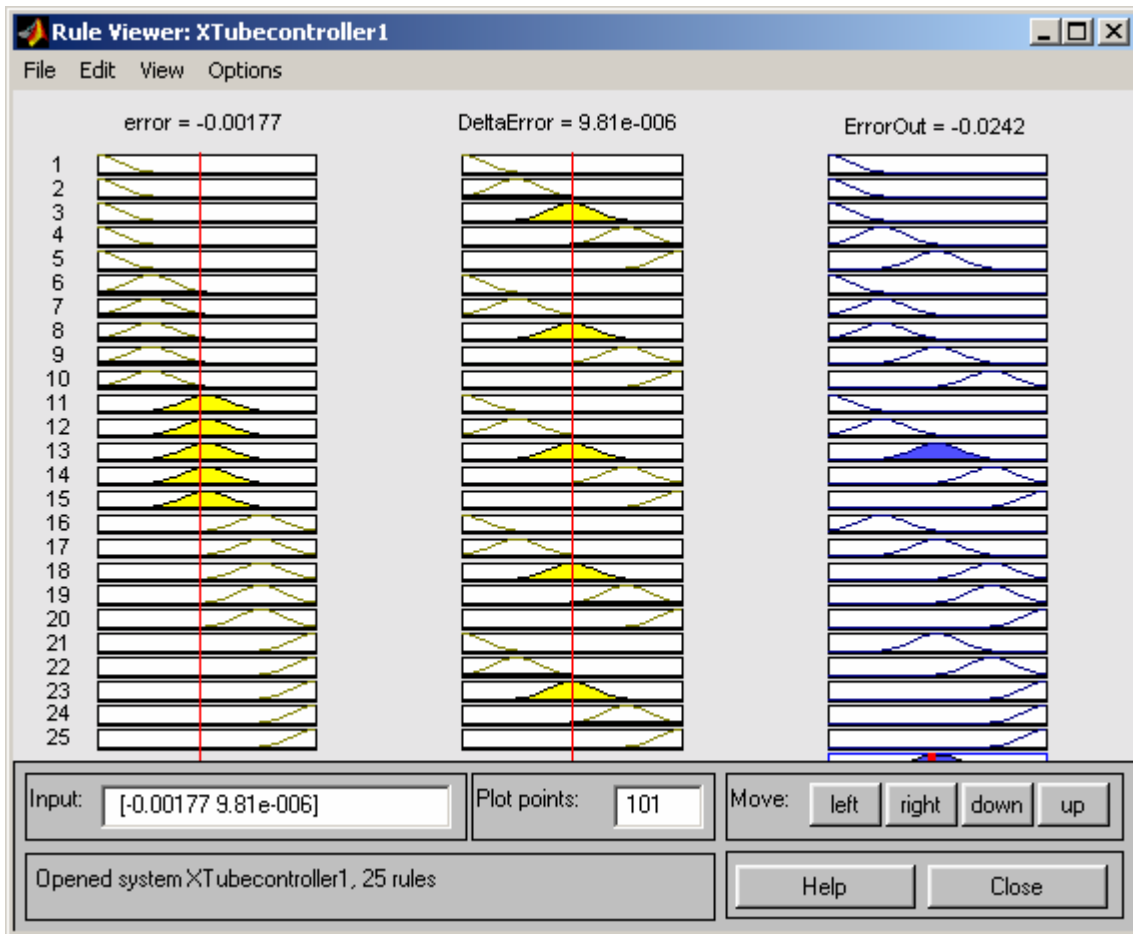


**Figure 44. Ruleviewer for simulation with gaussian Membership functions**

In *figure 44*, we can see that with the same values of inputs as those in *figure 32* in chapter 3, the output generated by the differently shaped membership functions is different. (ErrorOut is -0.0121 using trapezoidal membership functions and -0.0242 when using gaussian membership functions). This difference is emphasized only to substantiate the differences in system output produced after simulation. The surface view of this fuzzy controller (*figure 45*) also shows the difference of output from the previous fuzzy model.

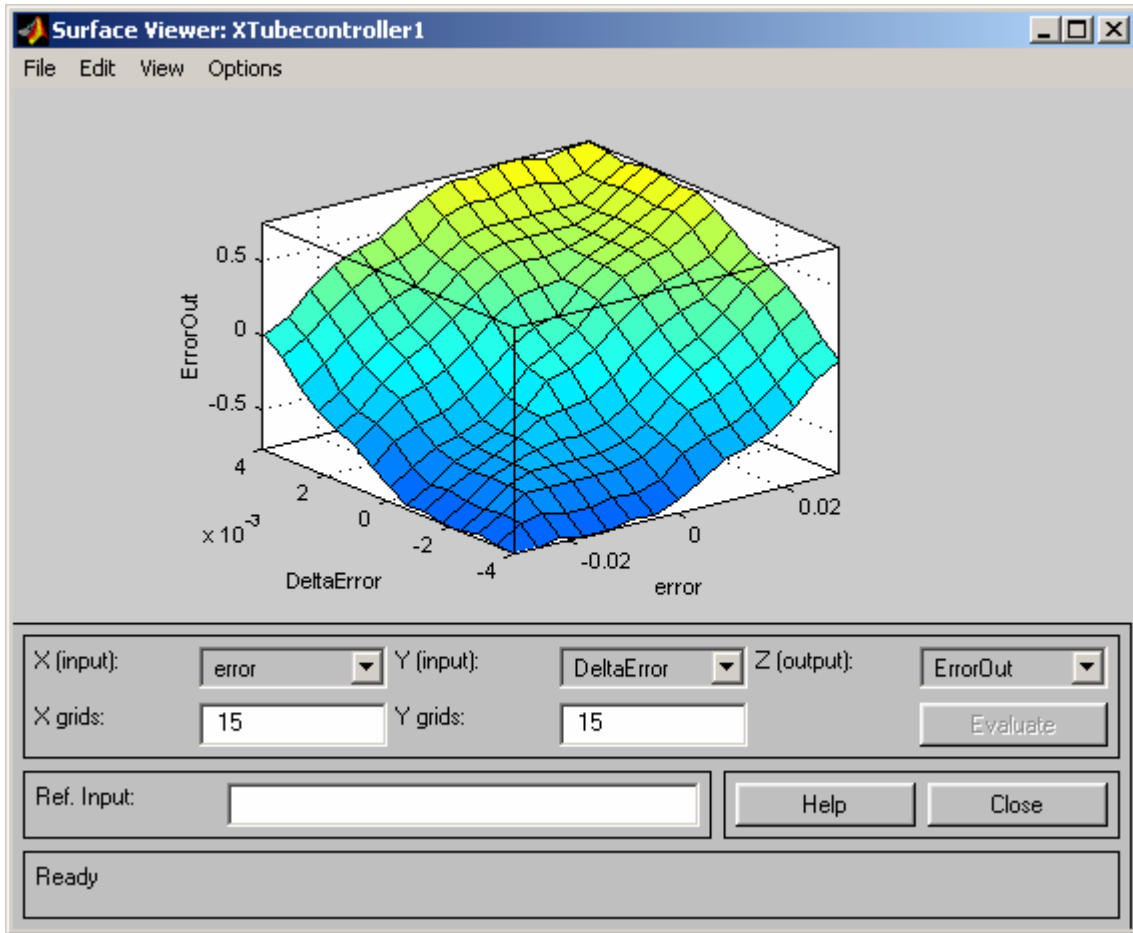


**Figure 45. Surface view of Fuzzy Controller using Gaussian Membership Functions**

#### 4.2.1 Percentage Error between reference signal and actual output of system

This is the error signal generated by the system. (*Figure 46*) Note the distinct difference between this signal and that in *figure 39* in chapter 3. The magnitude of error is almost the same range of value but this signal is much smoother than the earlier one. This is the difference produced by the change of membership functions. This fuzzy controller produces a more uniform error and would therefore be a better choice for use in the model of the X-Ray tube. However, there are some disadvantages to Gaussian membership functions (e.g., more computational effort in the real-time implementation), which make the choice of membership functions dependent on several factors.

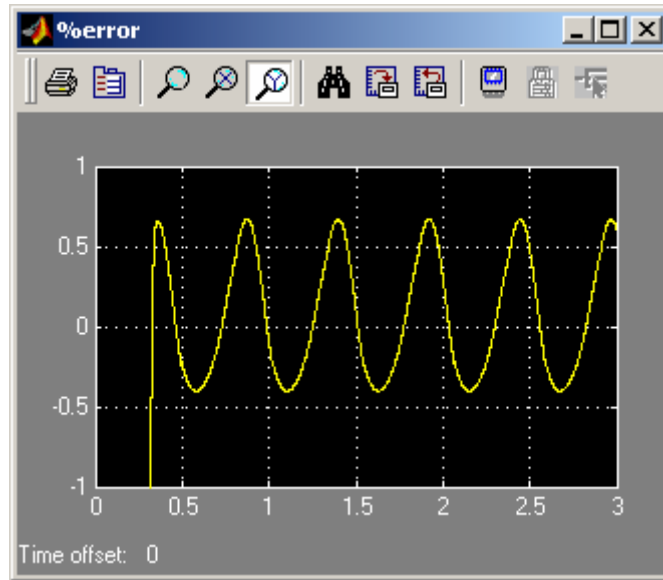


**Figure 46. Error of System using Gaussian Membership Functions**

Vertical Axis shows percentage error.  
Horizontal Axis shows time in Seconds.

### 4.3 FREQUENCY LIMITATIONS

Now that we have an X-Ray Tube system model with a fuzzy controller that minimizes the error during dose modulation, let us find its limitations by varying some system parameters. Since Tube Voltage (KV) and mA are limited by the data in the look up tables of the model, these parameters cannot be varied beyond known values. This leaves only the frequency of the reference signal as a possible variable parameter to the user. Note that from now we will use the fuzzy controller with gaussian membership functions in our X-Ray tube model since it produces better results.

#### 4.3.1 Frequency of reference signal

All simulations of the model done so far have been at a reference frequency of 12 radians per second/ 2 hertz since this is the most commonly needed variation in the applications of the CT scanner.

Let us try simulations with both an increase and decrease of the reference frequency.

### 4.3.2 Simulation at 24 radians /second tube current reference (4 Hertz)

The error magnitude is higher than that at 2 hertz, but is still less than 1 % in both directions. (*Figure 47*) This is significantly lower than the error produced by the system without the fuzzy controller (-10 % to 14%, *figure 48*). So it seems like the controller is still quite effective.

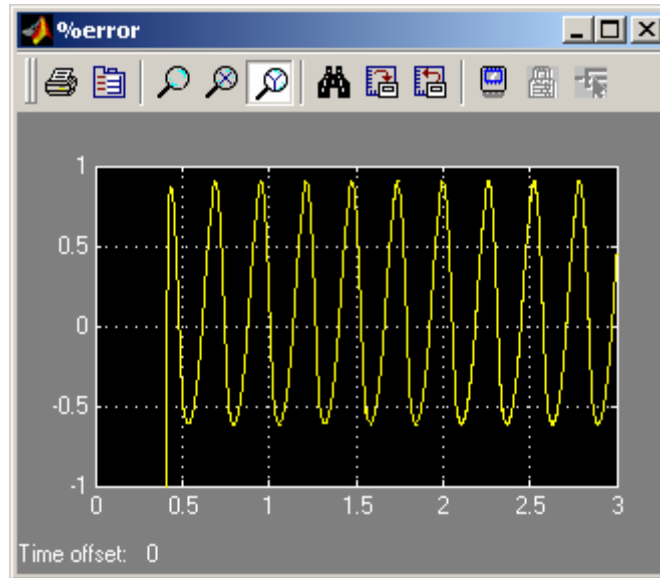


**Figure 47. Error at 4 Hertz.**

Vertical Axis shows percentage error.  
Horizontal Axis shows time in Seconds.

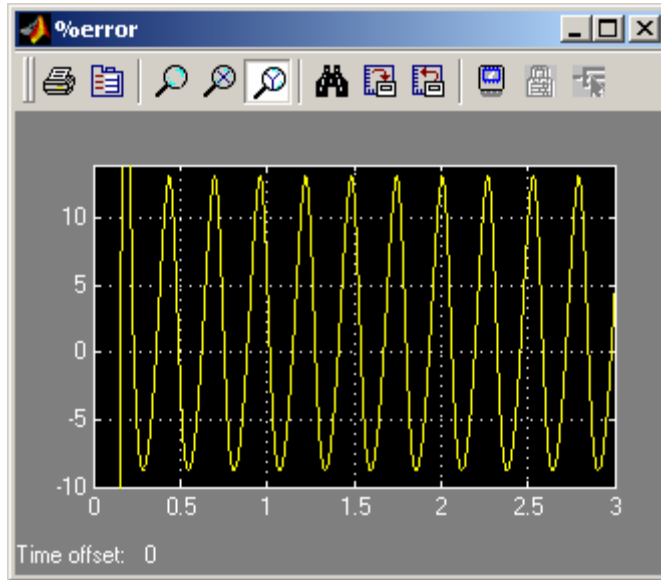


**Figure 48. Original Model Error at 4 Hertz.**

Vertical Axis shows percentage error.  
Horizontal Axis shows time in Seconds.

### 4.3.3 Simulation at 48 radians/second (8 Hertz) tube current reference

The error is in a range of  $-40$  to over  $10\%$  at  $8\text{ Hz}$  (*figure 49*). This is a high value as compared to that at lower frequencies. However this is to be expected since the reference is changing too rapidly for the controller to keep up with it. Since the requirements of a real CT scanner are not likely to be so high ( $4\text{ Hertz}$  maximum requirement of dose modulation), the system output at this frequency is not of much concern to us at this time.

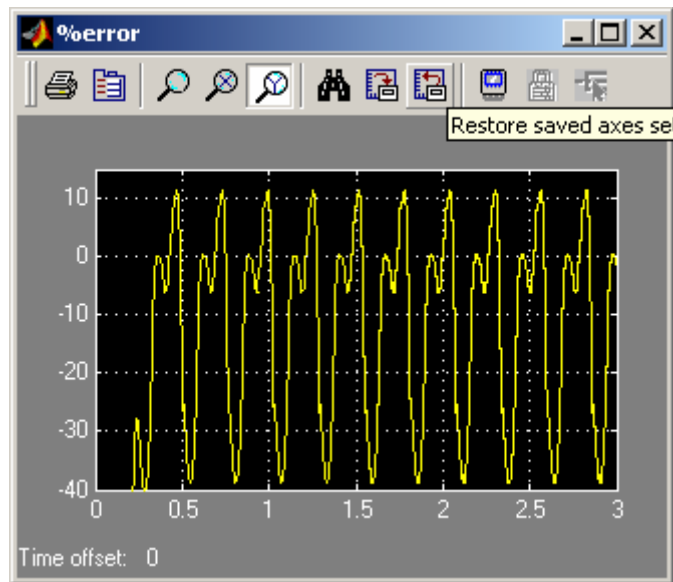


**Figure 49. Error at 8 Hertz Reference.**

Vertical Axis shows percentage error.  
Horizontal Axis shows time in Seconds.

Comparing this to the original model (*figure 50*), which has an error range of  $-15\%$  to  $20\%$ , we can see that the fuzzy model performs still significantly better.

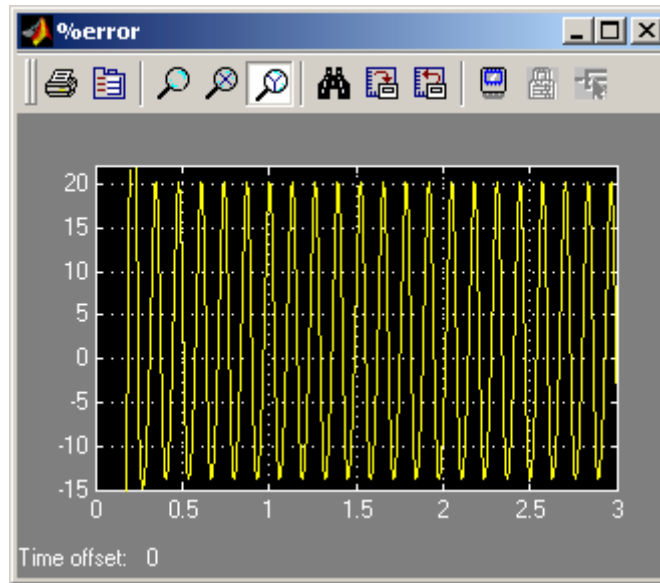


**Figure 50. Original Model Error at 8 Hertz**

Vertical Axis shows percentage error.  
Horizontal Axis shows time in Seconds.

#### 4.3.4 System Output at 48 radians/ second

The actual tube current is very distorted as can be seen (*figure 51*). So this confirms our conclusion that the error is relatively high.

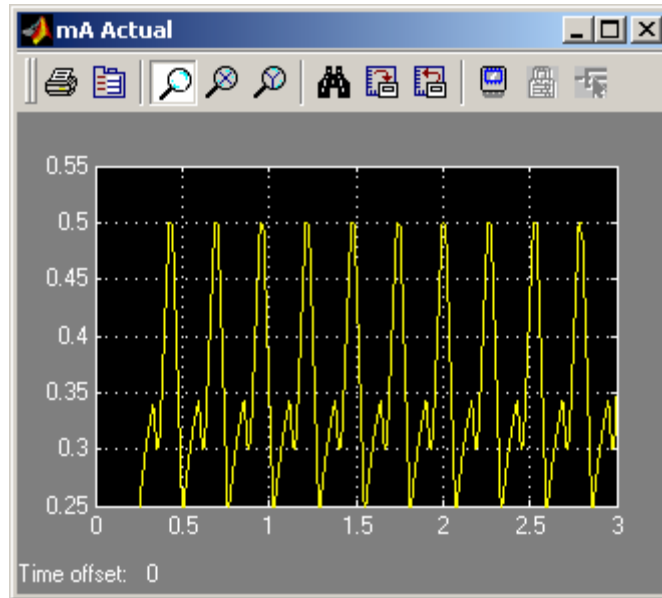


**Figure 51. System Output at 8 Hertz Reference Signal**

Vertical Axis shows current in Amps.  
Horizontal Axis shows time in Seconds.

According to the results observed for increasing frequencies, we can make an inference that (in the reverse case) the error would be lower for a decrease in frequency of reference. The simulation result of *figure 52* confirms this deduction.

#### 4.3.5 Simulation at 6 radians/second (1 Hertz) tube current reference

The magnitude of error is lower than that at higher frequencies and the waveform is also very smooth. (Figure 52) Of course, this simply bears out the fact that we got an error close to 0 % for the static current reference (0 Hertz) in chapter 1.

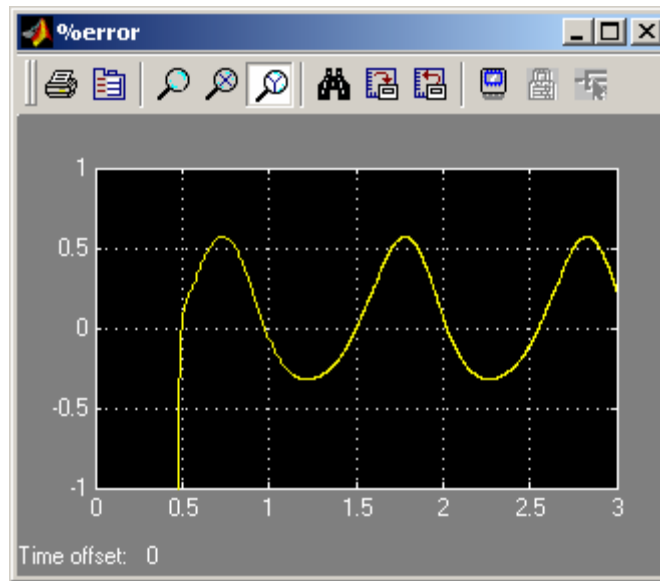


**Figure 52. Error at 1 Hertz.**

Vertical Axis shows percentage error.  
Horizontal Axis shows time in Seconds.

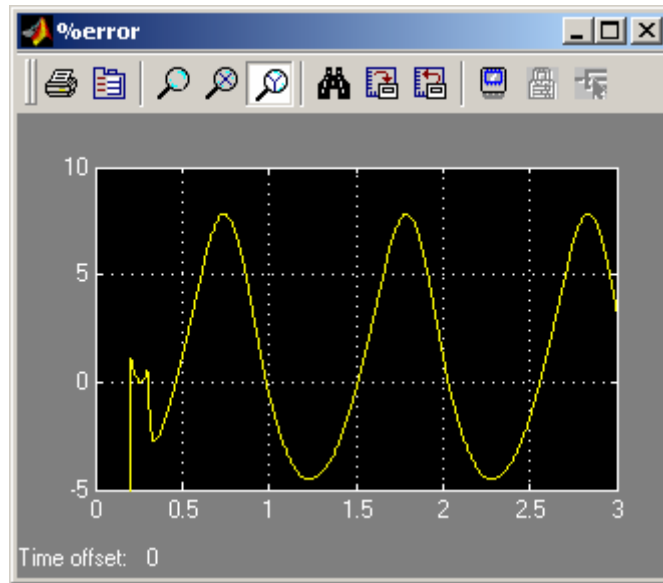


**Figure 53. Original System Error at 1 Hertz.**

Vertical Axis shows percentage error.  
Horizontal Axis shows time in Seconds.

Comparing the non-fuzzy systems output at this frequency (*figure 53*), we again see the significant difference in performance (-0.5 to 0.6 % in Fuzzy Enhanced system (*figure 52*) as compared to -5 to 8% in non-fuzzy).

We have thus explored the limits of the system with respect to the frequency of the tube current.

#### **4.4 ROBUSTNESS OF THE CONTROLLER TO NOISE CONDITIONS AND ANOMALIES**

The setup of *figure 54* shows a pulse generator input at the error-summing block. This will allow us to simulate certain noise conditions, which the tube experiences in real life. It is important to find out how Fuzzy Controller enhanced model responds to noise conditions that are sure to occur in the real system

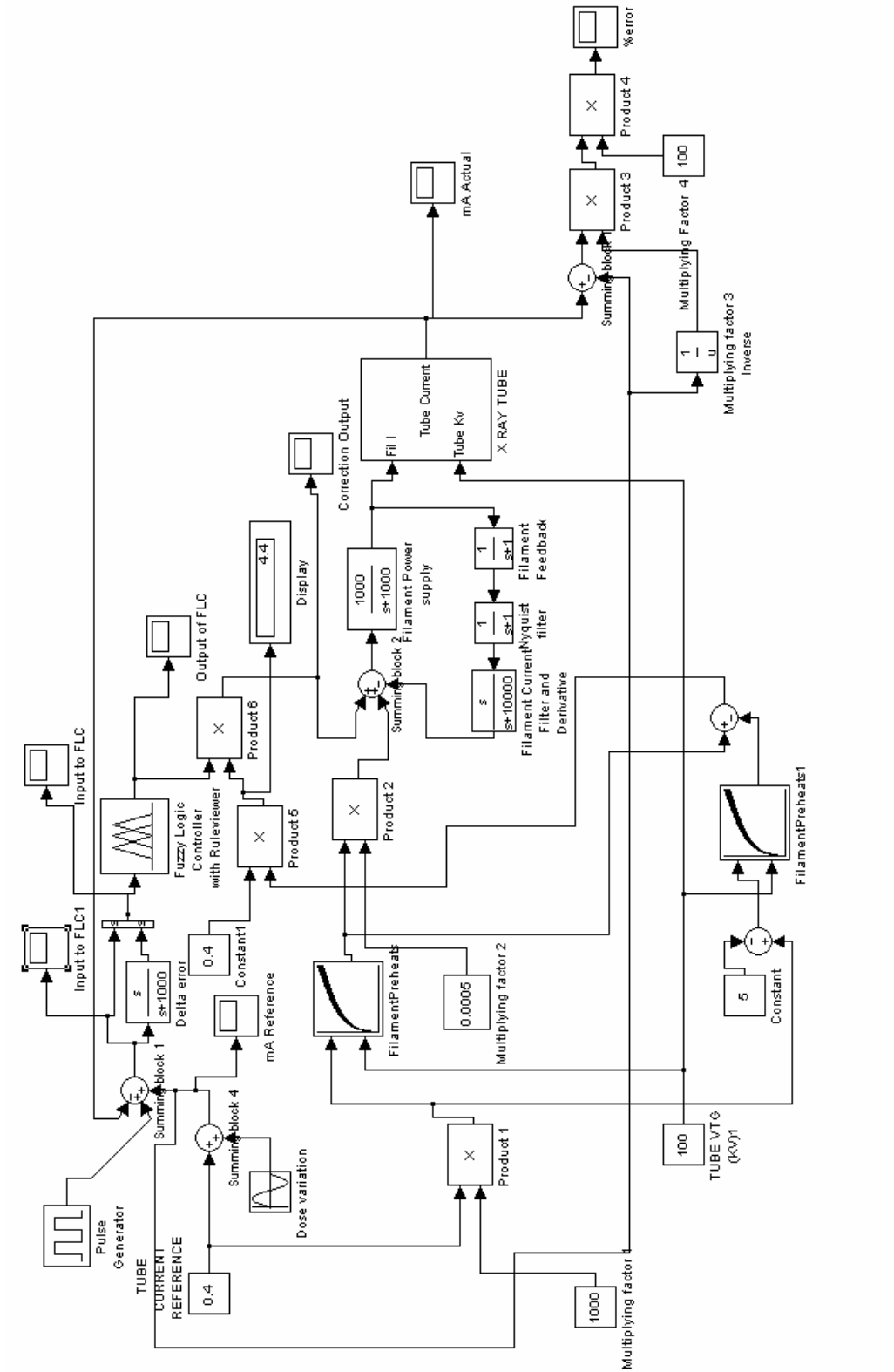
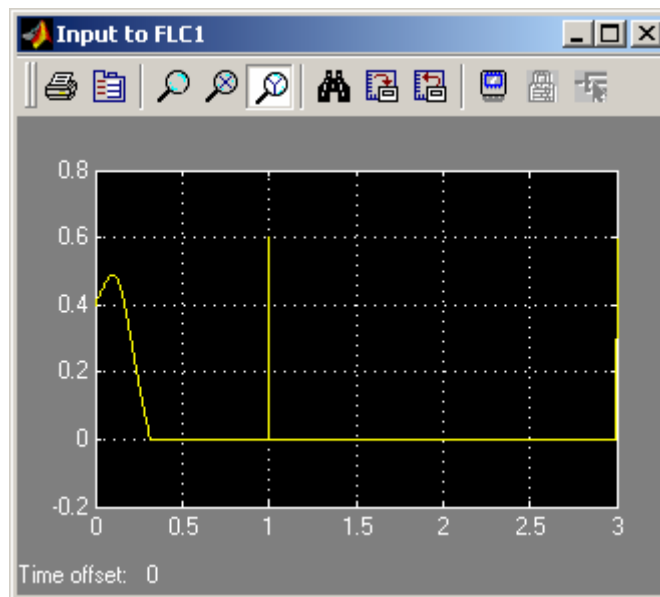


Figure 54. Setup for noise handling

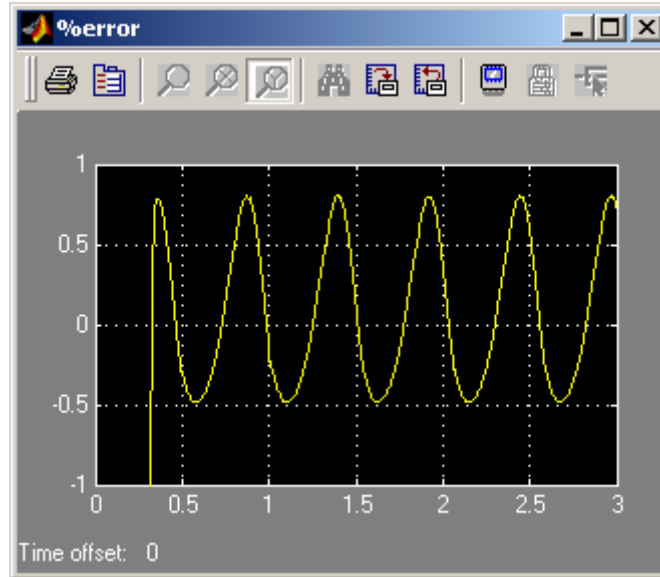
#### 4.4.1 Impulse of 600mA

Figure 55 shows an impulse input of 600mA being fed into the error loop of the system. An impulse very closely resembles a Tube “arc”, which is a spike in the tube current caused by noise conditions and other anomalies in the system. This is a common occurrence and the systems needs to be able to withstand them upto certain magnitudes.



**Figure 55. Error signal to the controller**

Vertical Axis shows signal magnitude.  
Horizontal Axis shows time in Seconds.



**Figure 56. Error of system with 600mA impulse noise**

Vertical Axis shows percentage error.  
Horizontal Axis shows time in Seconds.

As can be seen from *figure 56*, the system error remains unchanged even with the introduction of an impulse in the feedback loop. This is a good sign that shows our system performs well in noise conditions.

#### 4.4.2 Impulse of 2000mA (2 Amps)

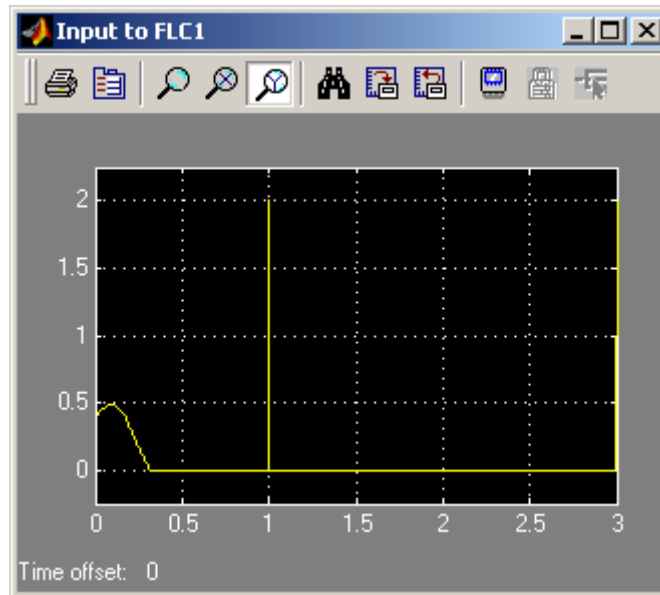


**Figure 57. Error signal to the controller**

Vertical Axis shows signal magnitude.  
Horizontal Axis shows time in Seconds.

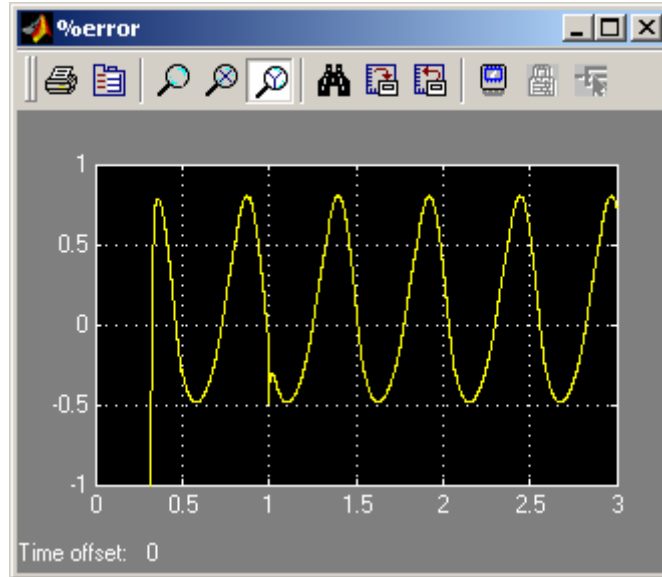


**Figure 58. Error of system with 2 Amps of impulse noise**

Vertical Axis shows percentage error.  
Horizontal Axis shows time in Seconds.

*Figures 57 and 58* show that the system still performs well at an impulse that is almost 150% larger than the reference signal magnitude. This is

#### 4.4.3 Impulse of 4000mA (4 Amps)

Figure 59 shows how the system stabilizes quickly even when subjected to an arc of 4 Amps. This is very positive for the design since real life tube arcs tend to be in the vicinity of 2 Amps. This shows that the system is very robust in noise conditions.

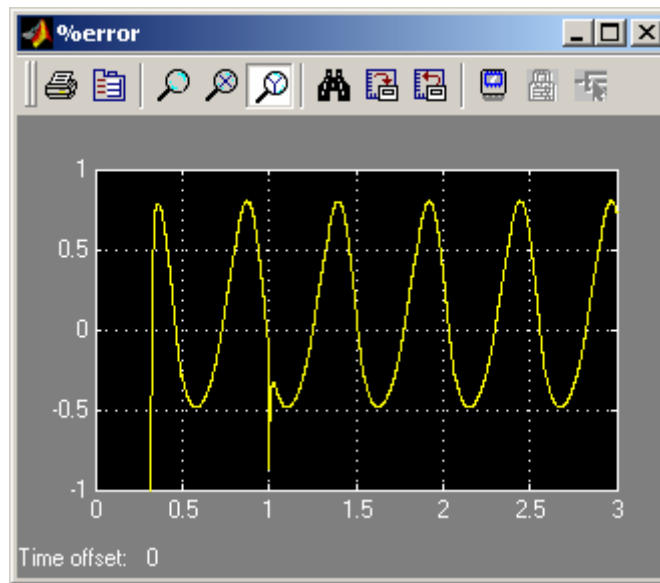


**Figure 59. Error of system with 4 Amps of impulse noise.**

Vertical Axis shows percentage error.  
Horizontal Axis shows time in Seconds.

#### 4.4.4 Impulse of 4000mA (4 Amps) on original model

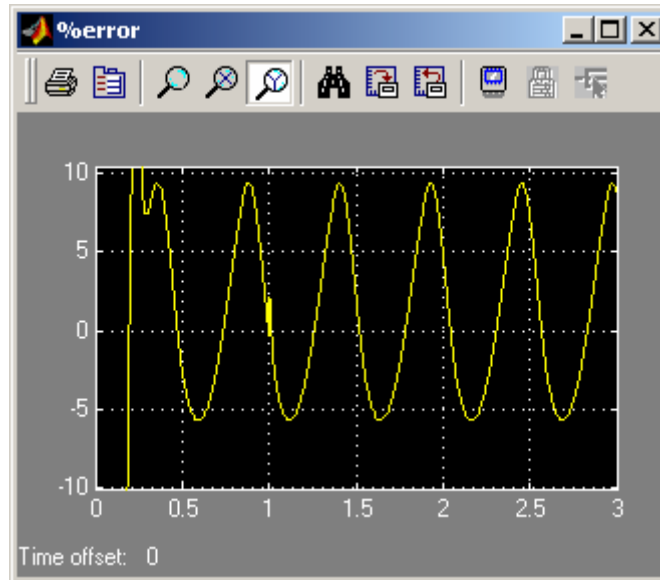


**Figure 60. Error of original system with 4 Amps of impulse noise.**

Vertical Axis shows percentage error.  
Horizontal Axis shows time in Seconds.

As can be seen from Figure 60, the original system performs well with impulse noise. So our enhanced system is consistent with its reduced error for all the same conditions.

## Chapter 5: CONCLUSION AND FUTURE DEVELOPMENTS

This thesis demonstrated the development of a control system of an X-Ray Tube as applied in a CT scanner. A model of the control system was simulated in Matlab-Simulink software and the model was verified as being in conformance with an existing Marconi Medical Systems CT System. This allows the evaluation of new control algorithms without resorting to experimental trial and error.”

Then an added performance requirement was introduced which enables the varying of X-Ray Tube current during one exposure cycle of the tube. It was seen that the original control system, which was not specifically designed for this dynamic application, performs relatively poorly under these requirements. The original model was enhanced with the addition of a Fuzzy Logic Controller in the control loop. The model was then seen to have immensely improved performance. As mentioned before, the benefits of this improvement are manifold:

- 1) There is better control of radiation dose to the patient, thus reducing risks of radiation related ailments like cancer. This is a very important safety issue.
- 2) Longer life of the X-Ray Tube, since higher current in the X-Ray Tube affects the life of the filament, thus resulting in cost savings, which has significant social benefits.
- 3) Better quality of images obtained from the CT Scans, as dose modulation optimizes the quantity of radiation required for different views of the body. A lower error in system output significantly affects this aspect.

This thesis description includes the development of the original X-Ray Tube current control system in Simulink based on the design of an existing system. Then the new requirement is introduced and the system is redesigned to accommodate this requirement. The enhancement to the original design, which includes the design of a Fuzzy Logic Controller, is presented in detail. Then the model is simulated after making modifications to the design and changing some parameters, and the effects of these changes and modifications are analyzed. This thesis work is significant in its treatment since the use of

Fuzzy Logic techniques in control systems in the medical field have not gained much popularity so far.

Now that the model has been simulated and it's improved performance noted, there is the possibility of implementation of the fuzzy model in the real system as and when the opportunity arises. Since it is possible to incorporate Fuzzy techniques in software in either Digital Signal Processors or Microcontrollers, this design could very well end up being a part of a real system. The development of hardware that implements Fuzzy logic could also make implementation of this design and others like it a reality.

Future development in this design would be to develop a design to achieve the same improved performance at even higher frequencies of reference, making the design specification restrictions tighter and lowering the allowable error to a minimum. This could involve using other ways of generating membership functions (such as gradient descent, genetic algorithms) Also, given the nonlinear behavior of the X-Ray Tube, it would be a good idea to explore the use of a hybrid intelligent controller which implements Neural Networks and Fuzzy Logic synergistically (Neuro-Fuzzy Control), since these techniques used in a complementary configuration have been known to produce exceptional results.

## APPENDIX

### LOOK-UP TABLE OF FILAMENT EMISSION CHARACTERISTICS.

```
tubefreq = 2; % cutoff freq to be used in tubemodel for simulink
s = sprintf('The xtube cutoff frequency of %4.2f hertz has been loaded',tubefreq);
disp(s);
% interpolated preheat table %
Xtuberow = [3.327:.03750:4.827]; %Filament Currents
Xtubecol = [80:20:120]; % Voltages
% Table of tube currents with given Tube Voltages and Filament currents

Xtubet = [0 0 0;1.24 1.52 1.79;2.48 2.78 3.06;3.71 4.03 4.34;5.00 5.28 5.60;6.19 6.54
6.89; 7.43 7.79 8.16;8.66 9.05 9.44;9.90 10.54 11.28;12.04 12.80 13.57;14.26 15.06
15.85;16.48 17.32 18.14;18.70 19.58 20.67;21.44 22.86 24.26;24.91 26.33 27.85;28.38
29.91 31.90; 32.45 34.56 36.65;37.06 39.25 41.72;42.03 44.85 47.58;47.67 50.73
54.07;53.93 57.61 61.17;60.72 65.10 69.15;68.45 73.29 78.07;76.90 80.23 87.76;86.15
92.25 98.41;96.25 103.13 110.00; 107.27 115.17 122.91;119.34 128.07 136.92;132.41
142.40 152.34;146.80 157.87 168.86;162.22 174.65 187.00;179.09 192.82 206.76;197.25
212.50 227.94;216.76 233.82 250.65;
237.94 256.77 275.52; 260.65 281.38 302.22; 285.17 308.15 330.80;311.48 336.54
361.74; 339.62 366.30 395.00;369.60 400.00 431.34;401.82 433.97 468.69];

disp('The preheats have been loaded');
plot(Xtuberow,Xtubet)
title('X-Ray tube emission characteristics')
xlabel('filament current in Amps')
ylabel('tube current in mA')
```

## FILAMENT PREHEAT TABLE

```
% $Revision: [pcom-host.pcomdb]/pcom/4_5dev/scan/xscp/include/preheat.h;1 $
% $Date: 1996/01/18 13:49:49 $%&&(++)
% *****
% **          CT SOFTWARE ENGINEERING          **
% *****
% ** THIS DOCUMENT CONTAINS PROPRIETARY INFORMATION.IT IS
THE EXCLUSIVE CONFIDENTIAL PROPERTY OF PICKER INTERNATIONAL,
INC. COPYRIGHT 1992, PICKER INTERNATIONAL . COPYING, DISCLOSURE
TO OTHERS, OR OTHER USE IS PROHIBITED WITHOUT THE EXPRESS,
WRITTEN AUTHORIZATION OF PICKER INTERNATIONAL, INC.
*****
%*
FILE:                preheat.h
%* CREATION DATE:    08-JUN-92
%* PROJECT:          CR XRAY GENERATOR (P-series)
%* GROUP:            CT XRAY ENGINEERING
%* PROGRAMMED BY:    WALT DUPUIS
%* CREATION ENVIRONMENT:    MUPS8
%* COMPUTER SYSTEM:  XSC (XRAY SYSTEM CONTROLLER)
%* OPERATING SYSTEM: PSOS
%* NOTES:
% This is 2 tables of default preheats. One for each filament.
% The values are in (filament ma)*2 since the preheat DAC has 0.5 ma
% The tables are organized as follows:
% 80 85 90.....160 165kv
% 0ma  n, n, n,.....
% 5ma  n, n, n,.....
% 395ma
% 400ma
```

%REVISION HISTORY

%DATE AUTH DESCRIPT

%4-jun-92 w.d. created file for rel 4.1

%09/02/97 DAD addition of mA stations from 401 to 600 for 600R generator

%04/29/97 MDH modified values in all mA stations to fit new 600R generator

\*\*\*\*\*

filrow = [0:5:600];

filcol = [80:5:165];

/\* ma 0-->600 in steps of 5 \*/

/\*kv --> \*/

/\*80 85 90 95 100 105 110 115 120 125 130 135 140 145 150 155 160 165

fili=[6654 6650 6645 6643 6638 6636 6632 6628 6624 6622 6619 6616 6615 6611 6608

6605 6602 6599

6957 6952 6946 6942 6937 6933 6928 6923 6918 6915 6911 6907 6904 6900 6896 6892

6888 6884

7260 7254 7247 7241 7236 7230 7224 7218 7212 7208 7203 7198 7193 7189 7184 7179

7174 7169

7453 7446 7438 7432 7426 7419 7413 7406 7400 7394 7389 7383 7378 7372 7367 7361

7356 7350

7598 7590 7582 7575 7568 7561 7554 7547 7540 7534 7528 7522 7516 7510 7504 7498

7492 7486

7715 7707 7698 7691 7683 7676 7668 7661 7653 7647 7641 7634 7628 7621 7615 7608

7602 7596

7814 7805 7797 7789 7781 7773 7765 7757 7749 7743 7736 7729 7722 7715 7709 7702

7695 7688

7901 7891 7882 7874 7865 7857 7849 7841 7833 7826 7818 7811 7804 7797 7790 7783

7776 7769

7977 7968 7958 7949 7941 7932 7924 7915 7907 7899 7892 7884 7877 7870 7862 7855

7848 7840

8046 8036 8027 8018 8009 8000 7991 7982 7974 7966 7958 7950 7942 7935 7927 7920  
7912 7905  
8110 8099 8089 8080 8071 8061 8052 8043 8035 8026 8018 8010 8002 7995 7987 7979  
7971 7963  
8168 8157 8147 8137 8128 8118 8109 8100 8091 8082 8074 8066 8057 8049 8041 8033  
8025 8017  
8222 8211 8200 8190 8180 8171 8161 8152 8143 8134 8126 8117 8108 8100 8092 8084  
8076 8067  
8272 8261 8250 8240 8230 8220 8210 8201 8191 8182 8174 8165 8156 8148 8139 8131  
8123 8114  
8319 8308 8297 8287 8276 8266 8256 8246 8237 8228 8219 8210 8201 8192 8184 8175  
8167 8158  
8364 8352 8341 8331 8320 8310 8300 8290 8280 8271 8261 8252 8243 8234 8226 8217  
8208 8199  
8406 8394 8383 8372 8361 8351 8341 8330 8320 8311 8302 8292 8283 8274 8265 8256  
8247 8238  
8446 8434 8423 8412 8401 8390 8380 8369 8359 8350 8340 8331 8321 8312 8303 8294  
8285 8276  
8484 8472 8461 8449 8438 8428 8417 8406 8396 8386 8377 8367 8357 8348 8339 8330  
8320 8311  
8521 8509 8497 8485 8474 8463 8452 8442 8431 8421 8412 8402 8392 8382 8373 8364  
8354 8345  
8556 8544 8531 8520 8509 8497 8486 8475 8465 8455 8445 8435 8425 8415 8406 8396  
8387 8377  
8590 8577 8565 8553 8541 8530 8519 8508 8497 8487 8477 8467 8457 8447 8437 8428  
8418 8409  
8622 8609 8597 8585 8573 8562 8551 8539 8529 8518 8508 8498 8487 8478 8468 8458  
8448 8438  
8653 8640 8628 8616 8604 8592 8581 8569 8559 8548 8538 8527 8517 8507 8497 8487  
8477 8467

8683 8670 8658 8645 8633 8622 8610 8599 8588 8577 8566 8556 8545 8535 8525 8515  
8505 8495  
8712 8699 8686 8674 8662 8650 8638 8627 8616 8605 8594 8583 8573 8563 8552 8542  
8532 8522  
8741 8727 8714 8702 8690 8678 8666 8654 8643 8632 8621 8610 8599 8589 8579 8569  
8558 8548  
8768 8754 8741 8729 8716 8704 8692 8680 8669 8658 8647 8636 8625 8615 8604 8594  
8584 8573  
8795 8781 8768 8755 8742 8730 8718 8706 8695 8683 8672 8661 8650 8640 8629 8619  
8608 8598  
8820 8806 8793 8780 8768 8755 8743 8731 8719 8708 8697 8686 8674 8664 8653 8643  
8632 8622  
8845 8831 8818 8805 8792 8780 8767 8755 8743 8732 8721 8709 8698 8687 8677 8666  
8655 8645  
8870 8856 8842 8829 8816 8804 8791 8779 8767 8755 8744 8733 8721 8710 8700 8689  
8678 8667  
8894 8879 8866 8853 8839 8827 8814 8802 8790 8778 8767 8755 8744 8733 8722 8711  
8700 8689  
8917 8902 8889 8875 8862 8849 8837 8824 8812 8800 8789 8777 8765 8754 8743 8733  
8722 8711  
8939 8925 8911 8898 8884 8871 8859 8846 8834 8822 8810 8799 8787 8776 8765 8754  
8742 8731  
8962 8947 8933 8919 8906 8893 8880 8867 8855 8843 8831 8819 8808 8796 8785 8774  
8763 8752  
8983 8968 8954 8941 8927 8914 8901 8888 8876 8864 8852 8840 8828 8817 8805 8794  
8783 8772  
9004 8989 8975 8962 8948 8935 8922 8908 8896 8884 8872 8860 8848 8836 8825 8814  
8803 8791  
9025 9010 8996 8982 8968 8955 8942 8928 8916 8904 8892 8879 8867 8856 8844 8833  
8822 8810

9045 9030 9016 9002 8988 8975 8961 8948 8935 8923 8911 8899 8886 8875 8863 8852  
8840 8829  
9065 9050 9036 9021 9007 8994 8980 8967 8954 8942 8930 8917 8905 8893 8882 8870  
8859 8847  
9085 9069 9055 9041 9026 9013 8999 8986 8973 8961 8948 8936 8923 8912 8900 8888  
8877 8865  
9104 9088 9074 9059 9045 9031 9018 9004 8991 8979 8966 8954 8941 8930 8918 8906  
8894 8883  
9122 9107 9092 9078 9063 9050 9036 9022 9009 8997 8984 8972 8959 8947 8935 8923  
8912 8900  
9141 9125 9110 9096 9081 9067 9054 9040 9027 9014 9002 8989 8976 8964 8952 8940  
8929 8917  
9159 9143 9128 9114 9099 9085 9071 9057 9044 9032 9019 9006 8993 8981 8969 8957  
8945 8933  
9176 9161 9146 9131 9116 9102 9088 9074 9061 9048 9036 9023 9010 8998 8986 8974  
8962 8949  
9194 9178 9163 9148 9133 9119 9105 9091 9078 9065 9052 9039 9026 9014 9002 8990  
8978 8965  
9211 9195 9180 9165 9150 9136 9122 9108 9095 9081 9068 9055 9042 9030 9018 9006  
8993 8981  
9228 9212 9197 9182 9166 9152 9138 9124 9111 9098 9084 9071 9058 9046 9034 9021  
9009 8997  
9244 9228 9213 9198 9183 9168 9154 9140 9127 9113 9100 9087 9074 9061 9049 9037  
9024 9012  
9261 9244 9229 9214 9199 9184 9170 9156 9142 9129 9116 9102 9089 9077 9064 9052  
9039 9027  
9277 9260 9245 9230 9214 9200 9186 9171 9158 9144 9131 9117 9104 9092 9079 9067  
9054 9042  
9293 9276 9261 9245 9230 9215 9201 9186 9173 9159 9146 9132 9119 9106 9094 9081  
9069 9056

9308 9292 9276 9261 9245 9230 9216 9201 9188 9174 9161 9147 9134 9121 9108 9096  
9083 9070  
9323 9307 9291 9276 9260 9245 9231 9216 9202 9189 9175 9162 9148 9135 9123 9110  
9097 9085  
9339 9322 9306 9291 9275 9260 9245 9231 9217 9203 9190 9176 9162 9149 9137 9124  
9111 9098  
9353 9337 9321 9305 9289 9275 9260 9245 9231 9217 9204 9190 9176 9163 9151 9138  
9125 9112  
9368 9351 9335 9320 9304 9289 9274 9259 9245 9232 9218 9204 9190 9177 9164 9151  
9138 9126  
9383 9366 9350 9334 9318 9303 9288 9273 9259 9245 9231 9217 9204 9191 9178 9165  
9152 9139  
9397 9380 9364 9348 9332 9317 9302 9287 9273 9259 9245 9231 9217 9204 9191 9178  
9165 9152  
9411 9394 9378 9362 9346 9331 9316 9301 9287 9272 9258 9244 9230 9217 9204 9191  
9178 9165  
9425 9408 9392 9376 9359 9344 9329 9314 9300 9286 9272 9257 9243 9230 9217 9204  
9191 9178  
9439 9422 9405 9389 9373 9358 9342 9327 9313 9299 9285 9270 9256 9243 9230 9217  
9204 9190  
9452 9435 9419 9403 9386 9371 9356 9340 9326 9312 9298 9283 9269 9256 9243 9229  
9216 9203  
9466 9448 9432 9416 9399 9384 9369 9353 9339 9325 9310 9296 9282 9268 9255 9242  
9228 9215  
9479 9462 9445 9429 9412 9397 9381 9366 9352 9337 9323 9308 9294 9281 9267 9254  
9241 9227  
9492 9475 9458 9442 9425 9410 9394 9379 9364 9350 9335 9321 9306 9293 9280 9266  
9253 9239  
9505 9488 9471 9454 9438 9422 9407 9391 9377 9362 9348 9333 9319 9305 9292 9278  
9265 9251

9518 9500 9484 9467 9450 9435 9419 9403 9389 9374 9360 9345 9331 9317 9303 9290  
9276 9263  
9531 9513 9496 9479 9463 9447 9431 9416 9401 9386 9372 9357 9342 9329 9315 9302  
9288 9274  
9543 9525 9509 9492 9475 9459 9443 9428 9413 9398 9384 9369 9354 9340 9327 9313  
9300 9286  
9555 9538 9521 9504 9487 9471 9455 9440 9425 9410 9395 9381 9366 9352 9338 9325  
9311 9297  
9568 9550 9533 9516 9499 9483 9467 9451 9437 9422 9407 9392 9377 9363 9350 9336  
9322 9308  
9580 9562 9545 9528 9511 9495 9479 9463 9448 9433 9418 9403 9389 9375 9361 9347  
9333 9320  
9592 9574 9557 9540 9523 9507 9491 9475 9460 9445 9430 9415 9400 9386 9372 9358  
9344 9330  
9604 9585 9568 9551 9534 9518 9502 9486 9471 9456 9441 9426 9411 9397 9383 9369  
9355 9341  
9615 9597 9580 9563 9546 9529 9513 9497 9482 9467 9452 9437 9422 9408 9394 9380  
9366 9352  
9627 9609 9592 9574 9557 9541 9525 9508 9493 9478 9463 9448 9433 9419 9405 9391  
9377 9363  
9638 9620 9603 9586 9568 9552 9536 9519 9504 9489 9474 9459 9444 9429 9415 9401  
9387 9373  
9650 9631 9614 9597 9579 9563 9547 9530 9515 9500 9485 9469 9454 9440 9426 9412  
9398 9384  
9661 9642 9625 9608 9590 9574 9558 9541 9526 9511 9496 9480 9465 9451 9437 9423  
9409 9395 %/\*this is 405ma data\*/  
9673 9654 9637 9620 9602 9586 9570 9552 9537 9522 9507 9491 9476 9462 9448 9434  
9420 9406  
9685 9666 9649 9632 9613 9597 9581 9564 9549 9534 9518 9502 9487 9473 9459 9445  
9431 9417

9697 9678 9661 9644 9625 9609 9593 9575 9560 9545 9530 9513 9498 9484 9470 9456  
9442 9428  
9709 9690 9673 9656 9637 9621 9605 9587 9572 9557 9541 9525 9510 9495 9481 9467  
9453 9439  
9721 9701 9684 9667 9648 9632 9616 9598 9583 9568 9552 9536 9521 9506 9492 9478  
9464 9450  
9733 9713 9696 9679 9660 9644 9628 9609 9594 9579 9564 9547 9532 9517 9503 9489  
9475 9461  
9745 9725 9708 9691 9671 9655 9639 9621 9606 9591 9575 9558 9543 9528 9514 9500  
9486 9472  
9757 9737 9720 9703 9683 9667 9651 9632 9603 9602 9586 9569 9554 9539 9525 9511  
9497 9483  
9769 9749 9732 9715 9695 9679 9663 9644 9629 9614 9598 9581 9566 9551 9537 9522  
9508 9494  
9780 9760 9743 9726 9706 9690 9674 9655 9640 9625 9609 9592 9577 9562 9548 9533  
9519 9505  
9792 9772 9755 9738 9718 9702 9686 9666 9651 9636 9620 9603 9588 9573 9559 9544  
9530 9516  
9804 9784 9767 9750 9729 9713 9697 9678 9663 9648 9631 9614 9599 9584 9570 9555  
9541 9527  
9816 9796 9779 9762 9741 9725 9709 9689 9674 9659 9643 9625 9610 9595 9581 9566  
9552 9538  
9828 9808 9791 9774 9753 9737 9721 9701 9686 9671 9654 9637 9622 9606 9592 9577  
9563 9549  
9840 9819 9802 9785 9764 9748 9732 9712 9697 9682 9665 9648 9633 9617 9603 9588  
9574 9560  
9852 9831 9814 9797 9776 9760 9744 9723 9708 9693 9677 9659 9644 9628 9614 9599  
9585 9571  
9864 9843 9826 9809 9787 9771 9755 9735 9720 9705 9688 9670 9655 9639 9625 9610  
9596 9582

9876 9855 9838 9821 9799 9783 9767 9746 9731 9716 9699 9681 9666 9650 9636 9621  
9607 9593  
9888 9867 9850 9833 9811 9795 9779 9758 9743 9728 9711 9693 9678 9662 9648 9632  
9618 9604  
9899 9878 9861 9844 9822 9806 9790 9769 9754 9739 9722 9704 9689 9673 9659 9643  
9629 9615  
9911 9890 9873 9856 9834 9818 9802 9780 9765 9750 9733 9715 9700 9684 9670 9654  
9640 9626  
9923 9902 9885 9868 9845 9829 9813 9792 9777 9762 9744 9726 9711 9695 9681 9665  
9651 9637  
9935 9914 9897 9880 9857 9841 9825 9803 9788 9773 9756 9737 9722 9706 9692 9676  
9662 9648  
9947 9926 9909 9892 9869 9853 9837 9815 9800 9785 9767 9749 9734 9717 9703 9687  
9673 9659  
9959 9937 9920 9903 9880 9864 9848 9826 9811 9796 9778 9760 9745 9728 9714 9698  
9684 9670  
9971 9949 9932 9915 9892 9876 9860 9837 9822 9807 9790 9771 9756 9739 9725 9709  
9695 9681  
9983 9961 9944 9927 9903 9887 9871 9849 9834 9819 9801 9782 9767 9750 9736 9720  
9706 9692  
9995 9973 9956 9939 9915 9899 9883 9860 9845 9830 9812 9793 9778 9761 9747 9731  
9717 9703  
10007 9985 9968 9951 9927 9911 9895 9872 9857 9842 9824 9805 9790 9773 9759  
9742 9728 9714  
10018 9996 9979 9962 9938 9922 9906 9883 9868 9853 9835 9816 9801 9784 9770  
9753 9739 9725  
10030 10008 9991 9974 9950 9934 9918 9894 9879 9864 9846 9827 9812 9795 9781  
9764 9750 9736  
10042 10020 10003 9986 9961 9945 9929 9906 9891 9876 9857 9838 9823 9806 9792  
9775 9761 9747

```

10054 10032 10015 9998 9973 9957 9941 9917 9902 9887 9869 9849 9834 9817 9803
9786 9772 9758
10066 10044 10027 10010 9985 9969 9953 9929 9914 9899 9880 9861 9846 9828 9814
9797 9783 9769
10078 10055 10038 10021 9996 9980 9964 9940 9925 9910 9891 9872 9857 9839 9825
9808 9794 9780
10090 10067 10050 10033 10008 9992 9976 9951 9936 9921 9903 9883 9868 9850 9836
9819 9805 9791
10102 10079 10062 10045 10019 10003 9987 9963 9948 9933 9914 9894 9879 9861
9847 9830 9816 9802
10114 10091 10074 10057 10031 10015 9999 9974 9959 9944 9925 9905 9890 9872
9858 9841 9827 9813
10126 10103 10086 10069 10043 10027 10011 9986 9971 9956 9937 9917 9902 9884
9870 9852 9838 9824
];
%/*{9650 9631 9614 9597 9579 9563 9547 9530 9515 9500 9485 9469 9454 9440 9426
9412 9398 9384} MDH this the real 400ma data -see above */
fili1=fili*0.0005;
disp('filament preheat table loaded')
plot(fili1,filrow)
title('filament preheats')
xlabel('filament current in Amps')
ylabel('tube current in mA')

```

## REFERENCES

1. Abbod, M. F., von Keyserlingk, D. G., Linkens, D. A., and Mahfouf, M., (Department of Automatic Control & Systems Engineering, Sheffield Univ., UK) Survey of utilization of fuzzy technology in medicine and Healthcare, *Fuzzy Sets and Systems*, Vol. 120, no 2, pages 331-349, June 2001.
2. Changjiang Yan, Shoji Hirano, and Yutaka Hata, (Department of Computer Engineering, Himeji Inst. of Technology, Japan), Extraction of blood vessel in CT angiography's image aided by fuzzy Logic, *IEEE Proceedings of the 5<sup>th</sup> International Conference on Signal Processing*, vol. 2, pages 926-929, August 2000.
3. Kwan, M. F. Y., Cheung K. C and Gibson. I, (Department of Mechanical Engineering, Hong Kong University, China), Automatic boundary extraction and rectification of bony tissue in CT images using artificial intelligence techniques, *Proceedings of the International Society for Optical Engineering*, Vol. 3979, pt. 1-2, pages 896-905, February 2000.
4. Ock-Kyung Yoon, Dong-Min Kwak, Dong-Whee Kim and Kil-Houm Park (Department of Electrical Engineering, Kyungpook Nat. Univ., Taegu, South Korea), MR brain image segmentation using fuzzy clustering, *1999 IEEE International Fuzzy systems Conference Proceedings*, vol.2, pages 853-857, August 1999.
5. Hirano, S., Kamiura, N. and Hata, Y. (Department of Computer Engineering, Himeji Inst. of Technology, Hyogo, Japan.), Fuzzy expert system for foot CT image segmentation, *Proceedings of the 5<sup>th</sup> International Conference on Soft Computing and Information/Intelligent Systems*, vol.1, pages 337-340, October 1998.
6. Hata, Y., Kobashi, S. and Hirano, S. (Department of Computer Engineering, Himeji Inst. of Technology, Hyogo, Japan), Medical image segmentation by fuzzy logic

techniques, *1998 IEEE International Conference on systems, Man, and Cybernetics*, vol. 4, pages 4098-5103, October 1998.

7. Brown, M. S., McNitt-Gray, M. F., Mankovich, N. J., Goldin, J. G., Hiller, J., Wilson, L. S. and Aberie, D. R. (Department of Radiological Science, California Univ., Los Angeles, CA, USA), Method for segmenting chest CT image data using an anatomical model: preliminary results, *IEEE Transactions on Medical Imaging*, vol. 16, no. 6, pages 828-839, December 1997.

8. Udupa, J. K., Odhner, D., Jie Tian, Holland and G., Axel, L (Department of Radiology, Univ. of Pennsylvania Med. Center, Philadelphia, PA, USA), Automatic clutter-free volume rendering for MR angiography using fuzzy connectedness, *Proceedings of the International Society for Optical Engineering*, vol. 3034, pt.1-2, pages 114-119, February 1997.

9. Cosic, D. and Loncaric, S (Faculty of Electrical & Computer Engineering, Zagreb Univ., Croatia), Rule-based labeling of CT head images, *6<sup>th</sup> Conference on Artificial Intelligence in Medicine Europe, AIME' 97*, pages 453-456, March 1997.

10. Tabuchi, H., Miyoshi, T., Ichibashi, H. and Ohno, K. (Department of Industrial Engineering, Osaka Prefecture University, Japan), Computerized Tomography with radial basis functions network: a neuro-fuzzy approach, *Proceedings of the International Conference on Neural Networks*, vol. 5, pages 2258-2263, December 1995.

11. Banerjee, S., Mukherjee, D. P., Majumdar, D. D., Kohli, S. S. and Mishra, V. K., (Electronics & Communications Science Unit, Indian Statistical Institute, Calcutta, India), Fuzzy C-means approach to tissue classification in multimodal medical imaging, *Proceedings of The International Society for Optical Engineering*, vol. 2664, pages 58-63, February 1996.

12. Li, Hongyi, Deklerck, Rudi, De Cuyper, Bernard, Hermanus, A.

Nyssen, Edgard and Cornelis, Jan (Vrije Universiteit Brussel, Brussel, Belgium),  
Object recognition in brain CT-scans: knowledge-based fusion of data from multiple  
feature extractors, *IEEE Transactions on Medical Imaging*, vol 14, pages 212-229, 1995.

13. Michael Gies, Willi A. Kalender, Heiko Wolf, Christoph Suess (Institute of Medical  
Physics, University of Erlangen-Nuremberg, Krankenhausstr, Germany) and Mark T.  
Madsen (Department of Radiology, University of Iowa, Iowa City, Iowa), Dose Reduction  
in CT by anatomically adapted tube current modulation, *American Association of  
Medical Physics*, vol. 26, pages 2235-2253, November 1999.

14. Euclid Seeram, RT( R), BSc, MSc, *Computed Tomography- Physical Principles,  
Clinical Applications and Quality Control.* ( W.B. Saunders Company, Philadelphia,  
Pennsylvania , 1994)

15. Marconi Medical Systems service publications.

16. Fuzzy Logic Research and Life

Publication of Loyola College in Maryland.

Web URL: [http://itri.loyola.edu/kb/c5\\_s4.htm](http://itri.loyola.edu/kb/c5_s4.htm), Published May 1993.

17. J. -S.R. JANG, C. -T SUN, E. MIZUTANI, *Neuro-Fuzzy and Soft Computing – A  
Computational Approach to Learning and Machine Intelligence* (Prentice Hall 1997).

18. M.J. Patyra and D.M. Mlynek, *Fuzzy Logic: Implementations and Applications*  
(Wiley Teubner 1996.)

19. Theodore A. Resnick, Walter DuPuis, Closed loop X-Ray Tube current control. (U.S.  
Patent No 4775992, October 4, 1988.)